MATHEMATICAL MODELS FOR SYNOVIAL JOINTS

A LUBRICATION BIOMECHANICAL STUDY

By
PEEYUSH CHANDRA

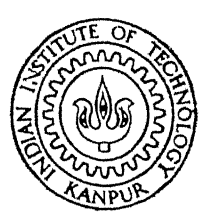

DEPARTMENT OF MATHEMATICS
INDIAN INSTITUTE OF TECHNOLOGY, KANPUR
JULY, 1975

MATHEMATICAL MODELS FOR SYNOVIAL JOINTS

A LUBRICATION BIOMECHANICAL STUDY

A Thesis Submitted
In Partial Fulfilment of the Requirements
for the Degree of
DOCTOR OF PHILOSOPHY

By
PEEYUSH CHANDRA

to the
DEPARTMENT OF MATHEMATICS
INDIAN INSTITUTE OF TECHNOLOGY, KANPUR
JULY, 1975

TO
MY LOVING
BROTHER AND SISTERS

ACKNOWLEDGEMENTS

The author expresses his deep sense of gratitude to his supervis Professor J.B. Shukla for introducing him to the field of Bio-Tribolo and his untiring guidance during the progress of this dissertation on this subject. His constructive criticisms and valuable suggestions had been a source of inspiration through out this work.

The author wishes to express his indebtedness to Prof.J.N.Kapu who introduced him to the new field of mathematics, called Bio-mathematics. The author also acknowledges his gratitudes to all his instructors and Dr. M.B. Banerjee in particular.

The author takes this opportunity to thank all his friends an the members of Bio-Tribology group for their co-operation and fruitfu discussions.

Though it is beyond the scope of any acknowledgement for what the author has received from his parents by way of inspiration and encouragement, yet he makes an effort to express his heartfelt and affectionate gratitudes to them.

The thanks are also due to C.S.I.R. and I.I.T., Kanpur for providing the financial assistance during this period.

Finally, the author expresses his thanks to Mr. G.L. Misra and Mr. S.K. Tewari for their unfailing patience in typecutting the ster and to Mr. Shyam Kumar for the neat cyclostyling. The keen interest taken by Mr. B.N. Srivastava in drawing the figures is also acknowle

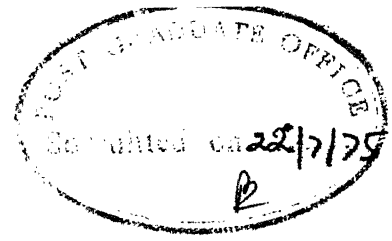

CERTIFICATE

This is to certify that the matter embodied in the thesis entitled "Mathematical Models For Synovial Joints" by Mr. Peeyush Chandra for the award of the Degree of Doctor of Philosophy of the Indian Institute of Technology, Kanpur, is a record of bonafide research work carried out by him under my supervision and guidance. The thesis has, in my opinion, reached the standard fulfilling the requirements of the Ph.D. degree. The results embodied in this thesis have not been submitted to any other University or Institute for the award of any degree or diploma.

(J. B. Shukla)
Thesis Supervisor
Department of Mathematics
Indian Institute of Technology
KANPUR

July - 1975

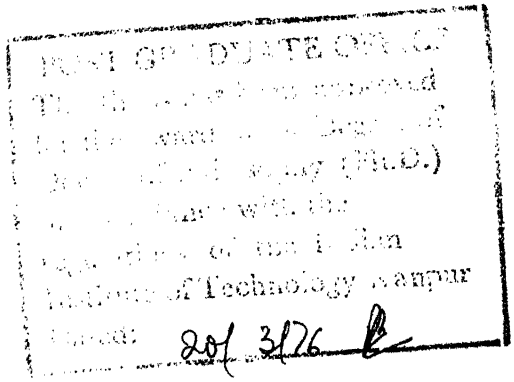

CONTENTS

LIST OF SYMBOLS

a_j = $\frac{1}{2\pi}$ (wave length of the jth roughness wave)

b = width of the rectangular zone

C = concentration of hyaluronic molecules in synovial fluid

C_o = concentration of hylauronate at the cartilage surface.

C_d = concentration of hyaluronate at the cartilage surface, in the case of diseased joint.

c_f = coefficient of friction

D = diffusion coefficient

e_{ij} = rate of deformation tensor

E_1, E_2 = Youngs' moduli of the cartilage surfaces

F = friction force (in chapter 6), otherwise as defined in equation (2.25)

G = boosting parameter

h = half the mean fluid film thickness

h_i = half the initial fluid film thickness

h_f = half the final fluid film thickness

h_m = half the minimum fluid film thickness

h_1 = half the fluid film thickness where pressure is maximum

h_r = half the fluid film thickness for rough surfaces

H = cartilage thickness

H_s = thickness of the superficial tangential zone

k_r = permeability in the radial direction

k_x = permeability in the x-direction

k_y = permeability in the y-direction

ℓ = half the length of the load bearing zone

ℓ_d = half the deformed length of load bearing zone

m = consistency index of synovial fluid

m_o = consistency index with no boosting effects

M = rate of increase in hyaluronate concentration

n = flow behaviour index of the fluid

N = number of superposed roughness waves

p = pressure in the fluid film region

P = pressure average in the porous region

P_o = constant pressure generated in the porous matrix due to compression at $x = \ell$

Q_x = Flow flux in x direction

Q_z = Flow flux in z direction

r = radial direction

r_o = radius of the load bearing zone

r_d = deformed radius of load bearing zone

R_1, R_2 = radii of the cartilage surfaces

t = time of squeezing

(u,v,w) = velocity components of the fluid

u_x = x component of velocity in porous region

U = surface velocity

V = squeeze velocity

V' = squeeze velocity of the cartilage surface ($y = h+H$) with respect to the surface, $y = h$

V_p = average velocity of the fluid in the porous region

v_h = resultant velocity at $y = h$

(x,y,z) = co-ordinate axes

W = load capacity

α = rate of decrease in concentration, in all the chapters except in chapter VI, where it is average inclination of the curved surface

ε_j = amplitude of jth roughness wave

μ = viscosity of synovial fluid

μ_o = viscosity of hyaluronate free synovial fluid

σ_1, σ_2 = Poisson's ratio of the cartilage surfaces

τ_{ij} = stress tensor

CHAPTER - I

GENERAL INTRODUCTION

1.1 INTRODUCTION

Since the beginning of civilization, man has been trying to understand nature which surrounds him. Because of his curiosity and continuous enhancement of knowledge, he has been involved in unveiling the mysteries of the universe by the space and other explorations. He has been asking questions such as 'why is the universe made as it is'; 'what is its origin'; 'how did the life originate on this planet' and so on. He has been contemplating the development of various organisms such as plants, animals and human beings and wondered how the changing environment effects their sequential growth. He has been trying to understand the origin of life itself and the mechanisms involved in making the life self-sustaining in an adequately optimised manner, Rashevsky [1973]. When one tries to answer some of the later questions from physico-mechanical points of view, the study is called Biomechanics. In short, Biomechanics is that branch of scientific knowledge which involves mechanics as well as biology. This encompasses studies regarding marphology and growth of plants and animals, functions and mechanisms of their parts, and their interaction with the environment.

One of the most important biomechanical systems is the human body itself where the synovial joints play an essential role during motion. In this thesis, we study the mechanism and functions of synovial joints by applying the well known theories in lubrication mechanics. Such studies fall into the general area of a new science called lubrication-biomechanics or biotribology. In fact, bio-tribology may be defined as the science of lubrication, friction and wear of a biomechanical system involving two surfaces in relative motion and separated by a very thin fluid film, Dowson and Wright [1973] . In this thesis, the emphasis has been given only to those aspects of synovial joints which can be investigated on the basis of hydrodynamic lubrication theory.

The investigations presented in this thesis give us a better understanding of joint-mechanism which would help in dealing with the problems of replacement of diseased joint, Wilson [1967], McKee [1967], arthroplasty of joints using foreign materials, Scales [1967] and in curing different kinds of rheumatisms. Since, the synovial joints are more complex and novel in nature, the study described here can also be used in studying the behaviour of equivalent mechanical joints, which at present may not be commonly used. Further, on the basis of this study, new bearings can be designed and constructed for use in modern mechanical systems.

1.2 SYNOVIAL JOINTS

A synovial joint may be described as a weight bearing system consisting of two mating bones with tangential or normal motion. The bone ends which are usually globular in appearance are covered with a soft sponge like material, called articular cartilage. The space between these cartilaginous extremities of the bones, known as joint cavity, is filled with a shear dependent fluid, called synovial fluid. The whole system is surrounded by a fibrous capsule which consists of a tough fibrous sheath of connective tissue. The integrity and stability of the joint in the capsule, under different conditions, are maintained by various ligaments. The general physical configuration of a synovial joint (knee or hip) is shown in fig. 1.1.

In a knee joint (fig. 1.2-a) the femur and tibia, two major bones of the leg undergo relative motion during body movements but the lateral bone, the fibula, normally does not take part in the articulating motion, Engine and Korde [1974] . It is the lower end of the femur, consisting of medial and lateral epicondyles and the upper end of the tibia, consisting of medial and lateral plateaus that are covered with the articulating cartilage. Steindler [1955] suggested that because of the obliquity of the femur axis more load is supported by the lateral condyle than medial one.

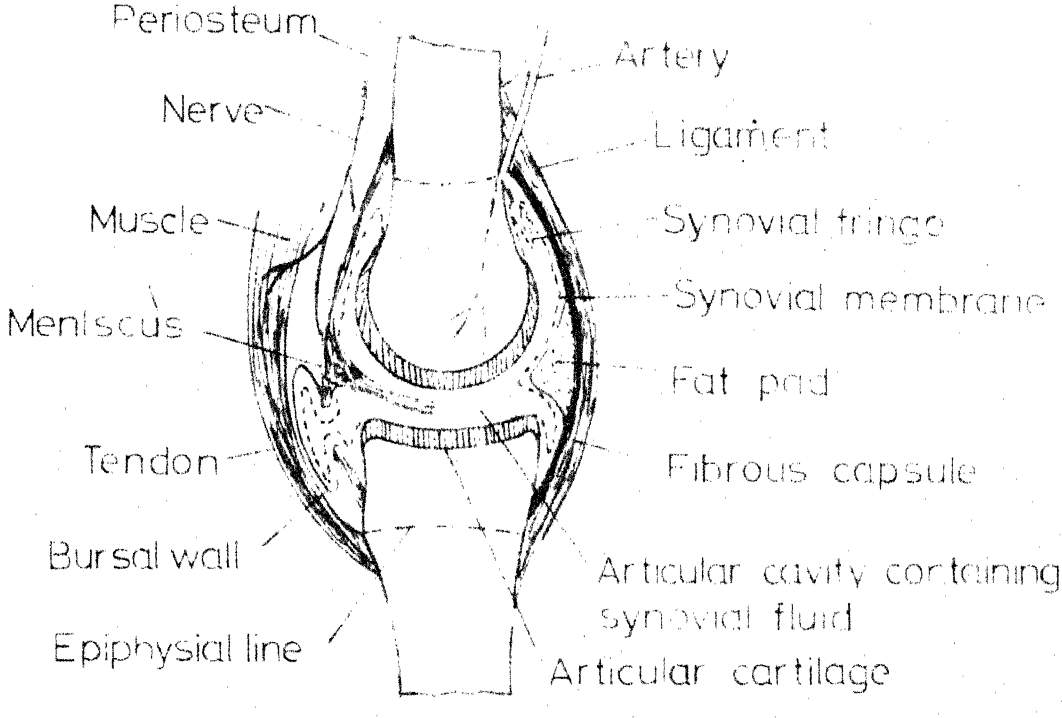

Fig. 1.1 Synovial joint

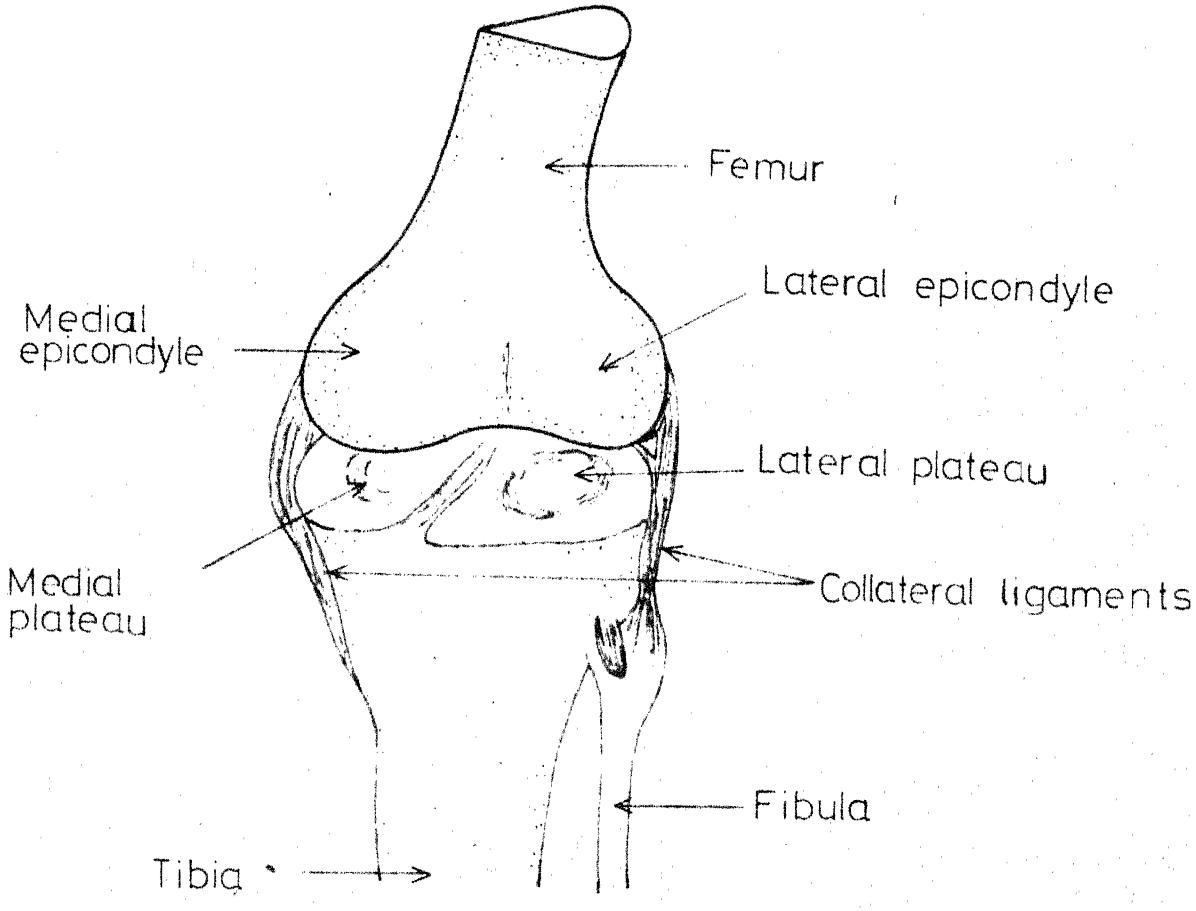

Fig. 1.2a. Knee joint.

In a hip, a ball and socket joint, the head of the femur forms the ball part of the joint and the acetabulum of the pelvis is the socket. The structure and stability of the joint are maintained by the congruence of the spherical femoral head within the acetabular cup and by various ligaments attached externally. The physical situation of a hip joint is shown in fig. 1.2-b.

The synovial joints have high degree of geometrical conformity between their surfaces. Geometrically, the hip joint can be represented by spherical surfaces while the knee joint by cylindrical surfaces. The radii of these surfaces vary from 2 to 100 cms.

The sliding speed in the joint varies from 0 to 10 cm/sec. The load support area is large in the case of a hip joint than a knee joint (4.7 sq.cm), Dowson [1967] . The structure of the joint is such that it can support load as high as four times the body weight by keeping the coefficient of friction as low as 10^{-2}, Paul [1967] , Morrison [1970] .

As the behaviour of the synovial joint is mainly governed by the characteristics of articular cartilage and synovial fluid, in the following, we describe their properties in detail, Wright et.al. [1974] , MacConaill [1967] .

Articular Cartilage :

The physical and chemical properties of the articular cartilage have been extensively studied by medical scientists

In a hip, a ball and socket joint, the head of the femur forms the ball part of the joint and the acetabulum of the pelvis is the socket. The structure and stability of the joint are maintained by the congruence of the spherical femoral head within the acetabular cup and by various ligaments attached externally. The physical situation of a hip joint is shown in fig. 1.2-b.

The synovial joints have high degree of geometrical conformity between their surfaces. Geometrically, the hip joint can be represented by spherical surfaces while the knee joint by cylindrical surfaces. The radii of these surfaces vary from 2 to 100 cms.

The sliding speed in the joint varies from 0 to 10 cm/sec. The load support area is large in the case of a hip joint than a knee joint (4.7 sq.cm), Dowson [1967] . The structure of the joint is such that it can support load as high as four times the body weight by keeping the coefficient of friction as low as 10^{-2}, Paul [1967] , Morrison [1970] .

As the behaviour of the synovial joint is mainly governed by the characteristics of articular cartilage and synovial fluid, in the following, we describe their properties in detail, Wright et.al. [1974] , MacConaill [1967] .

Articular Cartilage :

The physical and chemical properties of the articular cartilage have been extensively studied by medical scientists

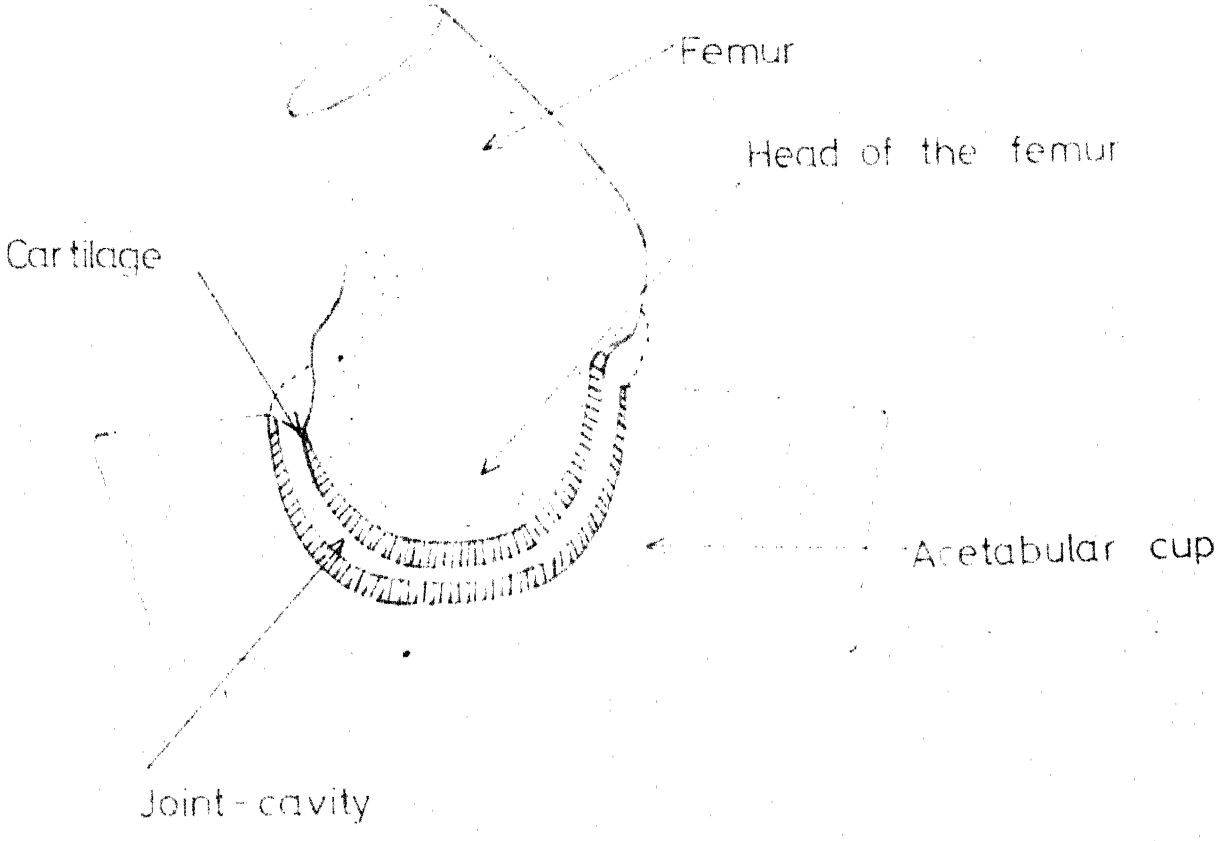

Fig. 1.2-b. Hip joint.

as well as engineers, Edwards [1967] , Mow [1969] , Walker et.al. [1968] , Mow et.al.[1974] . The articular cartilage is a soft glistening tissue with thickness varying between 1 to 7 mm. It consists of cells, the chondrocytes, embedded in a non-homogeneous, poroelastic matrix of collagen fibrils, Edwards [1967] . Sokoloff [1966] , Edwards [1967] have studied the elastic behaviour of the cartilage, which is due to the interaction of collagen fibrils and sulfated proteins with water like liquid present in the cartilage matrix, Wright et.al. [1974] . The Young's modulus of the cartilage has been found to be in the range $10^8 - 10^6$ dyne/cm^2 , McCutchen [1962-b] . The cartilage is slightly permeable and its permeability varies with the cartilage thickness and hydrostatic pressure, McCutchen [1962-b] . Its permeability is of the order 4.3×10^{-13} cm^4 dyne^{-1} sec^{-1} and the pore diameter is of the order 6×10^{-7} cm.

Clarke [1971-a] has made the scanning electron microscope study of articular cartilage and has pointed out that it is a layered medium (fig. 1.3), Meachim and Roy [1969] , Davies et.al. [1962] , Mittal and Millington [1971] . The upper layer of the cartilage, known as superficial tangential zone, consists of randomly woven collagen fiber bundles, $5-20 \times 10^{-7}$ cm in diameter, running parallel to the cartilage surface. The thickness of this sheet varies from 1µm to 20µm. The cells in this region are different from those in deeper zones and are of elliptic shape

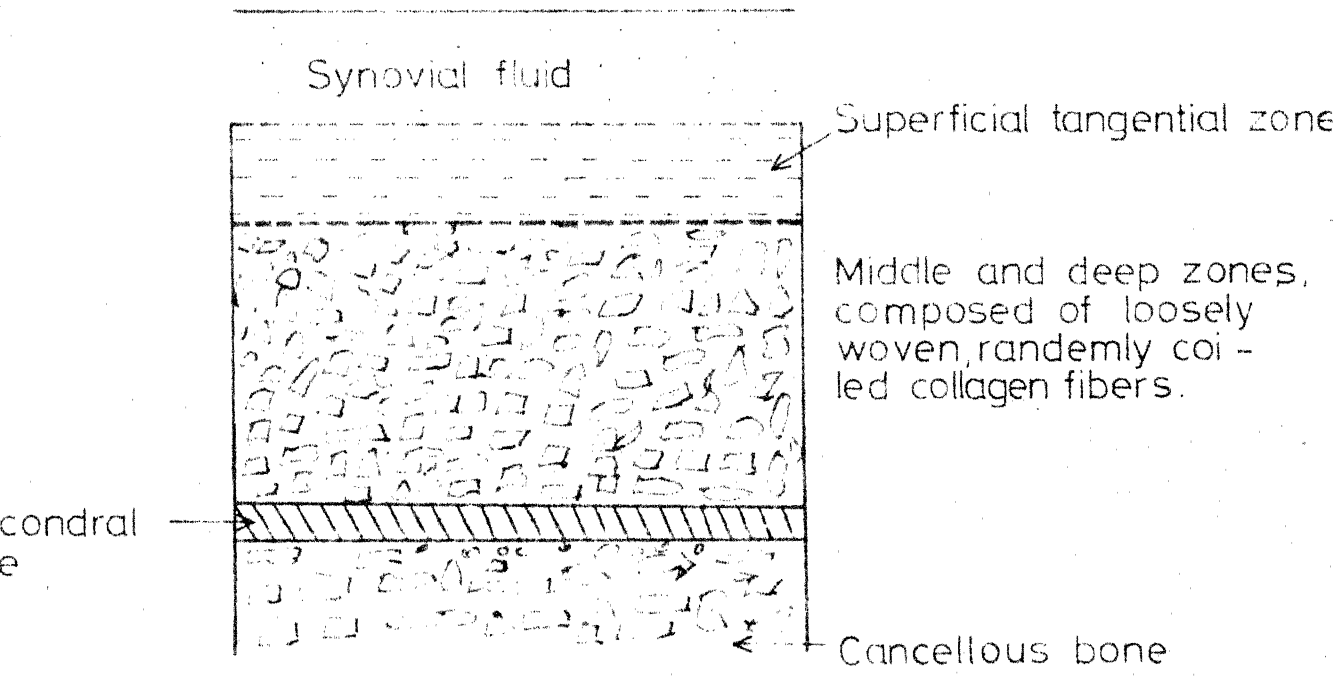

Fig 1.3 Representation of ultrastructural characteristics of the cartilage.

with long axes parallel to the articulating surfaces, Weiss et.al. [1968].

The surface roughness of the cartilage has been studied by Walker et.al. [1968] and it has been pointed out that the surfaces are wavy with a regular periodicity of 20-50 μm and amplitude of 2-5 μm. The existance of waviness of the surfaces has also been observed by Gardner and McGillivary [1971] and Clarke [1971-a].

Below the superficial tangential zone, there lie the middle and deep zones which are composed of more randomly oriented collagen fibrils, whose diameter ranges 30-5000 $\times 10^{-7}$ cm. In the deep layer of the cartilage, collagen fibers seem to have radial orientation, Mow et.al. [1974].

The upper cartilage zone is filled with (about 70% by weight) water like fluid, which could be described as 'dialysate phase of synovial fluid'. The collagen fibrils which surround the tissue cells, represent 47-66% of the dry weight, Matthews [1952], and provide strength to the tissue. The rest of the dry weight composition is mainly chondroitin sulfate which regulates the elasticity of the cartilage, Linn and Sokoloff [1965].

From the physico-chemical points of view, the cartilage structure can be regarded as a gel consisting of a liquid medium with solid colloidal particles dispersed in it. The colloidal

structure of the cartilage is helpful in accounting various mechanical properties such as viscoelasticity, Linn and Sokoloff [1965] , tensile strength and resistance to compression etc., Edwards [1967] .

Synovial Fluid :

The properties of synovial fluid have been studied by Davies [1966, 1967] , MacConaill [1966] , Walker et.al [1969] and surveyed by Mow [1969] and Wright et.al. [1974] . Synovial fluid is a clear or yellowish dialysate of blood plasma with the addition of a non sulfated mucopolysaccharide, known as hyaluronic acid. In a normal joint the concentration of the hyaluronic acid is 3.5 mg/g, Davies [1967] , Mow [1969] . The hyaluronic acid is a straight long chain polymer compound with molecular weight 500,000 and molecular length of the order $5 \times 10^{-5} - 10^{-4}$ cm, Dowson [1967] . It may be noted that the acid molecules, normally, can not pass through the cartilage pores because of their larger dimensions.

The important physical characteristic of the synovial fluid is its viscosity which depends upon the concentration of the hyaluronic acid molecules in it, Dintenfass [1963, 1966] , Davies [1967] . It also exhibits thixotropic and non-Newtonian pseudoplastic behaviour, Mow [1969] . Its viscosity ranges from 100 P at 10^{-2} sec^{-1} shear rate to 10 CP at 100 sec^{-1}, Dintenfass [1966]. Ogston and Staneir [1953] and Negami [1964] have also suggested the viscoelastic behaviour of the synovial fluid.

The viscosity variation with respect to shear rate in the case of synovial fluid has been shown in fig. 1.4. It can be seen that it decreases as the shear-rate increases, showing a pseudo-plastic behaviour. In the present study, included in this thesis, we have assumed that the behaviour of the synovial fluid may be represented by a pseudoplastic power law model whose stress-strain relation is as follows, Bird et.al. [1960] :

$$\tau_{ij} = m \left| \sqrt{e_{ij}\, e_{ji}} \right|^{n-1} e_{ij} \qquad (1.1)$$

$$i, j = 1, 2, 3$$

where τ_{ij} is the stress tensor, e_{ij} is the rate of deformation tensor, m is the consistency index and n is the flow behaviour index.

In one dimensional case equation (1.1) can be simplified as follows:

$$\tau = m \left| \frac{\partial u}{\partial y} \right|^{n-1} \frac{\partial u}{\partial y} \qquad (1.2)$$

where τ is the shear stress and $\frac{\partial u}{\partial y}$ is the shear rate. Comparing equation (1.2) with the usual Newtonian model, the viscosity μ can be written as follows:

$$\mu = m \left| \frac{\partial u}{\partial y} \right|^{n-1} \qquad (1.3)$$

or

$$\ln \mu = \ln m - (1-n) \ln \left| \frac{\partial u}{\partial y} \right| \qquad (1.4)$$

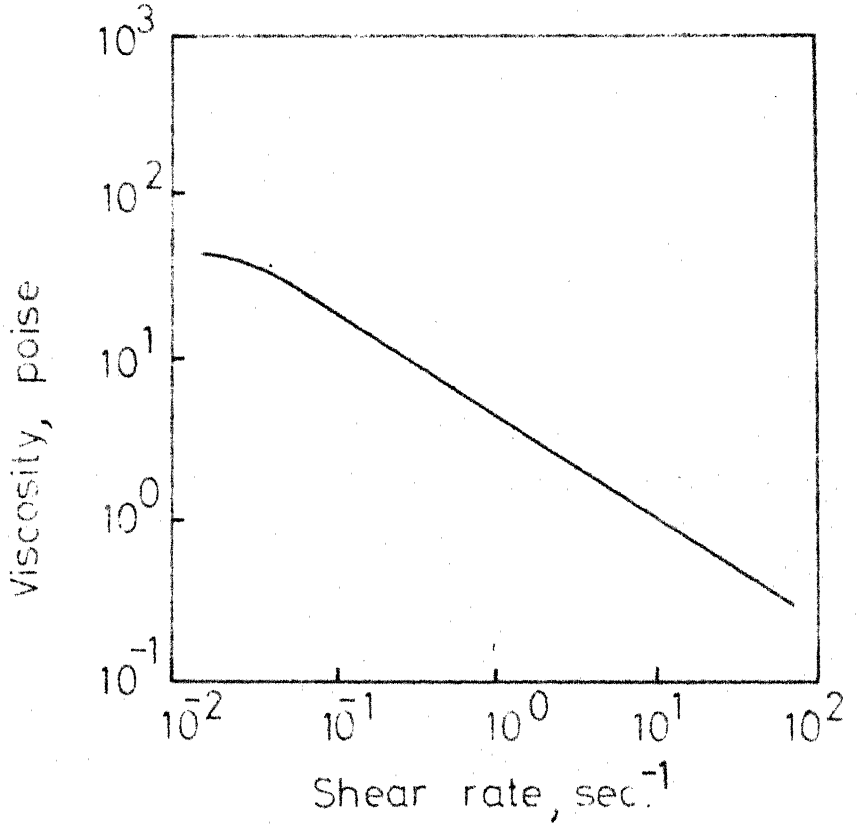

Fig. 1.4 Variation of viscosity with shear rate. (logarithmic representation)

These equations clearly show that for $n < 1$, the viscosity of the fluid decreases as shear-rate increases showing a pseudoplastic behaviour. By choosing $m \simeq 4.5$ dyne sec^n/cm^2, $n \simeq .37$, the graph corresponding to equation (1.4) can be approximately matched with the graph of fig. 1.4, and thus indicating that the choice of pseudoplastic power law model for the synovial fluid may be a desirable one.

Diseased Joint:

The properties of the components of synovial joint, just described, are for a normal joint. These characteristics show marked variations in the case of diseased or damaged joint. In a rheumatoid arthritic patient, the synovial fluid looses its non-Newtonian behaviour, Bloch and Dintenfass [1963]. Burch et.al. [1960] indicated that the concentration of hyaluronic acid in the synovial fluid decreases for a diseased joint. He also pointed out that the cartilage is affected at the sites of greatest pressure and becomes rough, frayed, blistered and cracked. For the old joints, the cartilage becomes softer, less resilient and may even wear out in certain cases. The hyaluronic acid molecules have a lower molecular weight for a rheumatoid joint. In such a case, the size of the cartilage pores becomeslarger, and hyaluronic molecules can pass through them. An injury can also cause an abnormality in the joint configuration and can effect the forces acting on the joint, Engine and Korde [1974] .

1.3 JOINT MECHANISM

In recent years, different modes of joint mechanism have been proposed on the basis of well known lubrication theories used in bearing systems. These theories are as follows, Dowson [1967] :

(i) Hydrodynamic/Hydrostatic lubrication.

(ii) Boundary lubrication.

(iii) Mixed lubrication.

(iv) Elastohydrodynamic lubrication.

The process of hydrodynamic lubrication, occuring between two relatively moving surfaces which are separated by a fluid film, is mainly determined by the viscous property of the lubricant and the dimensions of the fluid film, (10^{-4} - 10^{-3} cm), fig. 1.5-a. Here the surface roughness is much smaller than the fluid film thickness. The pressure in the fluid film is generated because of the relative motion of the surfaces and wedge action. When the surfaces are not moving and the pressure is generated because of external pumping, the term hydrostatic lubrication is used.

Boundary lubrication between two surfaces exists when the separation of bearing surfaces is of molecular dimensions (10^{-7} - 10^{-6} cm, fig. 1.5-d). The frictional behaviour of the system is determined by molecular properties of the lubricant

1.3 JOINT MECHANISM

In recent years, different modes of joint mechanism have been proposed on the basis of well known lubrication theories used in bearing systems. These theories are as follows, Dowson [1967] :

(i) Hydrodynamic/Hydrostatic lubrication.

(ii) Boundary lubrication.

(iii) Mixed lubrication.

(iv) Elastohydrodynamic lubrication.

The process of hydrodynamic lubrication, occuring between two relatively moving surfaces which are separated by a fluid film, is mainly determined by the viscous property of the lubricant and the dimensions of the fluid film, (10^{-4} - 10^{-3} cm), fig. 1.5-a. Here the surface roughness is much smaller than the fluid film thickness. The pressure in the fluid film is generated because of the relative motion of the surfaces and wedge action. When the surfaces are not moving and the pressure is generated because of external pumping, the term hydrostatic lubrication is used.

Boundary lubrication between two surfaces exists when the separation of bearing surfaces is of molecular dimensions (10^{-7} - 10^{-6} cm, fig. 1.5-d). The frictional behaviour of the system is determined by molecular properties of the lubricant

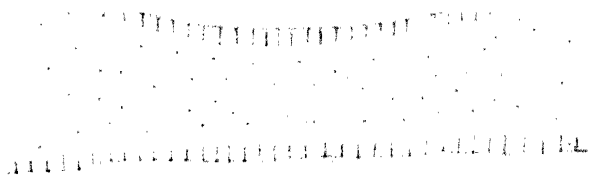

(a) Hydrodynamic lubrication, $h \simeq 10^{-4} - 10^{-3}$ cm.

(b) Elastohydrodynamic lubrication, $h \simeq 10^{-5} - 10^{-4}$ cm.

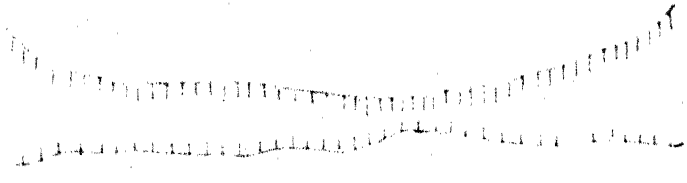

(c) Mixed lubrication, $h \simeq 10^{-5} - 10^{-6}$ cm

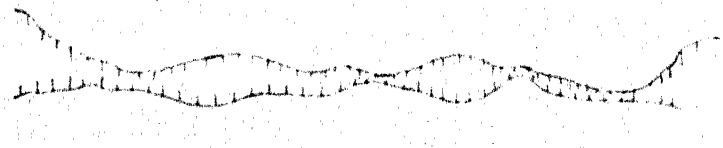

(d) Boundary lubrication

Fig. 1.5 Lubrication regimes

and the topography of the surface. The viscosity of the lubricant does not play any part in the process of boundary lubrication, Dowson [1967].

When the lubrication between the two surfaces is determined both by the viscosity of the lubricant and molecular structure of the polar compound, the process is known as mixed lubrication. The range of film thickness in this case varies between 10^{-6} and 10^{-5} cm (fig. 1.5-b).

Elastohydrodynamic lubrication is a hydrodynamic process in which fluid film pressure causes elastic deformation of bearing surfaces, which in turn modifies the pressure in the film region. The pressure variation can cause substantial changes in the film-thickness and fluid viscosity. The elastohydrodynamic action maintains a fluid film even under conditions of heavy loading (fig. 1.5-c).

Keeping these theories in view, efforts have been made to explain the low friction coefficient in the joint by considering the characteristics of its various components. First attempt in this direction was made by MacConaill [1932]. He proposed that the "lubrication mechanism in synovial joints is similar to hydrodynamic bearings and is due to the formation of wedge shaped film between the cartilage surfaces". However, Charney [1959] disputed the idea of hydrodynamic lubrication, "firstly

because this mode of lubrication is not suitable for reciprocating motion (which the joint movements certainly have); and secondly, he doubted the existance of fluid film between slow moving surfaces under highly loaded conditions". Charney observed that "the friction coefficient remains constant for all speeds of the movements and hence it must be a case of boundary lubrication". He explained that "the molecules of the hyaluronic acid have chemical affinity for the cartilage surfaces and do not break away even under high loading. Thus, a film (proportional to molecular size) is maintained to avoid actual contact of the cartilage surfaces".

Both MacConaill and Charney did not take note of the properties of the cartilage, such as porosity and elasticity, in their theories. McCutchen [1959] was first to account the porous behaviour of the cartilage in explaining the mechanism of the joints. In his view "cartilage is a weeping bearing and load is carried by the hydrostatic pressure of the fluid which cartilage weeps under loading". However, if "the squeezing is maintained indefinitely, the liquid content of the porous cartilage would be expelled and there would be an increase in friction coefficient". He explained that "the wringing out of water from the porous matrix follows a longer and difficult path, while resoaking is easy",McCutchen [1962-a] . This concept is known as "weeping lubrication" and has been supported recently by Mow and Ling [1969]and Radin et.al. [1970], [1972] . McCutchen [1966, 1967] further suggested that the weeping lubrication is

not the sum total of the joint lubrication but it is accompanied by boundary and osmotic lubrication.

Keeping in view the elastic nature of the cartilage, Dintenfass [1963] and Tanner [1966] suggested that both synovial fluid and cartilage play an important role in the joint lubrication. Dintenfass put forward the concept of elastohydrodynamic lubrication and concluded that the lateral deformation of the cartilage is important in generating the pressure in the film. He also considered the macromolecular structure of the synovia and stated that the joint lubrication depends upon the thixotropic and elastic nature of the synovial fluid. Tanner [1966] supported the concept of elastohydrodynamic lubrication.

Dowson [1967] also supported the existance of elastohydrodynamic conditions in the synovial joints during normal body movement such as walking and pointed out that"under severe conditions, such as jumping, boundary lubrication may also prevail. But under conditions of little or no movement, the joints function as elastohydrodynamic squeeze films". Fein [1967] studied the elastic effects in joints under squeeze film conditions.

Walker et.al. [1968] used the results of cartilage surface analysis to introduce a new concept of lubrication which they termed as 'Boosted lubrication'. The mechanism of boosted lubrication suggests that "when two cartilage surfaces are

pressed against each other nominal contact areas would be formed due to roughness waves of the cartilages. The synovial fluid is trapped in these nominal areas and the trapped pool of fluid will contain high concentration of hyaluronic acid molecules, as water and other low molecular substances will diffuse through the cartilage pores". This action of entrapment and enrichment is important in the load bearing phase of the joint. The increase in hyaluronate molecule concentration enables the joint to support more load, Dowson et.al. [1970].

A review of the above mentioned theories has been presented by Mow [1969] and, Radin and Paul [1972] . Mow pointed out that the rheological behaviour of synovial fluid and the cartilage should also be considered to explain the joint mechanism. Radin and Paul [1972] presented a consolidated view for the joint mechanism and suggested that "the effect of hyaluronate in cartilage to cartilage lubrication is very much limited and the term boosted lubrication seems to be a poor choice to describe the phenomena". It has been suggested that the joint mechanism is a combination of various lubricating mechanisms at different stages. "Boundary lubrication is favoured at low shear rate, because of the presence of a boundary layer of glycoprotein molecules at the cartilage surface. However, at high loads, these molecules are squeezed out and squeeze film action seems to be appropriate". In addition to it, "weeping action seems

probable during motion just in advance of the area of impending contacts".

Recently, Ling [1974], presented a new model for the cartilage, accounting for its nonlinearity and poroelastic nature. His model suggests that "the cartilage is composite which can imbibe and exudate and offers resistance in tension and compression". Thus, using Biot's theory of consolidation, he showed that "the theories of weeping and boosted lubrication are not exclusive to each other. The two modes operate in the beginning, but weeping lubrication becomes important after some time". Higginson and Norman, [1974] have also studied the effects of poroelasticity of the cartilage on the functioning of human joints.

1.4 CONCLUSIONS AND SUMMARY

In view of the above, it can be noted that the functioning of the synovial joints depends upon the following:

(i) Articular Cartilage: colloidal nature of its matrix, its porous and elastic behaviour, pore size, surface roughness, its non-linearity etc.

(ii) Synovial fluid: its viscosity, its non Newtonian character, concentration of hyaluronic acid in the fluid, the size and structure of the acid molecules; its interaction with cartilage surfaces etc.

(iii) Dynamics of the fluid flow: Laminar or turbulant, diffusive flow, reciprocating or normal movements, Darcy's flow in the porous matrix etc.

(iv) Joint geometry and position: Its shape, size and conformity, curvature of the joint surfaces, its position in the body etc.

It may be summarized here that in standing position the mechanism of synovial joint is mainly governed by a combination of hydrodynamic, elastohydrodynamic or poro-elastic squeeze films and weeping lubrication. However, when the standing position is prolonged or in the case of jumping, the possibility of taking over boundary lubrication does exist.

In the case of usual walking cycle or conditions of running, the mechanism is similar to poroelastic rollers under reciprocating motion coupled with the squeeze film action.

It may be further noted that the lubrication behaviour of the knee joint is enhanced due to the increase in the hyaluronate concentration, affinity of hyaluronic acid molecules with cartilage surfaces, pseudoplastic behaviour of synovial fluid, cartilage porosity, elasticity and its surface roughness.

In this thesis which consists of eight chapters we make a theoretical study of the following aspects in the case of synovial joints from the point of hydrodynamic lubrication.

(i) Effects of pseudoplastic behaviour of the synovial fluid.

(ii) Effects of cartilage surface roughness.

(iii) Effects of elastic nature of the cartilage matrix.

(iv) Effects of porous nature of the cartilage.

(v) Effects of change in concentration of the hyaluronic acid molecules in the synovial fluid.

Chapter I gives the general introduction, highlighting the structure of the synovial joint and the characteristics of its components. It is suggested that the synovial fluid may be represented by a pseudoplastic power law model. The various theories, proposed for joint mechanism, have also been described.

In chapter II, we have made the mathematical formulation of the synovial joint system by taking into account the pseudo-plastic behaviour of the synovial fluid, the viscosity variation with the concentration of hyaluronic acid molecules, the porosity of the cartilage, etc. The basic equation governing the pressure in the fluid film has been derived by considering synovia as a power law fluid. This equation, in fact, is a generalized form of Reynolds equation for power law lubricants.

The equation governing the pressure in the cartilage matrix has also been obtained in an approximate form. These two equations, which are non-linearly related, form the basis of the entire study under different physical conditions.

In chapter III, the effects of cartilage surface roughness and pseudoplastic behaviour of the synovia on the mechanism of knee and hip joints have been investigated under standing positions. The load bearing regions in cases of knee and hip joints have been approximated by two rectangular and circular parallel plates models respectively. It has been pointed out that the time of approach increases due to cartilage surface roughness and due to the pseudoplastic behaviour of the synovial fluid when considered with respect to the film-thickness function. Further, it is also noted that the boosting effect enhances the behaviour of the joint in presence of cartilage surface roughness.

Chapter IV describes the combined effects of elasticity of the cartilage matrix and pseudoplastic behaviour of the synovial fluid on the mechanism of joints. It has been pointed out that the time of squeezing increases due to the elastic nature of the cartilage. Further, it is also noted that elasticity of the cartilage and pseudoplastic behaviour of the synovia enhance the hydrodynamic conditions in the joint. It is suggested that synovial joints function as elastohydrodynamic non-Newtonian squeeze films.

Chapter V deals with the effects of porosity of the cartilage on the mechanism of joints by taking into account the pseudoplastic behaviour of the synovial fluid. It is shown that the load capacity and time of approach of the joints

increase with the permeability of the cartilage matrix in the normal direction but decrease with the permeability in the direction parallel to the cartilage surface. Thus, it is indicated that for better performance of the joint function, the permeability of the cartilage in the normal direction should be greater than its value in the tangential direction. In fact, this situation does exist in the case of synovial joint.

In chapter VI, the effects of sliding of the joint surfaces, on the mechanism have been studied by considering the pseudoplastic behaviour of the synovial fluid. Due to elasticity of the cartilage the loaded region in the joint is assumed to be approximated by a linear wedge. This situation is applied under walking or running conditions. It is shown that the coefficient of friction depends upon the conformity of the joint and it decreases as conformity increases.

In chapter VII, the effects of cartilage porosity on the joint mechanism have been studied by considering the Newtonian behaviour of the synovial fluid whose viscosity varies with the concentration of the hyaluronic acid molecules in the fluid. It has been found that the load capacity and time of approach of joints increase as the concentration of hyaluronic acid molecules increases due to their consolidation and trapping in the synovial film. The effects of porosity are same as mentioned in Chapter V.

Chapter VIII describes the behaviour of diseased joints such as in the case of arthrities. It is found that the load capacity and time of approach of this joint decrease as the joint becomes more and more diseased.

CHAPTER - II

MATHEMATICAL MODEL FOR THE MECHANISM OF SYNOVIAL JOINTS

2.1 INTRODUCTION

As pointed out in chapter I, the well known concepts of lubrication mechanics can be applied to equivalent biological situations such as synovial joints and very useful and interesting results may be obtained. One of the important aspects of the study dealt here, is to make a realistic and simplified mathematical model of the system and then to find its solution in a tangible form which could be utilised by medical scientists and others. Since 1932, it has been realized that the human and mechanical joints function almost on the similar principles. However the human joints give better performance due to their complexity and novelty in character. In fact, the joints in human body are excellent bearings provided by nature so that the movements of various body parts can be effected by minimum loss of energy. It may be conjectured that joints in nature might be functioning under the most optimal conditions.

In this chapter, an attempt has been made to present an idealized mathematical model governing the behaviour of the joint from the point of view of hydrodynamic lubrication theory. The emphasis has been given on the poroelastic behaviour of the cartilage and the viscous property of synovial fluid which is due to the suspension of

proteins and hyaluronic acid molecules.

It is well known that when an additive is added to a solution to form a suspension, the viscosity of the suspension increases as the concentration of the additive increases, Einstein [1906] , Rutgers [1962], Mow [1969] , Shukla [1972] . Keeping this in view, the behaviour of synovial fluid can be considered in two ways; firstly as a Newtonian fluid whose viscosity varies with the concentration of hyaluronate molecules, secondly as a non-Newtonian fluid with pseudoplastic behaviour. It is assumed here that the pseudoplastic behaviour of synovial fluid may be represented by a power law model as pointed in chapter I, Bird et. al.[1960] .

2.2 EQUATION FOR PRESSURE IN THE SYNOVIAL FLUID FILM

The physical structure of the synovial joint has already been described in chapter I and shown in fig. 1.1. It has also been pointed out there that geometrically the joints may be represented as two cylindrical or spherical surfaces. Since the cartilage is porous and saturated with a liquid, the system of synovial joint may be considered as two curved surfaces with porous liners lubricated by synovial fluid. The simplified physical configuration of the synovial joints is shown in fig. 2.1. Here H denotes the average thickness of the cartilage which includes both superficial tangential zone and middle deep zones and H_s denotes the thickness of superficial tangential zone only. The surface velocities of the cylindrical surfaces, in

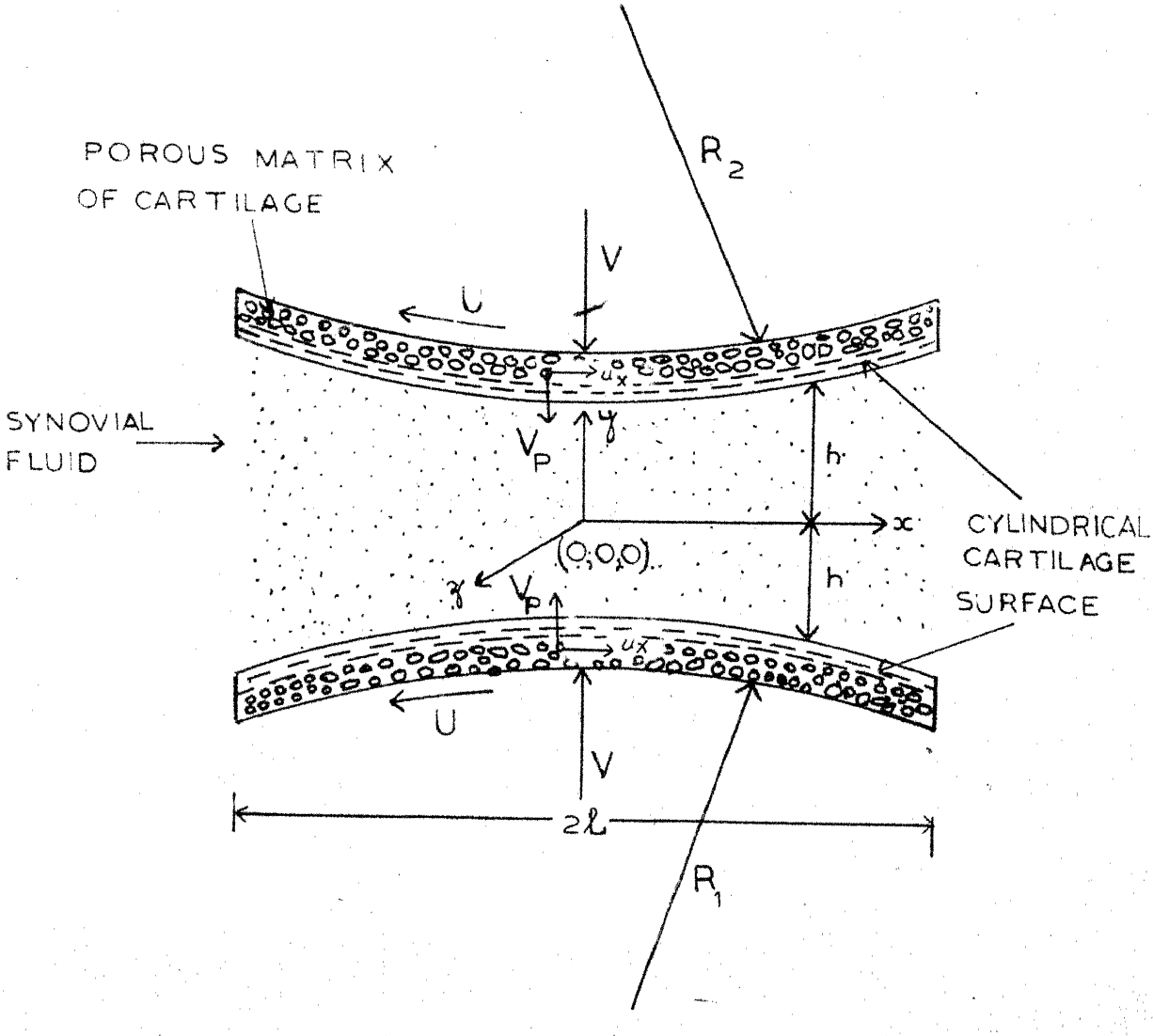

FIG. 2.1 THE GEOMETRICAL MODEL OF THE KNEE JOINT.

contact with the synovial film of thickness 2h, are denoted by U and V which are assumed to be acting in the directions shown in the figure, such that the behaviour of the system is symmetrical during motion.

Under the well known assumptions of lubrication theory, Pinkus and Sternlicht [1961], Dowson [1962] and using power law model for the synovial fluid, Bird et. al. [1960], Kapur [1963], Shukla [1963, 1964,a,b], Isa [1974], the basic equations governing the motion of synovial fluid in the joint cavity can be written as follows :

$$\frac{\partial p}{\partial x} = \frac{\partial}{\partial y}\left\{ m \left| \sqrt{\left(\frac{\partial u}{\partial y}\right)^2 + \left(\frac{\partial w}{\partial y}\right)^2} \right|^{n-1} \frac{\partial u}{\partial y} \right\} \qquad (2.1)$$

$$\frac{\partial p}{\partial z} = \frac{\partial}{\partial y}\left\{ m \left| \sqrt{\left(\frac{\partial u}{\partial y}\right)^2 + \left(\frac{\partial w}{\partial y}\right)^2} \right|^{n-1} \frac{\partial w}{\partial y} \right\} \qquad (2.2)$$

where $m = m(x,y,z)$ is the consistency index and n is the flow behaviour index assumed to be constant.

The equation of continuity is given by

$$\frac{\partial u}{\partial x} + \frac{\partial v}{\partial y} + \frac{\partial w}{\partial z} = 0 \qquad (2.3)$$

where u,v, w are the velocity components of the fluid in the region $-h \leq y \leq h$.

As the system is symmetrical with x-axis, it is sufficient to consider the system in the region $y \geq 0$, $z \geq 0$ for determination of velocities. Keeping the symmetry in view,the boundary conditions for u and w can be written as follows :

$$u = -U \qquad \text{at } y = h$$
$$\frac{\partial u}{\partial y} = 0 \qquad \text{at } y = 0 \tag{2.4}$$

$$w = 0 \qquad \text{at } y = h$$
$$\frac{\partial w}{\partial y} = 0 \qquad \text{at } y = 0 \tag{2.5}$$

where 2h is the fluid film thickness and may be a function of x, z.

For $n \neq 1$, equations (2.1) and (2.2) are non-linear and it is not possible to get their solution exactly. However, for $n = 1$, the non-linear term disappears and these equations can be solved exactly. To achieve their solution in the general case ($n \neq 1$), since there is no surface velocity in the z-direction, it may be assumed that

$$|u| \gg |w|$$

and $$\left|\frac{\partial u}{\partial y}\right| \gg \left|\frac{\partial w}{\partial y}\right|$$

Under these assumptions, the equations (2.1) and (2.2) may be simplified to the following form,

$$\frac{\partial p}{\partial x} = \frac{\partial}{\partial y}\left\{m\left|\frac{\partial u}{\partial y}\right|^{n-1}\frac{\partial u}{\partial y}\right\} \tag{2.6}$$

$$\frac{\partial p}{\partial z} = \frac{\partial}{\partial y}\left\{m\left|\frac{\partial u}{\partial y}\right|^{n-1}\frac{\partial w}{\partial y}\right\} \tag{2.7}$$

The equations (2.6) and (2.7) involve absolute value of velocity gradient $\frac{\partial u}{\partial y}$, and it is required to give the appropriate sign to it. For this, we resort to the physical situation of synovial fluid flow

as shown in fig. 2.2, where pressure and velocity profiles are qualitatively drawn. It can be pointed out here that the pressure becomes ambient at the points out side the zone considered and it takes a maximum value at $x = x_1$, $z = 0$ i.e.

$$\frac{\partial p}{\partial x} = 0 \qquad \text{at} \quad x = x_1$$

$$\frac{\partial p}{\partial z} = 0 \qquad \text{at} \quad z = 0 \tag{2.8}$$

The last condition is due to symmetrical pressure in the z-direction.

Thus, in the region $x_1 \leq x \leq \ell$, $z \geq 0$, $\frac{\partial p}{\partial x} \leq 0$, $\frac{\partial p}{\partial z} \leq 0$ and in the region $x_2 \leq x \leq x_1$, $z \geq 0$, $\frac{\partial p}{\partial x} \geq 0$, $\frac{\partial p}{\partial z} \leq 0$.

Keeping this in view, it may be noted that

$\frac{\partial u}{\partial y} \leq 0$ in the region $x_1 \leq x \leq \ell$, $y \geq 0$; and

$\frac{\partial u}{\partial y} \geq 0$ in the region $x_2 \leq x \leq x_1$, $y \geq 0$.

It may be noted here that the problem of generalizing Reynolds equation in two dimensions for power-law fluid has been lying unsolved since the start of non-Newtonian lubrication theory nearly two decades ago. It is because of these physical considerations that we have been able to proceed further.

Thus, from equations (2.6) and (2.7) we have

——— PRESSURE PROFILE

– – – – VELOCITY PROFILE

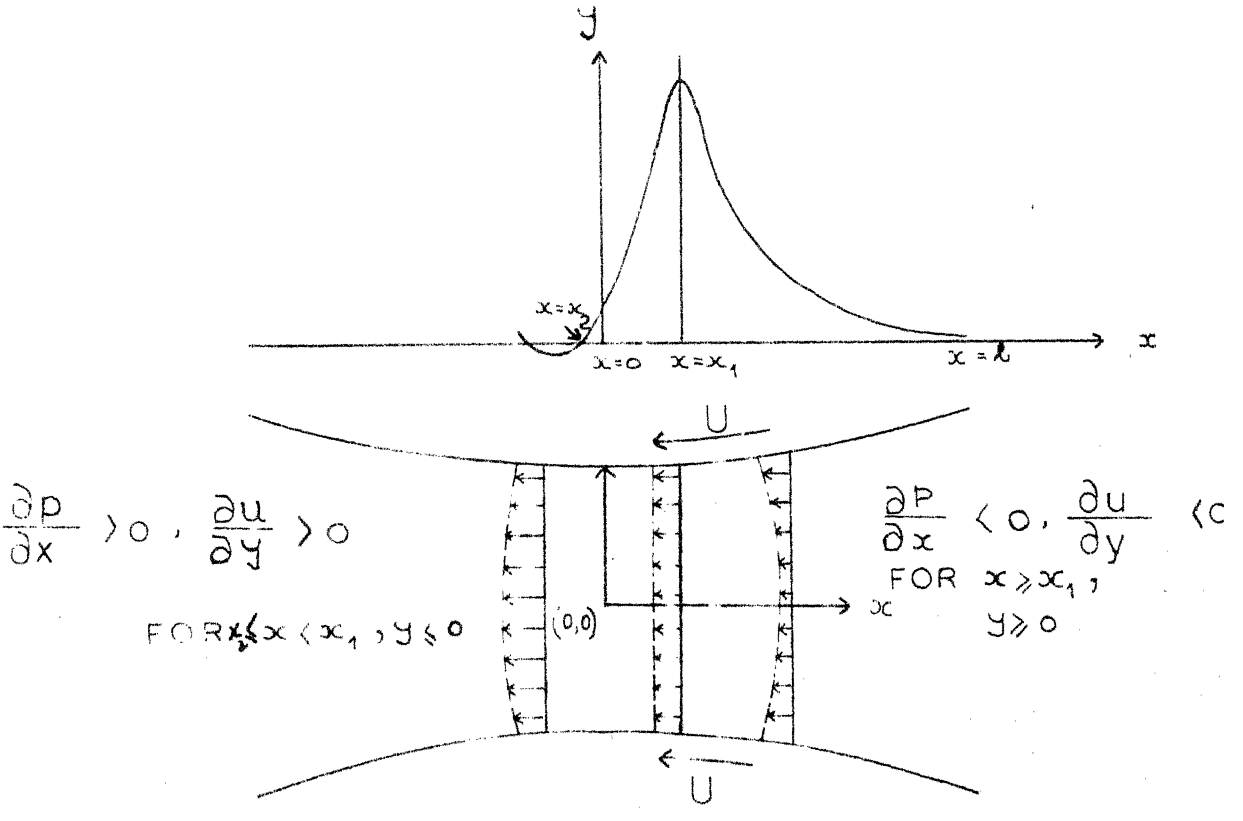

FIG. 2.2 QUALITATIVE PROFILES OF PRESSURE AND VELOCITY.

$$\frac{\partial p}{\partial x} = - \frac{\partial}{\partial y} \{ m \left(- \frac{\partial u}{\partial y}\right)^n \} \tag{2.9}$$

$$\frac{\partial p}{\partial z} = \frac{\partial}{\partial y} \{ m \left(- \frac{\partial u}{\partial y}\right)^{n-1} \frac{\partial w}{\partial y} \} \tag{2.10}$$

in the region $x_1 \leq x \leq \ell$, $y \geq 0$, $z \geq 0$;

$$\frac{\partial p}{\partial x} = \frac{\partial}{\partial y} \{ m \left(\frac{\partial u}{\partial y}\right)^n \} \tag{2.11}$$

$$\frac{\partial p}{\partial z} = \frac{\partial}{\partial y} \{ m \left(\frac{\partial u}{\partial y}\right)^{n-1} \frac{\partial w}{\partial y} \} \tag{2.12}$$

in the region $x_2 \leq x \leq x_1$, $y \geq 0$, $z \geq 0$.

Solving equations(2.9) to (2.12) with the boundary conditions (2.4) and (2.5) in the two regions, we get

$$u = - U - \left(- \frac{\partial p}{\partial x}\right)^{1/n} \int_h^y \left(\frac{y}{m}\right)^{1/n} dy \tag{2.13}$$

$$\frac{\partial u}{\partial y} = - \left(- \frac{\partial p}{\partial x}\right)^{1/n} \left(\frac{y}{m}\right)^{1/n} \tag{2.14}$$

$$w = \left(- \frac{\partial p}{\partial x}\right)^{(1-n)/n} \left(\frac{\partial p}{\partial z}\right) \int_h^y \left(\frac{y}{m}\right)^{1/n} dy \tag{2.15}$$

$$\frac{\partial w}{\partial y} = \left(- \frac{\partial p}{\partial x}\right)^{(1-n)/n} \frac{\partial p}{\partial z} \left(\frac{y}{m}\right)^{1/n} \tag{2.16}$$

in the region $x_1 \leq x \leq \ell$; and

$$u = - U + \left(\frac{\partial p}{\partial x}\right)^{1/n} \int_h^y \left(\frac{y}{m}\right)^{1/n} dy \tag{2.17}$$

$$\frac{\partial u}{\partial y} = \left(\frac{\partial p}{\partial x}\right)^{1/n} \left(\frac{y}{m}\right)^{1/n} \tag{2.18}$$

$$w = \left(\frac{\partial p}{\partial x}\right)^{(1-n)/n} \left(\frac{\partial p}{\partial z}\right) \int_h^y \left(\frac{y}{m}\right)^{1/n} dy \tag{2.19}$$

$$\frac{\partial w}{\partial y} = \left(\frac{\partial p}{\partial x}\right)^{(1-n)/n} \frac{\partial p}{\partial z} \left(\frac{y}{m}\right)^{1/n} \tag{2.20}$$

in the region $x_2 \leq x \leq x_1$.

The flow flux in the x and z directions are defined as

$$Q_x = \int_o^h u \, dy$$

$$Q_z = \int_o^h w \, dy$$

which on using equations (2.13), (2.15), (2.17) and (2.19) give

$$Q_x = - U h + F\left(- \frac{\partial p}{\partial x}\right)^{1/n} \tag{2.21}$$

$$Q_z = - F \left(- \frac{\partial p}{\partial x}\right)^{\frac{1-n}{n}} \frac{\partial p}{\partial z} \tag{2.22}$$

in the region $x_1 \leq x \leq \ell$, and

$$Q_x = - U h - F\left(\frac{\partial p}{\partial x}\right)^{1/n} \tag{2.23}$$

$$Q_z = - F \left(\frac{\partial p}{\partial x}\right)^{\frac{1-n}{n}} \frac{\partial p}{\partial z} \tag{2.24}$$

$$F = \int_0^h y \left(\frac{y}{m}\right)^{1/n} dy \qquad (2.25)$$

Integrating equation of continuity (2.3) with respect to y and using the symmetry conditions $v = v_h$ at $y = h$ and $v = 0$ at $y = 0$, we get

$$-v_h = \left[\frac{\partial}{\partial x}\int_0^h u\, dy + U\frac{\partial h}{\partial x} + \frac{\partial}{\partial z}\int_0^h w\, dy\right] \qquad (2.26)$$

Here, v_h is velocity in the y-direction at $y = h$ and includes the squeeze velocity V, the normal components of the surface velocity U and the velocity of fluid, flowing from the cartilage to the synovial fluid film due to compression of the porous cartilage under loading i.e.

$$v_h = -V - V_p - U\frac{\partial h}{\partial x} \qquad (2.27)$$

where V_p is the velocity of the fluid in the porous matrix to be determined by using Darcy's law.

Now, substituting the respective values of u and w from equations (2.13) , (2.15), (2.17) and (2.19) in equation (2.26); and on simplifying we get the following equations for determining the pressure in the two regions of the synovial fluid film.

$$\frac{\partial}{\partial x}\left\{F\left(-\frac{\partial p}{\partial x}\right)^{1/n}\right\} - \frac{\partial}{\partial z}\left\{F\left(-\frac{\partial p}{\partial x}\right)^{(1-n)/n}\frac{\partial p}{\partial z}\right\} = \qquad (2.28)$$

$$V + V_p + U\frac{\partial h}{\partial x}$$

$x_1 \leq x \leq \ell$,

$$\frac{\partial}{\partial x}\left\{F\left(\frac{\partial p}{\partial x}\right)^{1/n}\right\} + \frac{\partial}{\partial z}\left\{F\left(\frac{\partial p}{\partial x}\right)^{(1-n)/n}\frac{\partial p}{\partial z}\right\} = \qquad (2.29)$$

$$-V - V_p - U\frac{\partial h}{\partial x}$$

$x_2 < x < x_1$

The above equations take into account the squeezing (standing or jumping position) as well as sliding (walking or running position) effects of the joint movements.

These equations may also be seen as a generalized form of Reynolds equation applicable in the case of non-Newtonian power law model lubricant.

To determine the pressure, the following boundary conditions may be used for solving equations (2.28) and (2.29), respectively,

$$\begin{aligned} p &= 0 \quad \text{at } x = \ell \\ \frac{\partial p}{\partial x} &= 0 \quad \text{at } x = x_1 \\ p &= 0 \quad \text{at } z = b/2 \\ \frac{\partial p}{\partial z} &= 0 \quad \text{at } z = 0 \end{aligned} \tag{2.30}$$

for the region $x_1 \leq x \leq \ell$, $z \geq 0$ and,

$$\begin{aligned} \frac{\partial p}{\partial x} &= 0 \quad \text{at } x = x_1 \\ p &= 0 \quad \text{at } x = x_2 \\ p &= 0 \quad \text{at } z = b/2 \\ \frac{\partial p}{\partial z} &= 0 \quad \text{at } z = 0 \end{aligned} \tag{2.31}$$

in the region $x_2 \leq x \leq x_1$, where x_1 is to be determined by using the continuity of pressure.

When there is no or little leakage in the z-direction i.e. $\frac{\partial p}{\partial z} \approx 0$, the equation (2.28) and (2.29) reduces to the following simple form :

$$\frac{\partial}{\partial x}\{F\,(-\frac{\partial p}{\partial x})^{1/n}\} = U\,\frac{\partial h}{\partial x} + V + V_p \qquad (2.32)$$

for $x_1 \leq x \leq \ell$

$$\frac{\partial}{\partial x}\{F\,(\frac{\partial p}{\partial x})^{1/n}\} = -\,U\,\frac{\partial h}{\partial x} - V - V_p \qquad (2.33)$$

for $x_2 \leq x \leq x_1$.

In the case of walking cycle equation governing the pressure in the fluid, can be written as follows [from equations (2.32) and (2.33)],

$$\frac{\partial}{\partial x}\{F\,(-\frac{\partial p}{\partial x})^{1/n}\} = U\,\frac{\partial h}{\partial x} \qquad (x_1 \leq x \leq \ell), \qquad (2.34)$$

$$\frac{\partial}{\partial x}\{F\,(\frac{\partial p}{\partial x})^{1/n}\} = -\,U\,\frac{\partial h}{\partial x} \qquad (x_2 \leq x \leq x_1) \qquad (2.35)$$

However, in the case of standing position ($U = 0$), the two regions become symmetrical and the following equation determining the pressure is applicable,

$$\frac{\partial}{\partial x}[F\,(-\frac{\partial p}{\partial x})^{1/n}] = V + V_p \qquad (2.36)$$

in the region $0 \leq x \leq \ell$.

In the above cases when m is a constant, the function F reduces to,

$$F = \frac{h^{2+1/n}}{m^{1/n}\,(2 + 1/n)} \tag{2.37}$$

2.3 EQUATION FOR PRESSURE IN THE CARTILAGE MATRIX

Many investigators have studied the effects of porosity of bearing surfaces by using Darcy's law in the porous matrix and an appropriate Reynolds equation in the fluid film region, Mori et. al. [1969], Wu [1970], Hsing [1971]. As the cartilage surfaces are also porous, the same methods can be applied to investigate the effects of porosity in synovial joints, Ling [1974]. It has been pointed out by Mow et. al. [1974] that under walking conditions, a typical loading cycle takes approximately one second, Kempson [1968], and for such a short duration the porosity effects may be neglected. In view of this, we consider the effects of porosity in the case of standing position (squeeze film) only, by neglecting curvature and other effects in the model.

The physical situation, representing the flow behaviour in the cartilage matrix under squeeze film conditions is shown in fig.2.3. The equations governing the flow in the porous region ($h \leq y \leq h+H$, $x > 0$) can be written as, Mori et. al. [1964],

$$u_x = -\frac{k_x}{\mu_o}\frac{\partial P}{\partial x} \tag{2.38}$$

and

$$V_p = \frac{k_y}{\mu_o}\frac{P - p}{H_s} \tag{2.39}$$

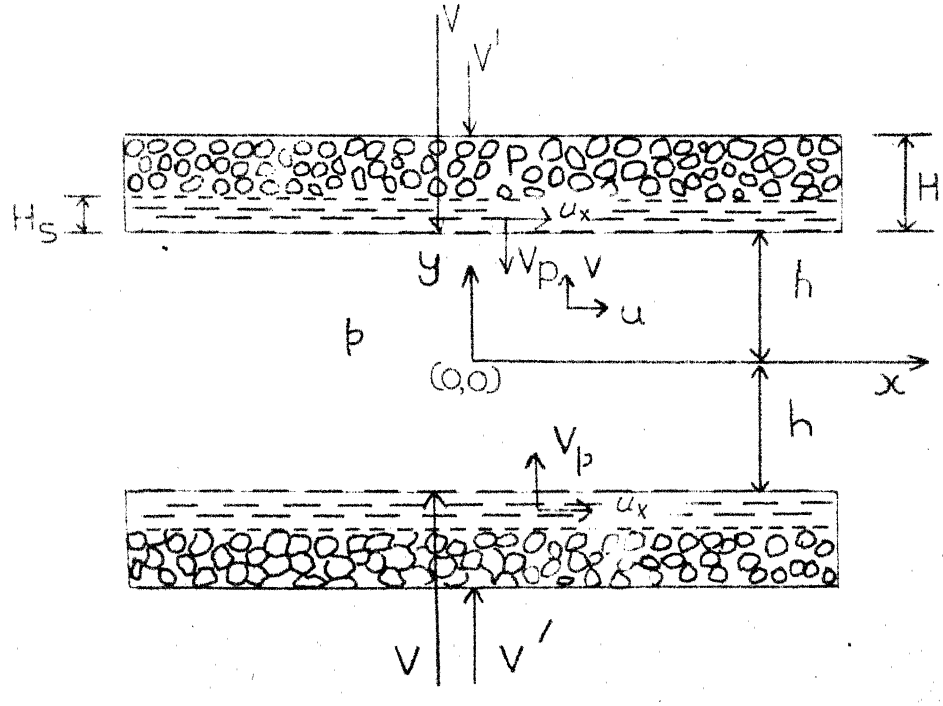

FIG. 2.3 FLOW THROUGH POROUS CARTILAGE IN THE CONTACT ZONE DUE TO LOADING

Here u_x is the average velocity with respect to the cartilage thickness in the x-direction and V_p is the average velocity of the fluid flowing from the porous matrix of cartilage towards the synovial film, P(x) is the average pressure of the fluid in the matrix with respect to the cartilage film-thickness H, H_s is the thickness of the superficial tangential zone, k_x permeability in the x-direction, k_y permeability in the y-direction and μ_o is the viscosity of the fluid present in the cartilage matrix.

Using continuity condition in the porous matrix, we have from equations (2.38) and (2.39)

$$\frac{\partial}{\partial x}\left(-\frac{Hk_x}{\mu_o}\frac{\partial P}{\partial x}\right)+\frac{k_y}{\mu_o}\cdot\frac{P-p}{H_s}=-\frac{\partial H}{\partial t}=V' \qquad (2.40)$$

where, V' is the squeeze velocity of the cartilage surface at y = h+H with respect to the cartilage surface y = h, in the direction of synovial fluid film.

In the case of squeezing for which the equation (2.40) is valid, the boundary conditions for P are,

$$\frac{dP}{dx}=0 \text{ at } x=0$$
$$P=P_o \text{ at } x=\ell \qquad (2.41)$$

where P_o is the pressure generated in the porous matrix due to the compression of the cartilage matrix.

For $k_x \approx 0$, i.e. when there is no flow in the x-direction of the cartilage matrix, the equation (2.40) can be approximated as follows

$$V' = -\frac{\partial H}{\partial t} \approx \frac{k_y}{\mu_o H_s} (P-p) \qquad (2.42)$$

To see the effects of porosity of the cartilage on the joint mechanism, equations (2.36), (2.39) and (2.40) should be solved simultaneously.

2.4 A PARTICULAR CASE

As pointed out earlier, the behaviour of the synovial fluid can also be considered as a Newtonian fluid whose viscosity varies with concentration of hyaluronic acid molecules. In such a case, the equation governing the pressure in the synovial fluid film can be easily written from equation (2.28) or (2.29) as follows, by taking $n = 1$,

$$\frac{\partial}{\partial x}\left(F \frac{\partial p}{\partial x}\right) + \frac{\partial}{\partial z}\left(F \frac{\partial p}{\partial z}\right) = -V - V_p - U \frac{\partial h}{\partial x} \qquad (2.43)$$

where

$$F = \int_o^h \frac{y^2}{\mu} dy \qquad (2.44)$$

and μ is the viscosity of the synovial fluid to be determined as a function of concentration.

To see the effects of porosity, in this case also equation (2.43) should be combined with equation (2.40).

Determination of μ :

To determine the viscosity μ of the synovial fluid as a function of concentration, C, of the hyaluronic acid molecules, it is assumed that μ is linearly related to C, Rutgers [1962] , Negami [1964], Shukla [1972] .

$$\mu = \mu_o (1 + \lambda C) \tag{2.45}$$

where μ_o is the viscosity of the fluid present in the porous matrix of the cartilage and λ is a constant.

The concentration C of the hyaluronate depends upon whether the joint is normal or diseased. It also depends upon the processes such as diffusion, biochemical reaction, consolidation, trapping, etc. during joint movement.

To determine C in the case of a normal joint, it is assumed that the concentration C is determined from the following equation (convection etc. are neglected)

$$D \frac{\partial^2 C}{\partial y^2} + M = 0 \tag{2.46}$$

where D is the diffusion co-efficient and M is the rate of increase of hyaluronate concentration due to consolidation and trapping because of cartilage surface waviness, Walker et. al. [1968] . In the case of a normal joint, since the size of hyaluronic acid molecules is larger than the cartilage pores, no mass transfer at the cartilage

surface takes place. In such a case M may be assumed to be a constant.

Due to symmetry in the system, the following boundary conditions for C are applicable,

$$D \frac{\partial C}{\partial y} = 0 \quad \text{at } y = 0$$
$$C = C_o \quad \text{at } y = h \tag{2.47}$$

where C_o is the concentration at the cartilage surface.

Solving equation (2.46) and using the boundary conditions (2.47), we get

$$C = C_o + \frac{M}{2D} (h^2 - y^2) \tag{2.48}$$

which on combining with equation (2.45) gives the final expression for the viscosity of the synovial fluid in this case,

$$\mu = \mu_o \left[1 + \lambda C_o + \frac{\lambda M}{2D} (h^2 - y^2) \right] \tag{2.49}$$

However, in the case of a diseased joint (if cartilage is diseased or hyaluronic acid molecules in the synovial fluid are being destroyed by bacterial reaction), the concentration is assumed to be given by the following form of diffusion equation

$$D \frac{\partial^2 C}{\partial y^2} - \alpha C = 0 \tag{2.46-a}$$

where $\alpha > 0$ is the rate of decrease in concentration.

The boundary conditions in this case can be written as follows

$$D \frac{\partial C}{\partial y} = 0 \quad \text{at} \quad y = 0$$

$$C = C_d \text{ at } y = h \qquad (2.47\text{-a})$$

where C_d is the concentration at the surface of the diseased cartilage.

Solving equation (2.46-a) and using the conditions (2.47-a), we get the concentration distribution of hyaluronic acid molecules in the case of a diseased joint, as follows :

$$C = C_d \frac{\cosh \gamma y}{\cosh \gamma h} \qquad (2.48\text{-a})$$

where $\gamma = \sqrt{\alpha/D}$

Finally the expression for μ in this case can be written by combining equations (2.45) and (2.48-a) as follows :

$$\mu = \mu_0 \left[1 + \lambda C_d \frac{\cosh \gamma y}{\cosh \gamma h} \right] \qquad (2.49\text{-a})$$

2.5 CONCLUSIONS

In this chapter we have derived the basic equation governing the pressure in the synovial fluid film by considering it as a non-Newtonian power law fluid. The equation governing the pressure in the porous cartilage matrix is also given.

The equation determining the pressure in the synovial film, for Newtonian fluid model of synovial fluid whose viscosity varies with

concentration of the hyaluronic acid molecules, is also obtained as a particular case.

In the following chapters some of these equations would be used to study the mechanism of the joint by taking into account the non-Newtonian behaviour of the synovial fluid, cartilage surface roughness, cartilage elasticity, cartilage porosity etc.

CHAPTER - III

EFFECTS OF CARTILAGE ROUGHNESS AND PSEUDOPLASTIC BEHAVIOUR OF SYNOVIAL FLUID

3.1 INTRODUCTION

The electron microscopic studies have shown that the cartilage surfaces are wavy, Walker et.al. [1968] . It has been suggested that "this wavy nature of the surface is due to regular array of large collagen bundles embedded in a porous matrix immediately adjacent to the surface". Clarke [1971-b] put forward a different point of view for this wavy character and suggested that the surface contours are created by the collapse of sub-adjacent lacunae, Mow et.al. [1974] . It has also been pointed out that due to waviness of the cartilage surfaces, a phenomenon, known as boosted lubrication, takes place. The consolidation and trapping of the hyaluronic acid molecules in the roughness grooves, under squeezing process, result in boosted lubrication, Walker et.al. [1968] , Dowson et.al. [1970] .

In view of this, the effects of surface roughness and boosted lubrication have been studied in this chapter. Here, the synovial fluid has been considered as a pseudoplastic fluid. The effects of cartilage porosity have not been taken into account and would be considered later. The following two cases have been taken for the joint geometry,

1. Rectangular Plates Model: Here the load bearing region of the joint has been approximated to two rectangular parallel plates. This model is applicable to the case of a knee joint.

2. Circular Plates Model: Here the load bearing region of the joint has been approximated to two circular parallel plates. This model is more suited to the case of a hip joint.

To see the effects of surface roughness theoretically, it is assumed that the surface waviness is represented by a superposition of cosine waves (fig. 3.1). The fluid film thickness function can then be written as follows

$$h_r = h \left[1 + \sum_{j=1}^{N} \frac{\varepsilon_j}{h} \cos \frac{x}{a_j}\right] \tag{3.1}$$

in the case of knee joint model and

$$h_r = h \left[1 + \sum_{j=1}^{N} \frac{\varepsilon_j}{h} \cos \frac{r}{a_j}\right] \tag{3.2}$$

in the case of hip joint model. Here, 2h is the mean film-thickness of synovial fluid film, ε_j and $2\pi a_j$ are the amplitude and wave-length respectively of the jth wave representing the waviness of the cartilage surface. It may be noted here, that ε_j (for all $j = 1,N$) are much smaller than the mean fluid film thickness, 2h, under hydrodynamic conditions for lubrication. Further, for fixed ε_j, when the wave-length $2\pi a_j$ decreases, the asperities get closer and the surface becomes more rough, but in

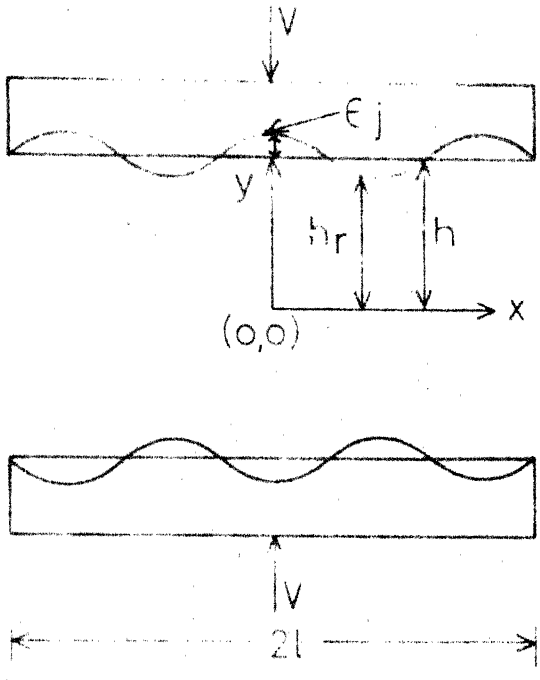

(a) Rectangular plates model (knee joint)

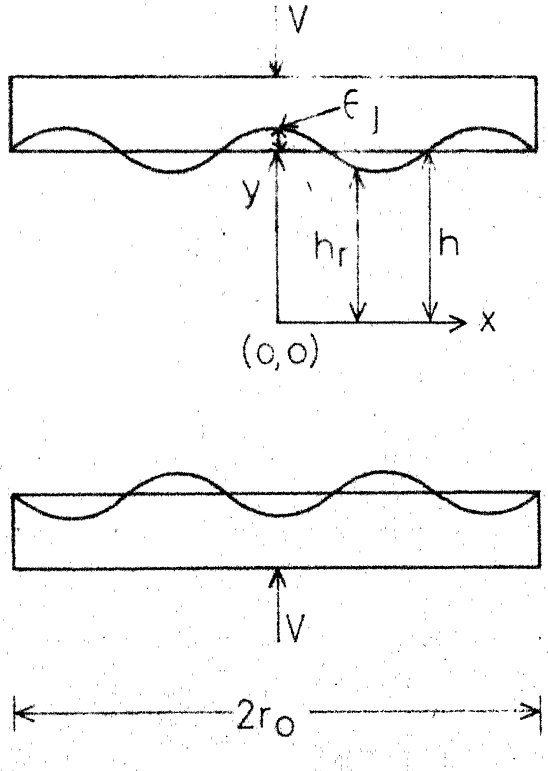

(b) Circular plates model (hip joint)

Fig. 3.1 Joint geometries with surface-roughness.

case $2\pi a_j$ increases, the surface tends towards smoothness, Shukla and Prasad [1966].

The effects of boosted lubrication have been accounted by considering the consistency index m, of the power law model of the synovial fluid, to be related with film-thickness function as follows

$$m = m_o \left[1 + \frac{G}{h_r}\right] \tag{3.3}$$

where G is a constant and accounts for the boosting effect and m_o is the consistency index of the synovial fluid when there are no boosting and no squeezing effects, Dowson et. al. [1970].

In the following, the various characteristics of the joints are studied in the case of standing or jumping positions (squeeze films).

3.2 RECTANGULAR PLATES MODEL (KNEE JOINT)

The physical situation in this case is shown in fig. (3.1-a). The basic equation governing the pressure in the synovial fluid film is obtained from equation (2.36) by putting $V_p = 0$ and replacing h by h_r, as follows

$$\frac{d}{dx}\left[\frac{h_r^{2+1/n}}{2+1/n}\left(-\frac{1}{m}\frac{dp}{dx}\right)^{1/n}\right] = V \tag{3.4}$$

where h_r is given by equation (3.1).

Solving equation (3.4) with the following boundary conditions

$$\frac{dp}{dx} = 0 \quad \text{at } x = 0$$

$$p = 0 \quad \text{at } x = \ell \tag{3.5}$$

the expression for pressure distribution is obtained as follows,

$$p = \left(\frac{2n+1}{n} V\right)^n \int_x^{\ell} \frac{m\, x^n}{h_r^{2n+1}}\, dx \tag{3.6}$$

The load capacity W of the joint is defined as

$$W = 2b \int_0^{\ell} p\, dx$$

which, on using equations (3.3) and (3.6), gives

$$W = 2b\, m_o \left(\frac{2n+1}{n} V\right)^n \int_0^{\ell} \frac{x^{n+1}}{h_r^{2n+1}} \left(1 + \frac{G}{h_r}\right) dx \tag{3.7}$$

The time of squeezing t, the time taken by the upper surface in approaching the position h_f from h_i under a constant load W, is given by,

$$t = \frac{2n+1}{n} \left(\frac{2b\, m_o}{W}\right)^{1/n} \int_{h_f}^{h_i} \left[\int_0^{\ell} \frac{x^{n+1}}{h_r^{2n+1}} \left(1 + \frac{G}{h_r}\right) dx\right]^{1/n} dh \tag{3.8}$$

In a particular case when roughness effects are neglected ($\varepsilon_j = 0$), the corresponding expression for load capacity and time of squeezing can be written from equations (3.7) and (3.8), as follows

$$W = \frac{2b\, m_o}{n+2} \left(\frac{2n+1}{n} V\right)^n \left(1 + \frac{G}{h}\right) \cdot \frac{\ell^{n+2}}{h^{2n+1}} \tag{3.9}$$

$$t = \frac{2n+1}{n+1} \left\{\frac{2\, m_o\, b}{(n+2)W}\right\}^{1/n} \frac{\ell^{1+2/n}}{h_f^{1+1/n}}\, \bar{t} \tag{3.10}$$

where,

$$\bar{t} = 1 - \left(\frac{h_f}{h_i}\right)^{1+1/n} + \frac{n+1}{n(2n+1)} \frac{G}{h_f} \left\{1 - \left(\frac{h_f}{h_i}\right)^{2+1/n}\right\} \qquad (3.11)$$

and $G/h_f << 1$.

It can be seen from equations (3.9) and (3.10) that both load capacity and time of approach increase as G increases (for $G/h_f << 1$). The case of Newtonian fluid is obtained by putting n = 1, and we get the same results as obtained by Dowson et. al. [1970].

To see the effects of pseudoplastic behaviour on the time of squeezing, the expression given by equation (3.11) is plotted in fig.3.2. It can be seen from this graph that $\bar{t}$ increases as n decreases i.e. as the pseudoplastic behaviour increases.

The effects of surface roughness on the load capacity and time of squeezing can be seen from equations (3.7) and (3.8) respectively, where h_r is given by equation (3.1). However, under hydrodynamic conditions $\frac{\varepsilon_j}{h} << 1$ and the various powers of h_r can be approximated as follows :

$$\frac{1}{h_r^s} \approx \frac{1}{h^s} \left[1 - s \sum_{j=1}^{N} \frac{\varepsilon_j}{h} \cos\frac{x}{a_j} + \frac{s(s+1)}{4} \sum_{j=1}^{N} \left(\frac{\varepsilon_j}{h}\right)^2 \left(1 + \cos\frac{2x}{a_j}\right)\right] \qquad (3.12)$$

where the terms of the order $\left(\frac{\varepsilon_j}{h}\right)^3$ are neglected.

To simplify the matter further, we assume that the cartilage surface is fairly rough. In such a case, as pointed out earlier, a_j

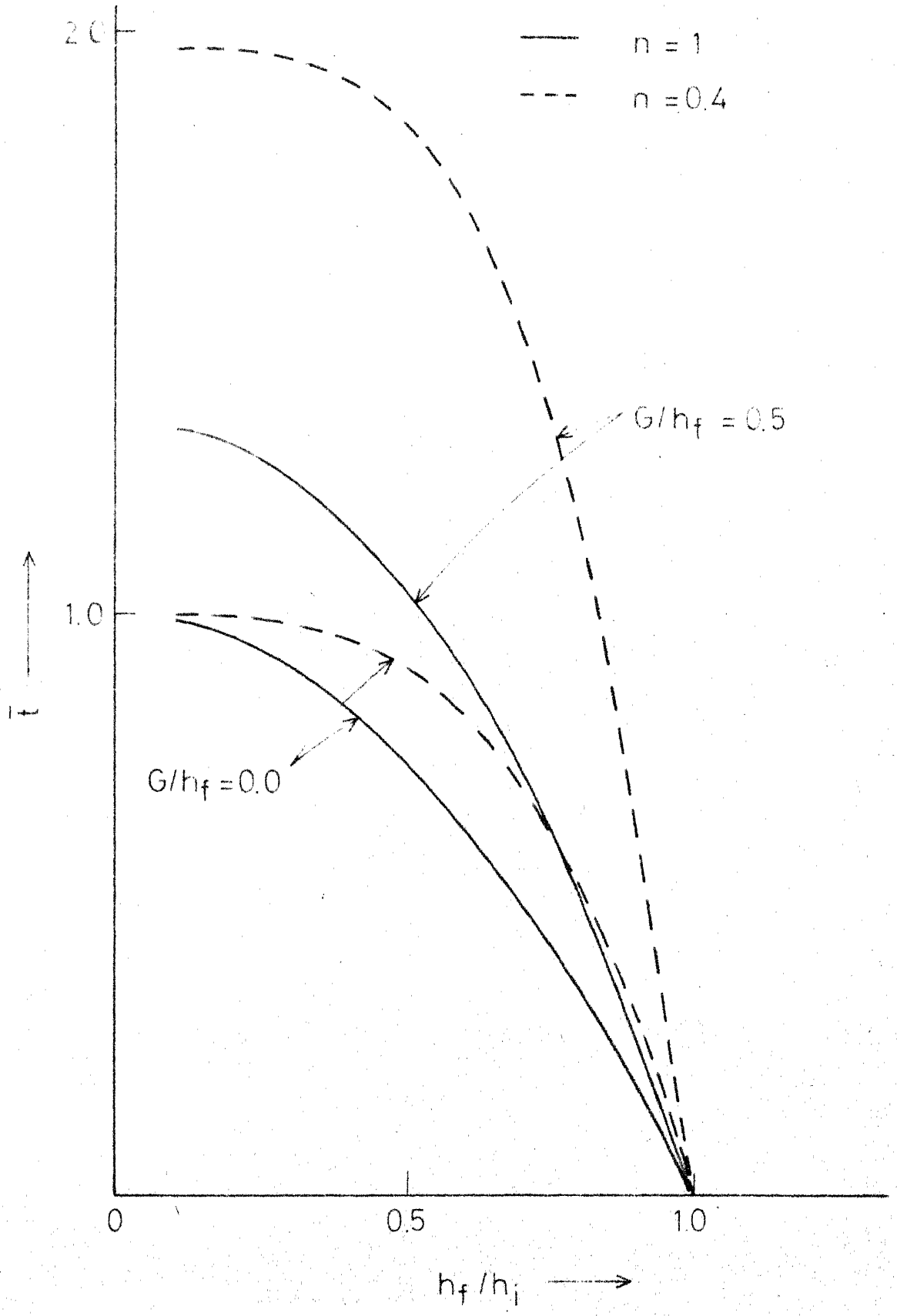

Fig. 3.2 Variation of $\bar{t}$ with h_f / h_i for smooth surface.

would tend to zero. Under this condition, it can be seen that the following integral

$$\int_0^{\ell} x^s \cos \frac{rx}{a_j}\, dx \qquad (3.13)$$

$$(\text{for } s \geq 1,\ r \geq 1)$$

tends to zero.

On using the above approximations, the equations (3.7) and (3.8) can be simplified as follows :

$$W = \frac{2b\, m_o}{n+2} \left(\frac{2n+1}{n} V\right)^n \frac{\ell^{n+2}}{h^{2n+1}} \cdot \bar{W} \qquad (3.14)$$

$$t = \frac{2n+1}{n+1} \left\{ \frac{2\, m_o\, b}{(n+2)W} \right\}^{1/n} \frac{\ell^{1+2/n}}{h_f^{1+1/n}} \bar{t} \qquad (3.15)$$

where,

$$\bar{W} = \left(1 + \frac{G}{h}\right) + \frac{n+1}{2} \left\{(2n+1) + (2n+3)\frac{G}{h}\right\} \sum_{j=1}^{N} \left(\frac{\varepsilon_j}{h}\right)^2 \qquad (3.16)$$

$$\bar{t} = \frac{n+1}{n} \int_1^{\bar{h}_i} \left[\left(1 + \frac{G}{h}\right) + \frac{n+1}{2} \left\{(2n+1) + (2n+3)\frac{G}{h}\right\} \cdot \sum_{j=1}^{N} \left(\frac{\varepsilon_j}{h}\right)^2\right]^{1/n} \frac{d\bar{h}}{\bar{h}^{2+1/n}} \qquad (3.17)$$

and $\bar{h} = h/h_f$, $\bar{h}_i = h_i/h_f$.

From equation (3.16), it is seen that $\bar{W}$ increases as G or ε_j increases. Thus, the load capacity of the knee joint increases due to cartilage surface roughness as well as due to the boosting effect.

It is also noted from the second term of equation (3.16) that the effect of boosting combined with the cartilage roughness further enhances the increase in $\bar{W}$.

To see the behaviour of $\bar{t}$, equation (3.17) is plotted in figures 3.3 to 3.5 . It is seen from fig. 3.3 that $\bar{t}$ increases as cartilage surface roughness increases or as n decreases. From fig. 3.4 it is noted that $\bar{t}$ increases as boosting increases and this effect is enhanced by pseudo-plastic behaviour of the synovial fluid. It is also seen from fig. 3.5 that $\bar{t}$ increases as roughness increases or as n decreases in presence of boosting also. From these graphs, it may also be concluded that the effects of boosting, roughness and pseudoplastic behaviour of the fluid are all favourable and enhance each others effect in combined form.

3.3 CIRCULAR PLATES MODEL (HIP JOINT)

The physical configuration of the hip joint represented by two circular plates is shown in fig. 3.1-b . The basic equation for determining pressure in this case can be written as follows :

$$\frac{1}{r}\frac{d}{dr}\left\{\frac{h_r^{2+1/n}}{2+1/n} \cdot r\left(-\frac{1}{m}\frac{dp}{dr}\right)^{1/n}\right\} = V \qquad (3.18)$$

where h_r is given by equation (3.2)

The boundary conditions determining pressure are,

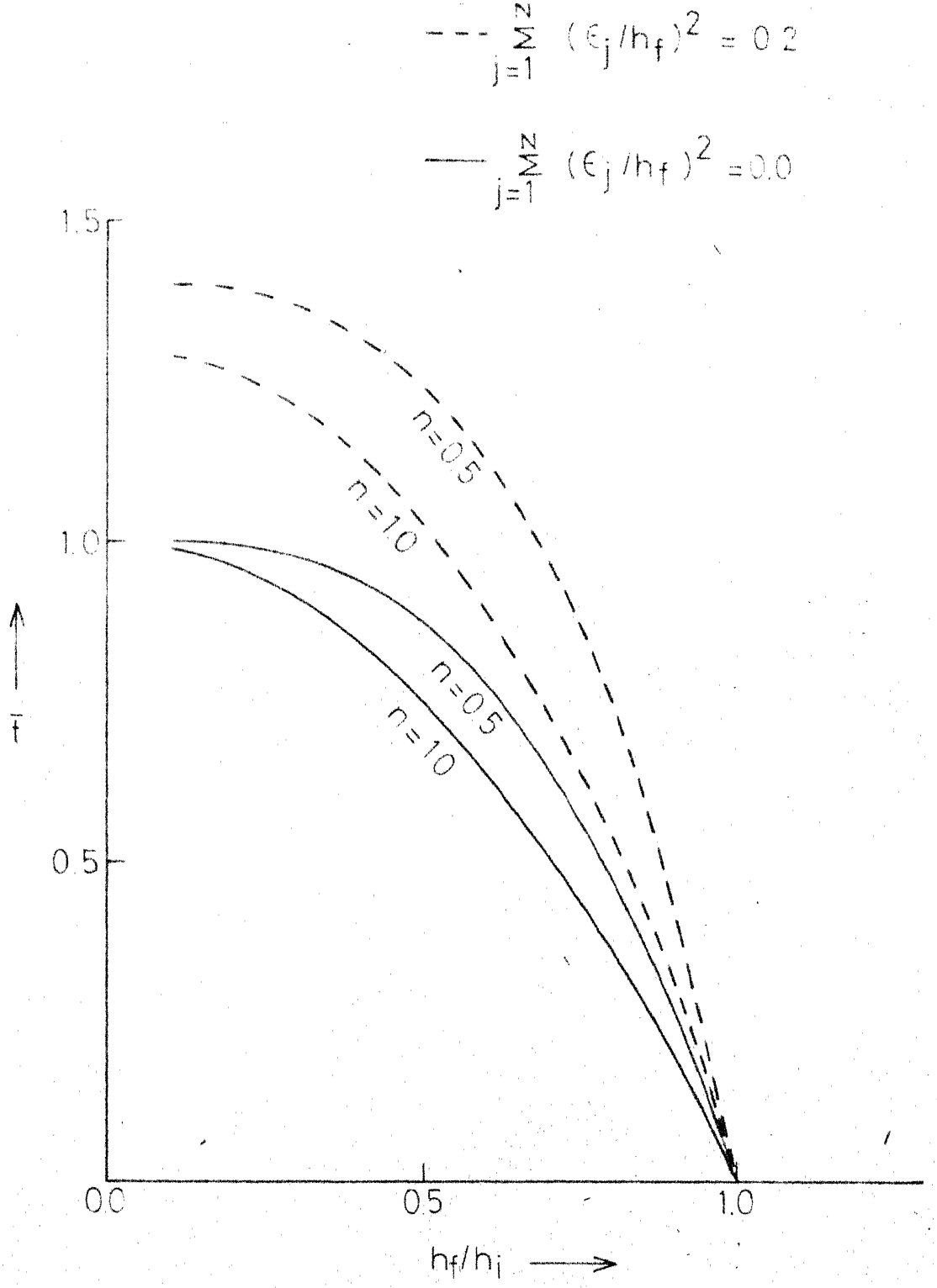

Fig.3.3 Variation of $\bar{t}$ with h_f/h_i for different values of n, $\sum_{j=1}^{N} (\epsilon_j/h_f)^2$ and $G/h_f = 0.0$

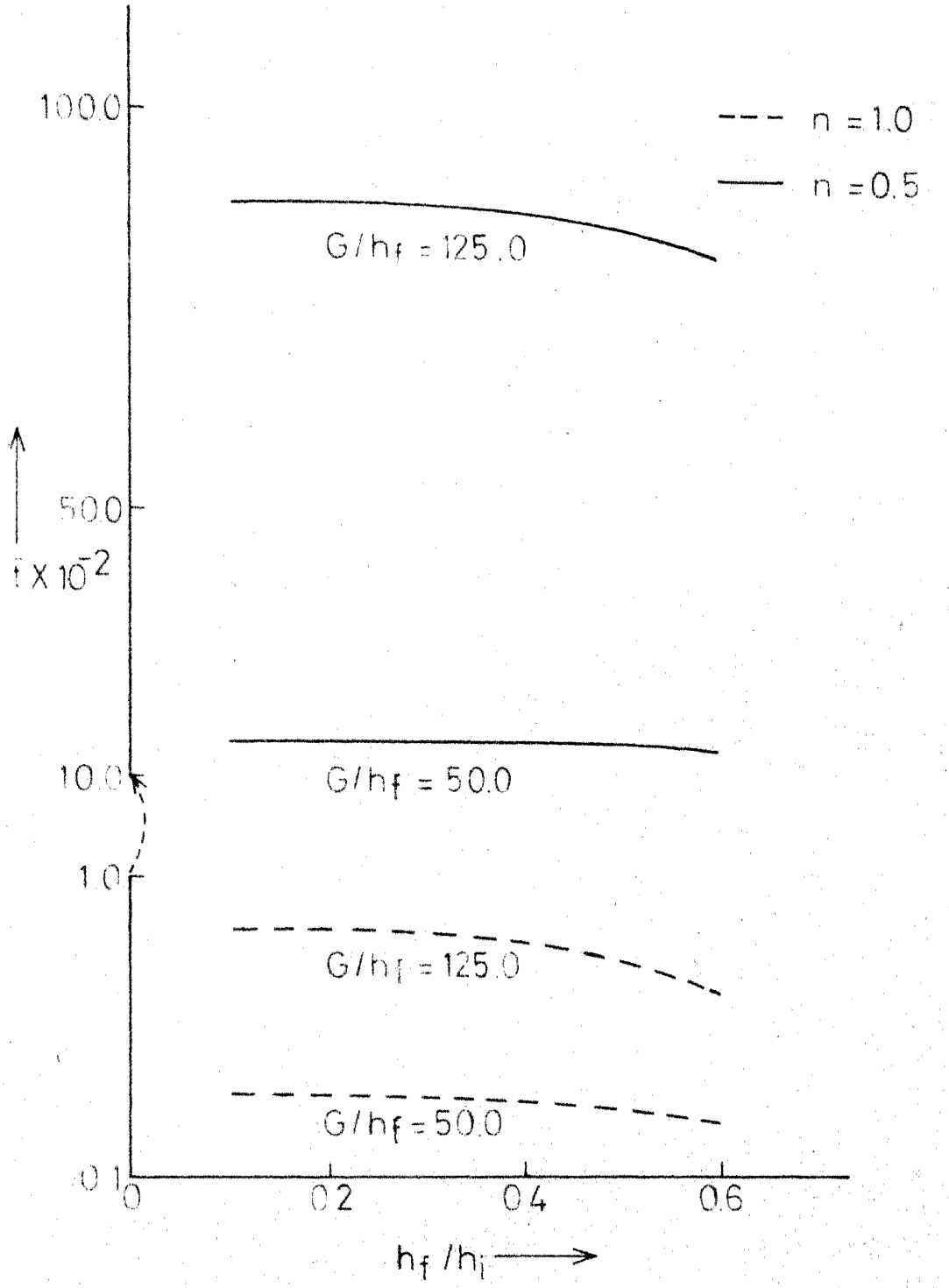

Fig. 3.4 Variation of $\bar{t}$ with h_f/h_i for different values of n, G/hf and $f_i = 0$

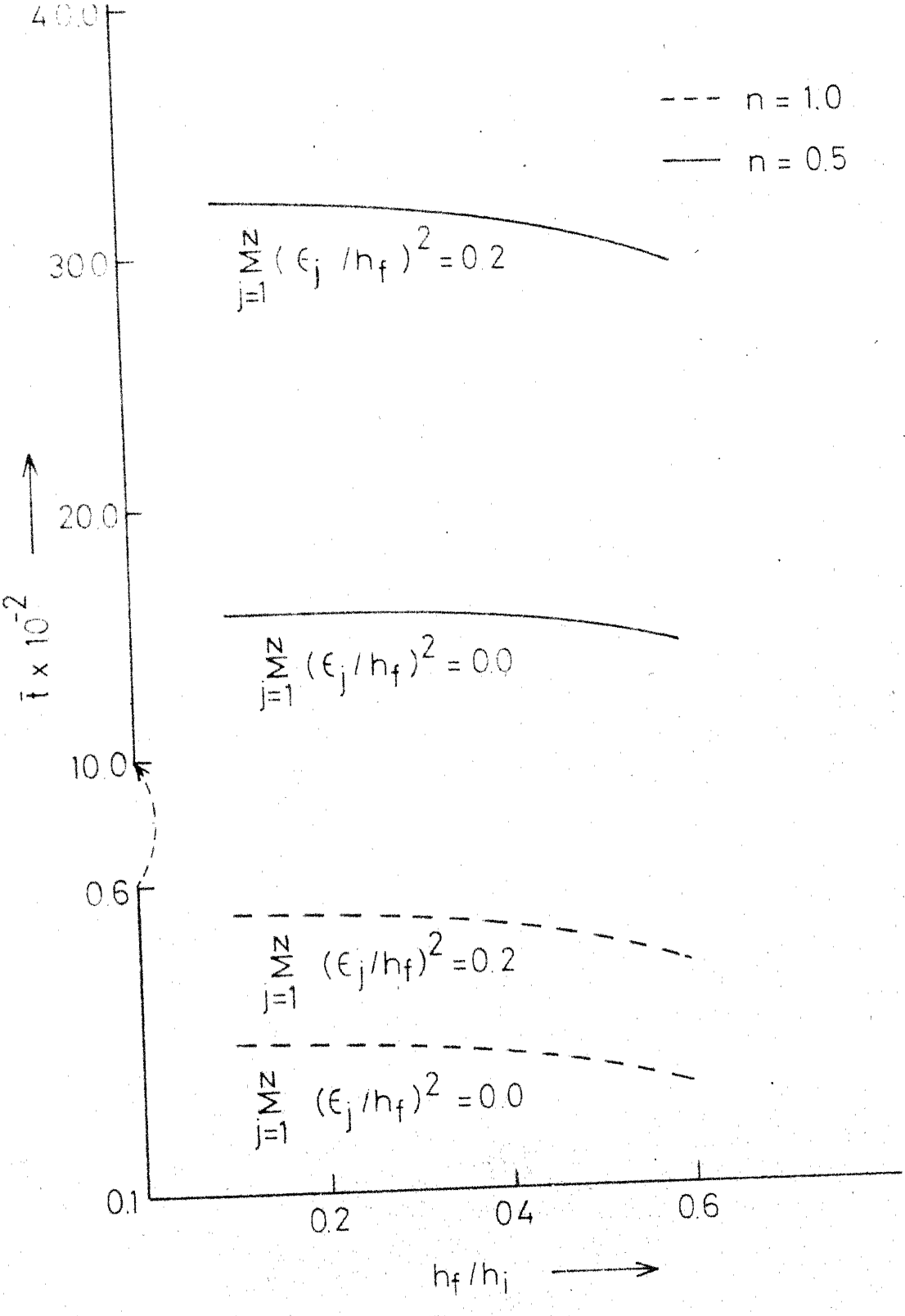

Fig. 3.5. Variation of $\bar{t}$ with h_f/h_i for different values of n and $\sum_{j=1}^{N} (\epsilon_j / h_f)^2$ and $G/h_f = 50.0$

$$p = 0 \quad \text{at } r = r_o$$
$$\frac{dp}{dr} = 0 \quad \text{at } r = 0 \tag{3.19}$$

where r_o is the radius of the circular zone.

As before, integrating equation (3.18) with the boundary conditions (3.19), the expression for pressure is obtained as

$$p = \left(\frac{2n+1}{2n} V\right)^n \int_r^{r_o} \frac{m r^n}{h_r^{2n+1}} dr \tag{3.20}$$

The load capacity in this case is defined as ,

$$W = \int_o^{r_o} 2\pi r\, p\, dr$$

which, on using expressions for p and m from equations (3.20) and (3.3) respectively, gives

$$W = \pi m_o \left(\frac{2n+1}{2n} V\right)^n \int_o^{r_o} \frac{r^{n+2}}{h_r^{2n+1}} \left(1 + \frac{G}{h_r}\right) dr \tag{3.21}$$

Now, the time of approach, t, for the upper surface to approach from the initial position h_i to final position h_f is given as follows :

$$t = \frac{2n+1}{2n} \left(\frac{\pi m_o}{W}\right)^{1/n} \int_{h_f}^{h_i} \left[\int_o^{r_o} \frac{r^{n+2}}{h_r^{2n+1}} \left(1 + \frac{G}{h_r}\right) dr \right]^{1/n} dh \tag{3.22}$$

In the case of smooth surface, $\varepsilon_j = 0$ the expressions for W and t can be written as follows :

$$W = \frac{\pi m_o}{n+3} \left(\frac{2n+1}{2n} V\right)^n \frac{r_o^{n+3}}{h^{2n+1}} \cdot \left(1 + \frac{G}{h}\right) \tag{3.23}$$

and

$$t = \frac{1}{2} \cdot \frac{2n+1}{n+1} \left\{ \frac{\pi m_o}{(n+3)W} \right\}^{1/n} \frac{r_o^{1+3/n}}{h_f^{1+1/n}} \bar{t} \qquad (3.24)$$

where,

$$\bar{t} = 1 - \left(\frac{h_f}{h_i}\right)^{1+1/n} + \frac{n+1}{n(2n+1)} \frac{G}{h_f} \left\{ 1 - \left(\frac{h_f}{h_i}\right)^{2+1/n} \right\} \qquad (3.25)$$

and $G/h_f << 1$.

From the above equations, it is seen that the effect of boosting parameter, G, is to increase the load capacity as well as the time of approach. The case of Newtonian lubricant can be obtained by putting $n = 1$ in the equations (3.23) and (3.25), which give similar results as obtained by Dowson et. al. [1970].

The effect of pseudoplastic behaviour of the lubricant is similar to the case of rectangular plates as $\bar{t}$ given by equation (3.25) is same as in equation (3.10) of the previous case.

To see the effect of surface roughness, equations (3.21) and (3.22) are integrated by substituting the value of h_r from equation (3.2). After making similar assumptions as in the previous case, the expressions for load capacity and time of approach are obtained as follows :

$$W = \frac{\pi m_o}{3+n} \left(\frac{2n+1}{2n} V\right)^n \cdot \frac{r_o^{n+3}}{h^{2n+1}} \cdot \bar{W} \qquad (3.26)$$

and

$$t = \frac{2n+1}{2n+2}\left(\frac{\pi}{n+3}\cdot\frac{m_o}{W}\right)^{1/n}\ \frac{r_o^{1+3/n}}{h_f^{1+1/n}}\cdot\bar{t} \qquad (3.27)$$

where,

$$\bar{W} = 1 + \frac{G}{h} + \frac{n+1}{2}\left\{(2n+1) + (2n+3)\frac{G}{h}\right\}\sum_{j=1}^{N}\left(\frac{\varepsilon_j}{h}\right)^2 \qquad (3.28)$$

$$\bar{t} = \frac{n+1}{n}\int_1^{\bar{h}_i}\left[\left(1+\frac{G}{h}\right) + \frac{n+1}{2}\cdot\left\{(2n+1) + (2n+3)\frac{G}{h}\right\}\cdot \sum_{j=1}^{N}\left(\frac{\varepsilon_j}{h}\right)^2\right]^{1/n}\cdot\frac{d\bar{h}}{\bar{h}^{2+1/n}} \qquad (3.29)$$

and,

$$\bar{h} = \frac{h}{h_f}\ ,\ \bar{h}_i = \frac{h_i}{h_f}$$

From equations (3.28) and (3.29) it is again noted that $\bar{W}$ and $\bar{t}$ increase due to boosting and cartilage surface roughness. This increase in $\bar{t}$ is further enhanced by the pseudoplastic behaviour of the synovial fluid. As the expressions for $\bar{W}$ and $\bar{t}$ are same as in the previous case, these results can also be noted from figures (3.2) to (3.5).

3.4 CONCLUSIONS

In this chapter, the effects of cartilage surface roughness and the pseudoplastic behaviour of the synovial fluid have been studied on the time of squeezing of synovial joints in the case of standing position (squeeze film). It is shown that the time of squeezing

increases due to cartilage surface roughness and due to pseudoplastic behaviour of the synovial fluid when seen with respect to the film-thickness function.

The effects of boosting is also considered and it is pointed out that the boosting effect combined with cartilage surface roughness increases the load capacity and further delays the time of squeezing.

It may be noted that the analysis presented here supports the concept of boosted lubrication even when the non-Newtonian behaviour of the synovial fluid is taken into account.

CHAPTER - IV

EFFECTS OF CARTILAGE ELASTICITY AND NON-NEWTONIAN BEHAVIOUR OF SYNOVIAL FLUID

4.1 INTRODUCTION

In chapter III, we have studied the effects of cartilage surface roughness and the non-Newtonian effects of synovial fluid on the characteristics of knee and hip joints by assuming that the load bearing region can be approximated as parallel plates. In this chapter, we study the effects of cartilage elasticity on the time of squeezing of synovial joints in the same two cases as discussed in chapter III.

The effects of surface deformation on the bearing surfaces have been extensively studied, Dowson et. al [1959, 1960, 1966] , Hooke et. al. [1966] , Kamal [1968] , Christensen [1969] , Herrebrugh [1973] , Castelli et. al. [1966] . To see the effects of cartilage elasticity on synovial joints, similar methods can be applied as have been pointed out by Ling [1974] , Mow et. al. [1974] , Higginson and Norman [1974] . However, when non-Newtonian behaviour of the fluid is taken into account, solution of similar problems are not available.

In view of this, here, we apply the same procedure as suggested by Fein [1967] in the study of squeeze films in synovial joints.

In the case of contact between two elastic cylinders (knee joint), the elastic effects can be taken into account by assuming that the length ℓ_d of the deformed contact zone under applied load W, is the same as in the case of dry contact, Barwell [1956] i.e.

$$\ell_d = 2\left[\frac{W}{\pi}\ \frac{R}{E}\right]^{1/2} \qquad (4.1)$$

In equation (4.1),

$R = \dfrac{R_1 R_2}{R_1+R_2}$, R_1 and R_2 are the radii of the two cylindrical surfaces and

$$\frac{1}{E} = \frac{1-\sigma_1^2}{E_1} + \frac{1-\sigma_2^2}{E_2} \qquad (4.2)$$

where E_1, E_2 are the Young's moduli of the two surfaces, and σ_1 , σ_2 are their respective poissons ratios. Here, it may be noted that ℓ_d increases as E decreases i.e. as the surfaces become more elastic.

Similarly, in the case of elastic contact between two circular surfaces, the radius r_d of the deformed zone, under applied load W, can be written as follows, Fein [1967] ,

$$r_d = 1.15\ \left(\frac{WR}{E}\right)^{1/3} \qquad (4.3)$$

where R is the equivalent radius and E is the equivalent Young's modulus of the spherical surfaces.

4.2 RECTANGULAR PLATES MODEL (KNEE JOINT)

Considering the squeezing of the synovial fluid between two elastic rectangular plates whose physical configuration is shown in fig. 4.1-a, the basic equation governing the pressure in the synovial fluid film can be rewritten as follows

$$\frac{d}{dx}\left[\frac{h^{2+1/n}}{2+1/n}\left(-\frac{1}{m}\frac{dp}{dx}\right)^{1/n}\right] = V \tag{4.4}$$

The boundary conditions in this case would be modified as follows,

$$\frac{dp}{dx} = 0 \quad \text{at } x = 0$$

$$p = 0 \quad \text{at } x = \ell_d = 2\left[\frac{W}{\pi}\frac{R}{E}\right]^{1/2} \tag{4.5}$$

As in chapter III, the expressions for pressure and load capacity of the knee joint can be obtained as ,

$$P = \frac{n}{n+1}\left(\frac{2n+1}{n}V\right)^{n}\frac{\ell_d^{n+1} - x^{n+1}}{h^{2n+1}} \tag{4.6}$$

$$W = \frac{2bm}{n+2}\left(\frac{2n+1}{n}V\right)^{n}\frac{\ell_d^{n+2}}{h^{2n+1}} \tag{4.7}$$

The time of squeezing, t, for approaching the upper surface from the position h_i to the final position h_f is given by using equations (4.1) and (4.7)

$$t = \frac{2n+1}{n+1}\left(\frac{2bm}{n+2}\right)^{1/n} W^{1/2}\left(\frac{4R}{\pi E}\right)^{\frac{n+2}{2n}} \cdot \frac{\bar{t}}{h_f^{1+1/n}} \tag{4.8}$$

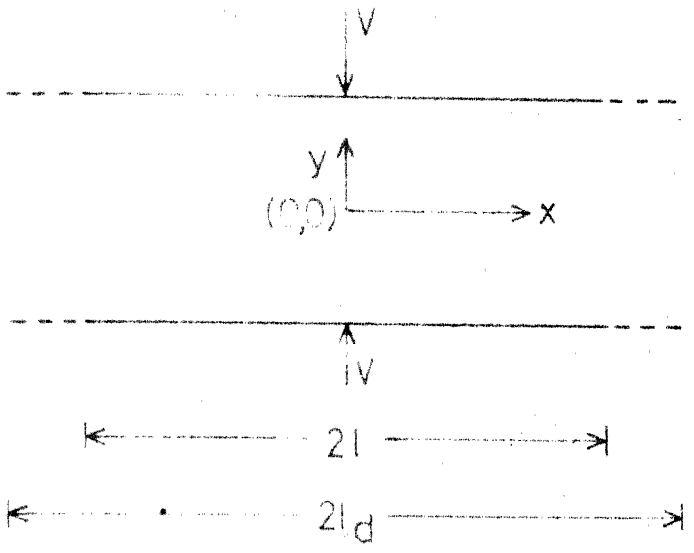

(a) Rectangular plates model

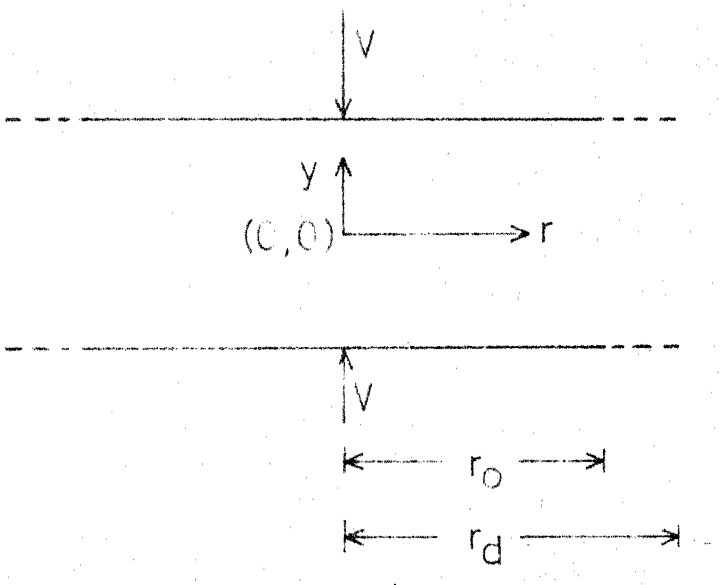

(b) Circular plates model

Fig. 4.1 Squeeze film model under elastic deformations.

where,

$$\bar{t} = 1 - \left(\frac{h_f}{h_i}\right)^{1+1/n} \qquad (4.9)$$

From equation (4.8) it is seen that the time of approach, t, increases as E decreases i.e. as the cartilage surface becomes more elastic. Again, as before, $\bar{t}$ decreases as n decreases (see fig. 4.2).

To find the various effects on the film thickness h_f, we write equation (4.8) as follows, for $\frac{h_f}{h_i} \ll 1$,

$$h_f = \left(\frac{2n+1}{n+1}\ \frac{1}{t}\right)^{\frac{n}{n+1}} \cdot \left(\frac{1}{n+2}\right)^{\frac{1}{n+1}} \left(\frac{4WR}{\pi E}\right)^{\frac{n}{2n+2}} \left(\frac{8b\ m\ R}{\pi E}\right)^{\frac{1}{n+1}} \qquad (4.10)$$

It can be noted from equation (4.10) that the film thickness h_f, at a given time after loading, increases with consistency m, load W, conformity R, and compliance $\frac{1}{E}$. It is also noted that when $n \ll 1$ $(n \to 0)$, the last factor in equation (4.10) dominates and the film thickness h_f essentially depends upon the consistency, conformity and the compliance but not on load, and it may increase as n decreases for $\frac{8b\ m\ R}{\pi E} > 1$. This implies that higher loads would not change h_f too much due to pseudoplastic behaviour of the synovial fluid. The film thickness, $2h_f$, calculated from equation (4.10) with the following data

$m = 4.5$ dyne sec^n/cm^2, $n = .37$,

$W = 10^8$ dyne, $E = 10^7$ dyne/cm^2,

$t = 1$ sec. , $R = 50$ cms. , $b = 2$ cms.

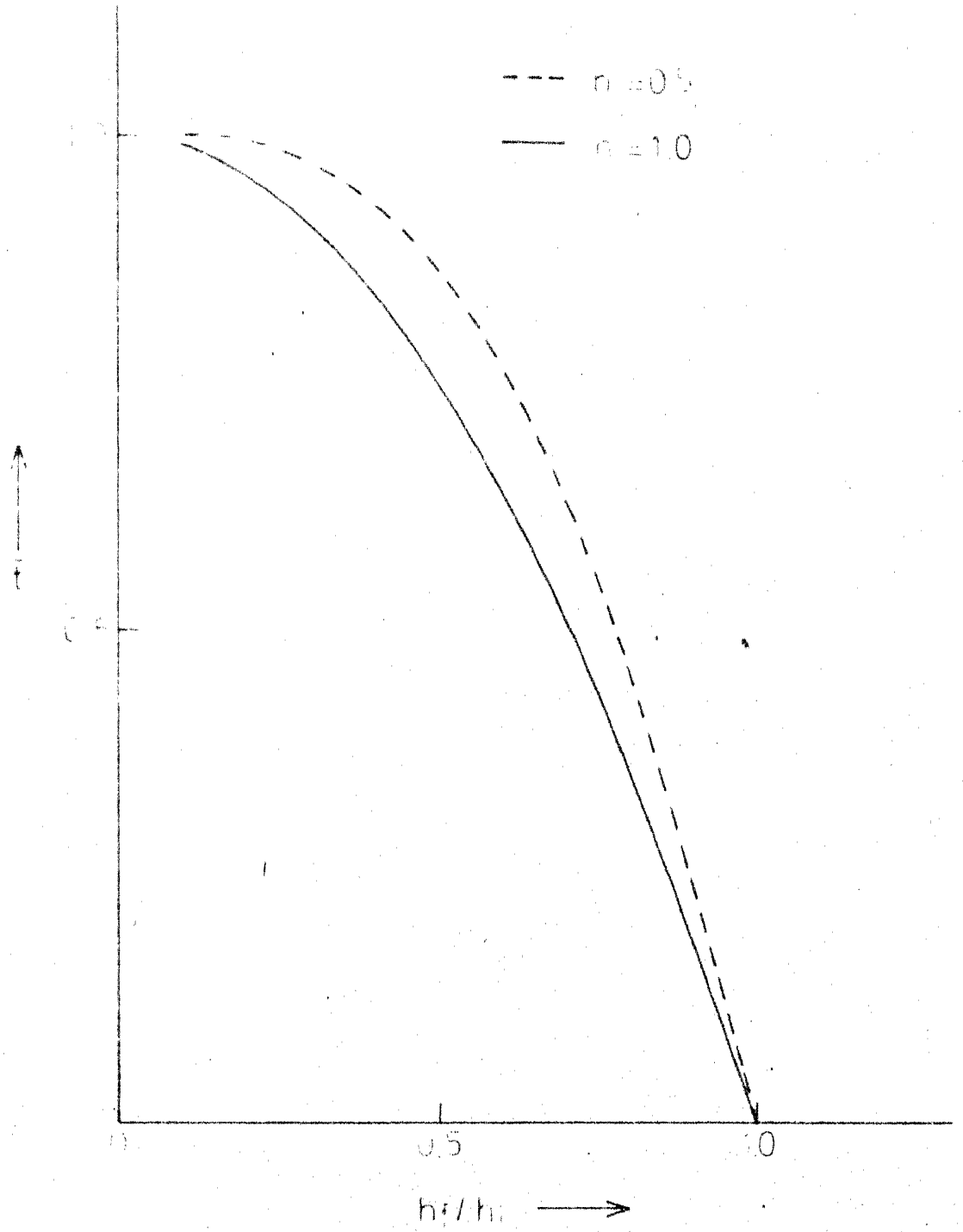

Fig. 3.2 Variation of $\bar{t}$ with h_f/h_i for n = 1.0 and n = 0.5

is found to be of the order 7×10^{-4} cm. Thus, it may be concluded that both the cartilage elasticity and pseudoplastic nature of the synovial fluid help in maintaining the hydrodynamic conditions in the joints.

4.3 CIRCULAR PLATES MODEL (HIP JOINT)

Let us consider the squeezing process in a hip joint whose physical configuration has been approximated by two circular parallel plates as shown in fig. 4.1-b. Proceeding along the same lines as in chapter III, the expressions for load capacity and time of approach can be rewritten as follows :

$$W = \frac{\pi n}{n+3} \left(\frac{2n+1}{2n} \cdot V\right)^n \frac{r_d^{n+3}}{h^{2n+1}} \tag{4.11}$$

$$t = \frac{1}{2} \frac{2n+1}{n+1} \left(\frac{\pi n}{n+3} \cdot \frac{1}{W}\right)^{1/n} r_d^{1+3/n} \left(\frac{1}{h_f^{1+1/n}} - \frac{1}{h_i^{1+1/n}}\right) \tag{4.12}$$

where r_d is given by equation (4.3).

Substituting the value of r_d in equation (4.12), the final expression for the time of squeezing can be written as follows :

$$t = \frac{1}{2} \cdot (1.15)^{\frac{n+3}{n}} \cdot \frac{2n+1}{n+1} \cdot \left(\frac{\pi n}{n+3}\right)^{\frac{1}{n}} \cdot W^{\frac{1}{3}} \cdot \left(\frac{R}{E}\right)^{\frac{n+3}{3n}} \frac{1}{h_f^{1+1/n}} \cdot \bar{t} \tag{4.13}$$

where

$$\bar{t} = 1 - \left(\frac{h_f}{h_i}\right)^{1+1/n} \tag{4.14}$$

It may be noted here again, as before, that the time of squeezing increases as E decreases and $\bar{t}$ increases as n decreases for fixed $(\frac{h_f}{h_i})$.

To see the various effects on the film thickness $2h_f$ we can write equation (4.13) as follows $(\frac{h_f}{h_i} << 1)$:

$$h_f = (1.15)^{\frac{n+3}{n+1}} \left\{\frac{2n+1}{2(n+1)\bar{t}}\right\}^{\frac{n}{n+1}} \left(\frac{1}{n+3}\right)^{\frac{1}{n+1}} \left(\frac{WR}{E}\right)^{\frac{n}{3n+3}} \left(\frac{\pi mR}{E}\right)^{\frac{1}{n+1}} \qquad (4.15)$$

Here, again it can be noted that the film-thickness h_f increases with consistency m, load W, conformity R and compliance $\frac{1}{E}$. Further when $n << 1$ $(n \to 0)$, h_f essentially depends upon the factor $(\frac{\pi mR}{E})^{\frac{1}{n+1}}$ and increases as n decreases for $(\frac{\pi mR}{E}) > 1$. Since in the case $(n \to 0)$ the film-thickness h_f is nearly independent of W it implies that even under jumping condition when the loads are high , the film-thickness h_f would nearly remain the same due to pseudoplastic behaviour of the synovial fluid.

Taking the following typical values of various parameters in the case of a hip joint,

$m = 4.5$ dyne $\sec^n/cm^2$ $\quad W = 10^8$ dyne $\quad E = 10^7$ dyne/cm^2

$n = .37$ $\quad R = 50$ cm $\quad r_o = 1$ cm

$t = 1$ sec.

the value of $2h_f$ is of the order 1.2×10^{-3} cm. which shows a hydrodynamic condition in the hip joint.

When n = 1, we get all the results as discussed by Fein [1967] .

4.4 CONCLUSIONS

In this chapter, we have studied the effects of cartilage elasticity and pseudoplastic behaviour of the synovial fluid on the time of squeezing in the cases of knee and hip joints. The following conclusions may be drawn :

(1) In both the cases the time of squeezing increases as the cartilage surface becomes elastic.

(2) In both the cases $\bar{t}$ increases as the pseudoplastic behaviour of the synovial fluid increases ($n < 1$).

(3) The film-thickness increases with consistency m, load W, conformity R and compliance $\frac{1}{E}$ in both the cases.

(4) For small values of flow behaviour index $n << 1$, the film-thickness $2h_f$, essentially depends upon the consistency m, conformity R and compliance $\frac{1}{E}$. Further, it increases as n decreases for $\frac{8m\ b\ R}{\pi E} > 1$ in the case of knee joint and $\frac{\pi mR}{E} > 1$ in the case of hip joint.

Thus, it may be pointed out here that the elastic behaviour of the cartilage and pseudoplastic behaviour of the synovial fluid are helpful in creating conditions of hydrodynamic lubrication in the joint and these joints function as elastohydrodynamic non-Newtonian squeeze films in standing or jumping position.

CHAPTER - V

EFFECTS OF CARTILAGE POROSITY AND PSEUDOPLASTIC BEHAVIOUR OF SYNOVIAL FLUID

5.1 INTRODUCTION

In previous chapters, we have studied the effects of cartilage surface roughness and cartilage elasticity on the time of squeezing in cases of knee and hip joints. In this chapter, we study the effects of cartilage porosity on the behaviour of these joints by considering the same physical situations as before. The main aim is to investigate the pseudoplastic behaviour of the synovial fluid on weeping lubrication in cases of knee and hip joints by approximating them as rectangular and circular parallel plates respectively.

5.2 RECTANGULAR PLATES MODEL (KNEE JOINT)

Let us consider the squeezing flow of synovial fluid through a knee joint as shown in fig. 5.1. Under loading, the thickness of the cartilage would decrease due to its poro-elasticity and the liquid present in the porous matrix would be expelled in accordance with Darcy's law. The basic equation governing the flow of the fluid (which is Newtonian in character) with viscosity μ_o is given by [see chapter II, equation(2.40)]

$$\frac{d}{dx}\left(-\frac{H k_x}{\mu_o}\frac{dP}{dx}\right) + \frac{k_y}{\mu_o}\frac{P-p}{H_s} = V' \qquad (5.1)$$

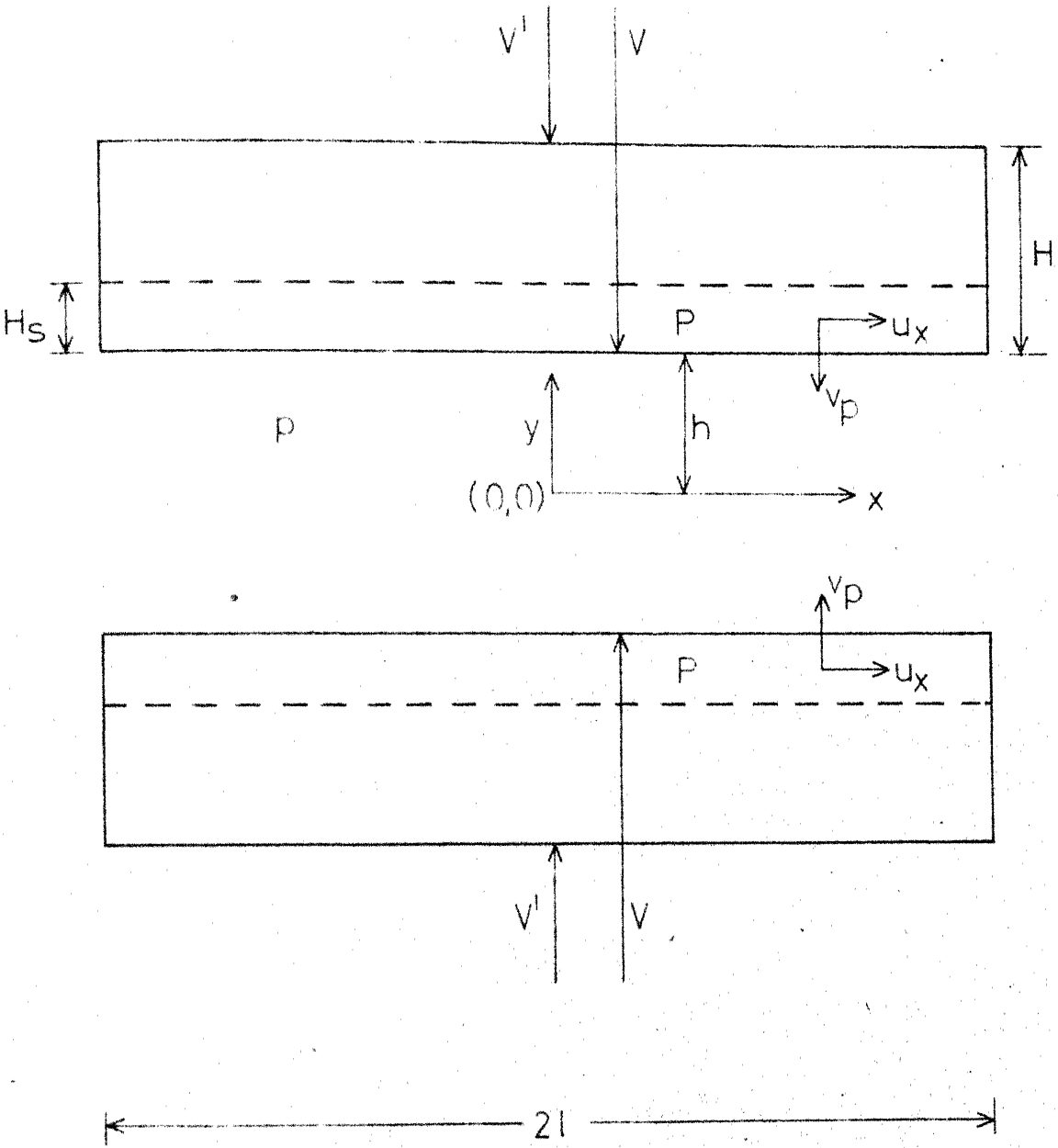

Fig. 5.1 Knee joint geometry with porous effects.

where P(x) is average pressure with respect to the film-thickness H of the cartilage. Other symbols are as explained in chapter II.

The equation governing the pressure in the synovial fluid with constant consistency m is obtained by combining the equations (2.36) and (2.37), as follows :

$$\frac{d}{dx}\left[\frac{h^{2+1/n}}{2+1/n}\left(-\frac{1}{m}\frac{dp}{dx}\right)^{\frac{1}{n}}\right] = V + \frac{k_y}{\mu_o}\frac{P-p}{H_s} \qquad (5.2)$$

Equations (5.1) and (5.2) should be solved simultaneously to get the pressure in the cartilage matrix and in the synovial fluid film.

The boundary conditions for the system are taken as follows :

$$\begin{aligned} \frac{dP}{dx} = \frac{dp}{dx} &= 0 && x = 0 \\ p &= 0 && x = \ell \\ P &= P_o && x = \ell \end{aligned} \qquad (5.3)$$

The last condition implies that at $x = \ell$ in the cartilage matrix, the pressure is non zero, Ling [1974] .

Adding equations(5.1) and (5.2),we have

$$\frac{d}{dx}\left[\frac{h^{2+\frac{1}{n}}}{2+\frac{1}{n}}\left(-\frac{1}{m}\frac{dp}{dx}\right)^{\frac{1}{n}} - \frac{H k_x}{\mu_o}\frac{dP}{dx}\right] = V + V' \qquad (5.4)$$

Integrating equation (5.4) and using the first of the boundary conditions (5.3), we get

$$\frac{h^{2+\frac{1}{n}}}{2+\frac{1}{n}}\left(-\frac{1}{m}\frac{dp}{dx}\right)^{\frac{1}{n}} = (V + V')\,x + \frac{H\,k_x}{\mu_o}\frac{dP}{dx} \qquad (5.5)$$

This equation is non-linear in general when $n \neq 1$ and its solution can not be found exactly. However, when $n = 1$, the equation (5.5) can be solved easily and this case would be dealt with in chapter VII where synovial fluid has been considered as a Newtonian fluid whose viscosity varies with the concentration of the hyaluronic acid molecules.

As a step towards understanding the present physical situation of the knee joint and for solving equation (5.5), we assume that the permeability k_x in the x-direction is small in comparison to the permeability k_y in the y-direction. This implies that flow in the cartilage along x-axis is much smaller than the flow from cartilage matrix to the synovial fluid film.

With this assumption, equation (5.1) can be approximated as follows :

$$V' \approx \frac{k_y}{\mu_o}\frac{P-p}{H_s} \qquad (5.6)$$

where $V' = -\frac{\partial H}{\partial t}$, assumed constant with respect x. This is again an assumption for the cartilage film-thickness which may as well vary with x.

Similarly equation (5.5) can also be approximated as follows by assuming that the second term on the right is smaller than the

first because of small k_x,

$$\left(-\frac{n}{2n+1}\right)^n \cdot h^{2n+1} \cdot \left(-\frac{1}{m}\frac{dp}{dx}\right) \approx (V + V')^n \cdot x^n \qquad (5.7)$$

Solving this and using the second boundary condition (5.3), we get the pressure distribution in the film :

$$p \approx \frac{n}{n+1}\left\{\frac{2n+1}{n} \cdot (V + V')\right\}^n \frac{\ell^{n+1} - x^{n+1}}{h^{2n+1}} \qquad (5.8)$$

On using equations (5.6) and (5.8), the pressure in the cartilage matrix can be written as,

$$P \approx \frac{\mu_o H_s}{k_y} \cdot V' + \frac{m}{n+1}\left\{\frac{2n+1}{n}(V + V')\right\}^n \frac{\ell^{n+1} - x^{n+1}}{h^{2n+1}} \qquad (5.9)$$

Combining the last boundary condition of (5.3) with equation (5.9), it may be seen that

$$P_o \approx \frac{\mu_c H_s}{k_y} V' \qquad (5.10)$$

This equation gives the relation between P_o and V'.

As before the load capacity of the joint can be written as follows :

$$W \approx \frac{2bm}{n+2}\left\{\frac{2n+1}{n}(V + V')\right\}^n \cdot \frac{\ell^{n+2}}{h^{2n+1}} \qquad (5.11)$$

This shows that the load capacity increases as V', the velocity of compression of the cartilage increases.

Again in this case, the time of squeezing is given by the following expression :

$$t = \frac{2n+1}{n+1}\left(\frac{2bm}{n+2}\cdot\frac{1}{W}\right)^{\frac{1}{n}}\cdot\frac{\ell^{1+\frac{2}{n}}}{h_f^{1+\frac{1}{n}}}\,\bar{t} \qquad (5.12)$$

where

$$\bar{t} = \frac{n+1}{n}\int_1^{\bar{h}_i}\frac{d\bar{h}}{\bar{h}^{2+\frac{1}{n}} - \frac{2n+1}{n}\cdot V'\cdot\frac{\ell^{1+\frac{2}{n}}}{h_f^{2+\frac{1}{n}}}\cdot\left(\frac{2bm}{n+2}\cdot\frac{1}{W}\right)^{\frac{1}{n}}} \qquad (5.13)$$

and $\bar{h} = \frac{h}{h_f}$, $\bar{h}_i = \frac{h_i}{h_f}$.

It is seen from equation (5.13) that t or $\bar{t}$ increases as V', the velocity of compression of the cartilage increases. Since, $V' \approx \frac{k_y P_o}{\mu_o H_s}$, it may also be pointed out here that the time of squeezing increases as the permeability coefficient k_y increases or H_s, the thickness of the superficial tangential zone of the cartilage decreases. Further, the effects of pseudoplastic behaviour of the synovial fluid is to increase the time of squeezing.

To see the effects of k_x approximately, let us write equation (5.5) as follows by using equation (5.9) for **P** as its value

corresponding to the first iteration

$$\frac{h^{2+\frac{1}{n}}}{2+\frac{1}{n}}\left(-\frac{1}{m}\frac{dp}{dx}\right)^{\frac{1}{n}} = (V + V')x - \frac{m H k_x}{\mu_o} .$$

$$\left\{\frac{2n+1}{n}(V + V')\right\}^n \frac{x^n}{h^{2n+1}} \qquad (5.14)$$

This equation determines the improved pressure distribution in the film as compared to equation (5.8) in terms of k_x.

We know from physical considerations that p is a continuously decreasing function of x in the region $0 \leq x \leq \ell$ with maximum at $x = 0$ and $\frac{dp}{dx} \leq 0$ in $0 \leq x \leq \ell$. It may then be seen from equation (5.14) that $\left(-\frac{1}{m}\frac{dp}{dx}\right)$ decreases as k_x increases for all x in the region $0 \leq x \leq \ell$. This implies that both pressure and load would decrease as k_x increases, and so this situation is unfavourable for joint characteristics.

Thus, it may be concluded from the above mathematical analysis for favourable effects on characteristics of knee joint, the permeability in the normal direction of the surface of the cartilage should be greater than the permeability in the tangential direction. In fact, this situation really does exist in synovial joint as reported by McCutchen [1962] .

For $n = 1$, i.e. when the synovial fluid behaves as a Newtonian fluid at high shear rate, the above described results are also true.

5.3 CIRCULAR PLATES MODEL (HIP JOINT)

In this case, the load bearing region is approximated by two circular plates whose physical configuration is shown in fig. 5.2. The basic equation governing the pressure in the cartilage and synovial fluid film can be written as follows [see equations(5.1) and (5.2)] :

$$\frac{1}{r}\frac{d}{dr}\left(-\frac{H k_r}{\mu_o} r \cdot \frac{dP}{dr}\right) + \frac{k_y}{\mu_o}\frac{P-p}{H_s} = V' \qquad (5.15)$$

$$\frac{1}{r}\frac{d}{dr}\left[\frac{h^{2+\frac{1}{n}}}{2+\frac{1}{n}} \cdot r \cdot \left(-\frac{1}{m}\frac{dp}{dr}\right)^{\frac{1}{n}}\right] = V + \frac{k_y}{\mu_o}\frac{P-p}{H_s} \qquad (5.16)$$

where k_r, k_y are the permeabilities in the radial and normal directions.

Adding equations(5.15) and (5.16) and integrating with respect to r with the conditions $\frac{dp}{dr} = \frac{dP}{dr} = 0$ at $r = 0$, we get

$$\frac{h^{2+\frac{1}{n}}}{2+\frac{1}{n}}\left(-\frac{1}{m}\frac{dp}{dr}\right)^{\frac{1}{n}} - \frac{H k_r}{\mu_o}\frac{dP}{dr} = (V + V')\frac{r}{2} \qquad (5.17)$$

The boundary conditions in this case also can be written as follows :

$$p = 0 \quad , \quad r = r_o$$
$$P = P_o \quad , \quad r = r_o \qquad (5.18)$$

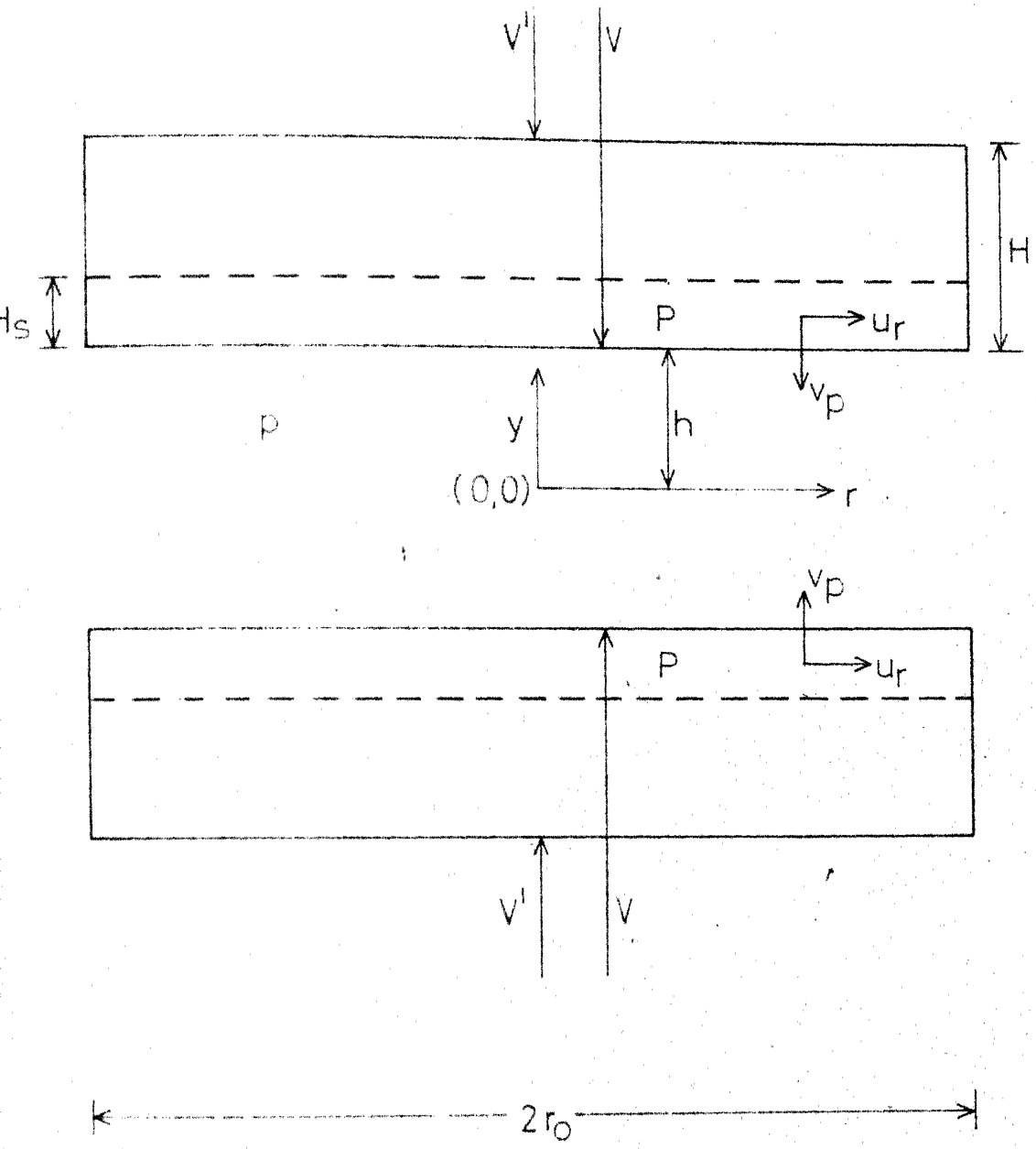

Fig. 5.2 Hip[illegible]rt geometry with porosity effects.

As in previous section, after assuming $k_r << k_y$ and V', a constant, we can write the following expressions from equations (5.16), (5.17) and (5.18) as follows, for the first approximation,

$$I \approx \frac{m}{n+1} \cdot \{\frac{2n+1}{2n} \cdot (V + V')\}^n \frac{1}{h^{2n+1}} (r_o^{n+1} - r^{n+1}) \qquad (5.19)$$

$$P \approx \frac{\mu_o H_s V'}{k_y} + p \qquad (5.20)$$

$$P_o \approx \frac{\mu_o H_s V'}{k_y} \qquad (5.21)$$

The load capacity in this case can be obtained as follows :

$$W = \frac{\pi m}{n+3} \cdot \{\frac{2n+1}{2n} \cdot (V + V')\}^n \cdot \frac{r_o^{n+3}}{h^{2n+1}} \qquad (5.22)$$

Here, also, the load capacity increases as V' increases.

The time of squeezing in this case can be written as

$$t = \frac{2n+1}{2n+2} \cdot \{\frac{\pi m}{(n+3)W}\}^{\frac{1}{n}} \cdot \frac{r_o^{1+\frac{3}{n}}}{h_f^{1+\frac{1}{n}}} \bar{t} \qquad (5.23)$$

where

$$\bar{t} = \frac{n+1}{n} \int_1^{\bar{h}_i} \frac{d\bar{h}}{\bar{h}^{2+\frac{1}{n}} - \frac{2n+1}{2n} \cdot V' \cdot \frac{r_o^{1+\frac{3}{n}}}{h_f^{2+\frac{1}{n}}} \cdot \{\frac{\pi m}{(n+3)W}\}^{\frac{1}{n}}} \qquad (5.24)$$

All the result described in the previous case of a knee joint

5.4 CONCLUSIONS

In this chapter, we have studied the effects of cartilage porosity and the pseudoplastic behaviour of the synovial fluid in cases of knee and hip joints. It is seen here that the load capacity and time of squeezing increase as the permeability, normal to the cartilage surface, increases but the permeability parallel to the cartilage surface has unfavourable effect on pressure developed in the synovial fluid film.

Thus it may be remarked that permeability in the normal direction to the cartilage surface should be greater than the permeability in the tangential direction for better performance of the joints. This, in fact, is the case in synovial joints as pointed by McCutchen [1962].

CHAPTER -VI

EFFECTS OF SLIDING AND PSEUDOPLASTIC BEHAVIOUR OF SYNOVIAL FLUID

6.1 INTRODUCTION

In previous chapters, we have considered the mechanism of joint, only under the condition of squeeze film which is applicable in the case of standing or jumping position. However, during walking cycle, the curvature of the joint surfaces does play an important role in producing the wedge film action similar to hydrodynamic lubrication theory, McConaill [1967] . This hydrodynamic action may be further enhanced by the poroelastic behaviour of the cartilage and the pseudoplastic nature of the synovial fluid. In this chapter, we consider the effects of sliding and the pseudoplastic behaviour of synovial fluid under walking condition. Since the time taken by a complete walking cycle is of the order of only one second, Mow et. al. [1974], the effects of the porosity of the cartilage on the flow may not be too significant to be considered in this case. Further due to the elasticity of the cartilage the loaded region of the joint is assumed to be of the form of convergent linear wedge in the direction of motion, though it may be little circular in reality (fig. 6.1). The film thickness function h in this case may be written as

$$\begin{aligned} h &= h_m + \alpha x \\ &= h_1 + \alpha(x - x_1) \end{aligned} \tag{6.1}$$

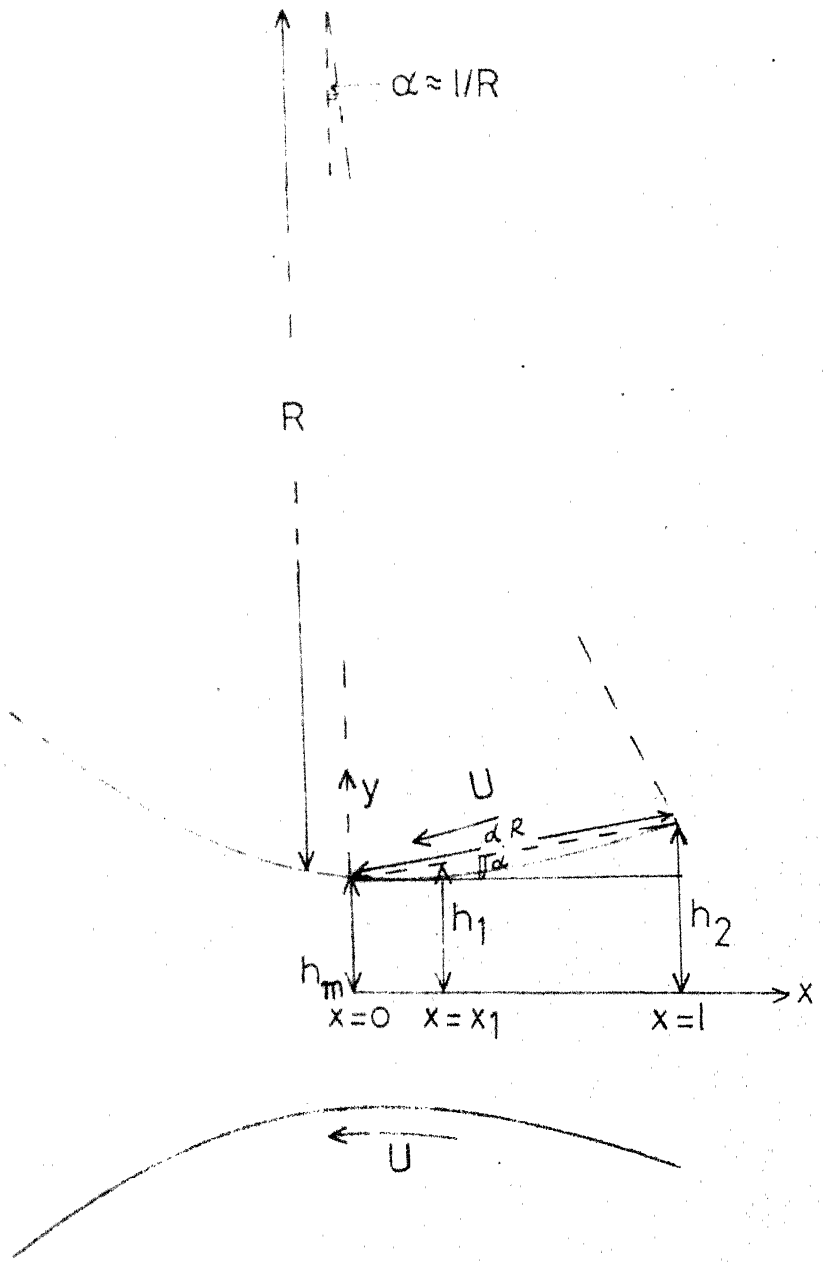

$$\alpha \simeq \tan \alpha = (h_2 - h_0)/l \quad , \alpha R \approx l$$

$$\alpha \simeq (h_2 - h_0)/l \approx l/R$$

Fig. 6.1 Effects of sliding in the synovial joint.

where α is the average inclination of the curved surface and is assumed to be very small.

As shown in fig. 6.1, the constant α has the following approximate relation with the conformity R of the joint and it decreases as R increases.

$$\alpha \approx \frac{\ell}{R} \ (<< 1) \tag{6.2}$$

Further, to observe the effects of cartilage elasticity on the joint mechanism, in this case, it may be assumed that the minimum film thickness function h_m can be given by similar expression as obtained by Archard and Kirk [1963] in the case of a point contact,

$$h_m = C_m \sqrt{RU/E} \tag{6.3}$$

where C_m is a constant and depends upon the consistency of the synovial fluid.

In the following we study the load capacity and the friction coefficient of the synovial joint under walking condition .

6.2 LOAD CAPACITY AND FRICTION COEFFICIENT OF THE JOINT

Noting that the maximum pressure lies at $x = x_1$, as explained in chapter II, the basic equation governing the pressure are [see equations (2.34) and (2.35)]

$$\frac{d}{dx}\left[\frac{h^{2+1/n}}{2+1/n}\left(-\frac{1}{m}\frac{dp_1}{dx}\right)^{1/n}\right] = U\frac{dh}{dx} \tag{6.4}$$

in the region I, $x_1 \leq x \leq \ell$, and

$$\frac{d}{dx}\left[\frac{h^{2+1/n}}{2+1/n}\left(\frac{1}{n}\frac{dp_2}{dx}\right)^{1/n}\right] = -U\frac{dh}{dx} \tag{6.5}$$

in the region II, $0 \leq x \leq x_1$, where pressure in the region $-\ell \leq x \leq 0$ is neglected because of the divergent film in that region.

The boundary conditions for p are

$$\begin{aligned} \frac{dp_1}{dx} = \frac{dp_2}{dx} &= 0 \qquad \text{at} \quad x = x_1 \\ p_1 &= 0 \qquad \text{at} \quad x = \ell \\ p_2 &= 0 \qquad \text{at} \quad x = 0 \end{aligned} \tag{6.6}$$

Solving equations(6.4) and (6.5) with the boundary conditions (6.6), we get the pressure distribution in the two regions as follows :

$$p_1 = n\left(\frac{2n+1}{n}U\right)^n \int_x^{\ell} \frac{(h - h_1)^n}{h^{2n+1}}\,dx \tag{6.7}$$

for $x_1 \leq x \leq \ell$, and for the region $0 \leq x \leq x_1$,

$$p_2 = n\left(\frac{2n+1}{n}U\right)^n \int_0^{x} \frac{(h_1 - h)^n}{h^{2n+1}}\,dx \tag{6.8}$$

where h is given by equation (6.1), $h_1 = h(x_1)$ and x_1 is found by using the matching condition

$$p_1 = p_2 \text{ at } x = x_1,$$

from the following equation

$$\int_{o}^{x_1} \frac{(h_1 - h)^n}{h^{2n+1}}\, dx = \int_{x_1}^{\ell} \frac{(h - h_1)^n}{h^{2n+1}}\, dx \qquad (6.9)$$

The load capacity W is defined as

$$W = b\left[\int_{o}^{x_1} p_2\, dx + \int_{x_1}^{\ell} p_1\, dx\right] \qquad (6.10)$$

or

$$W = -b\left[\int_{o}^{x_1} x\frac{dp_2}{dx}\, dx + \int_{x_1}^{\ell} x\frac{dp_1}{dx}\, dx\right] \qquad (6.10\text{-a})$$

which on using equations (6.7) and (6.8) gives,

$$W = b\, m\left(\frac{2n+1}{n}\, U\right)^n \left[\int_{x_1}^{\ell} \frac{x(h - h_1)^n}{h^{2n+1}}\, dx - \int_{o}^{x_1} \frac{x(h_1 - h)^n}{h^{2n+1}}\, dx\right] \qquad (6.11)$$

The force of friction F, on the surfee y = h is defined as,

$$-F = b\int_{o}^{\ell} \left(\tau_{xy}\Big|_{y=h}\right) dx$$

$$= b\left[\int_{o}^{x_1} m\left(\frac{\partial u}{\partial y}\right)^n_{y=h}\, dx - \int_{x_1}^{\ell} m\left(-\frac{\partial u}{\partial y}\right)^n_{y=h}\, dx\right] \qquad (6.12)$$

which on using equations (2.14) and (2.18) gives

$$-F = b\left[\int_{o}^{x_1} h\frac{dp_2}{dx}\, dx + \int_{x_1}^{\ell} h\frac{dp_1}{dx}\, dx\right] \qquad (6.13)$$

Integrating equation (6.13) by parts and using equations (6.1), (6.6) and (6.10) we get

$$F = \alpha W \tag{6.14}$$

The coefficient of friction c_f in the joint can then be written as

$$c_f = \alpha \approx \frac{\ell}{R} \tag{6.15}$$

It can be seen from equation (6.15) that the coefficient of friction decreases as the conformity (R) of the joint increases but it does not depend upon the nature of the fluid under the situation considered here.

To see approximately the various effects on other joint characteristics, we assume that $\frac{\alpha\ell}{h_m} << 1$. Under this assumption,

$$W = \frac{m\, b\, \ell^{n+2}}{h_1^{2n+1}} \left\{ \frac{2n+1}{n}\ \alpha U \right\}^n \left[\frac{\beta^{n+2} + (1-\beta)^{n+2}}{n+2} \right.$$

$$\left. - (2n+1)\, \frac{\alpha\ell}{h_1} \cdot \frac{(1-\beta)^{n+3} - \beta^{n+3}}{n+3} \right] \tag{6.16}$$

where

$$h_1 = h_m \left[1 + \frac{\alpha\ell}{h_m} \beta \right] \tag{6.17}$$

and β is given by the following expression

$$\left(\frac{\beta}{1-\beta}\right)^{n+1} = 1 - \frac{(n+1)(2n+1)}{(n+2)} \left(\frac{\alpha\ell}{h_m}\right) \tag{6.18}$$

or

$$\beta \approx \frac{1}{2} \left[1 - \frac{1}{2} \frac{2n+1}{n+2} \left(\frac{\alpha\ell}{h_m}\right) \right] \tag{6.19}$$

Substituting this value of β in equation (6.16), the final expression for W can be approximated as,

$$W = \frac{bm}{2(n+2)} \left[\frac{2n+1}{2n} \alpha U \right]^{n} \frac{\ell^{n+2}}{h_m^{2n+1}} \qquad (6.20)$$

It can be noted from equation (6.20) that the load capacity increases as αU increases, but this increase in W is greater in the case of pseudoplastic behaviour ($n << 1$) of the synovial fluid for small values of $\alpha U < 1$.

From equation (6.20), the expression for minimum film thickness can be written as follows :

$$h_m = \left\{ \frac{bm}{2(n+2)} \right\}^{\frac{1}{2n+1}} \left(\frac{2n+1}{2n} \right)^{\frac{n}{2n+1}} \ell^{\frac{n+2}{2n+1}} (\alpha U)^{\frac{n}{2n+1}} \frac{1}{W^{1/(2n+1)}} \qquad (6.21)$$

Taking particular values of the various parameters as below, $m = 4.5$ dyne sec^n/cm^2, $n = .37$, $W = 10^8$ dyne, $b = 2$ cm., $\ell = 1$ cm., $\alpha = \frac{\ell}{R} = .01$, $U = .1$ cm/sec. the value of the minimum film thickness, is found to be of the order 2×10^{-5} cm. Thus, it is noted that even when the pseudoplastic behaviour of the synovial fluid is considered, the hydrodynamic condition does prevail in the joint.

6.3 EFFECTS OF CARTILAGE ELASTICITY

To see the effects of elasticity approximately, let us write equation (6.20) with the help of equations (6.2) and (6.3) as follows :

$$W \approx \frac{bm}{2(n+2)} \left(\frac{2n+1}{2n}\right)^n \frac{\ell^{2n+2}}{C_m^{2n+1}} \frac{E^{n+1/2}}{U^{1/2} R^{2n+1/2}} \qquad (6.22)$$

Here it is seen that the load capacity W decreases as E decreases. Since $R >> 1$, it can also be observed that W decreases as R increases but the decrease is less in the case of $n << 1$. Further, when $n \to 0$, the load capacity mainly depends upon the factor

$$\frac{m\, E^{1/2}}{C_m\, U^{1/2}\, R^{1/2}}$$

indicating strong dependence of W on R, E, U and $\frac{m}{C_m}$ due to increased pseudoplastic behaviour of the synovial fluid.

6.4 CONCLUSIONS

In this chapter, we have studied the mechanism of synovial joint under walking conditions. It is seen that the load capacity increases as the sliding speed increases and this increase is enhanced by the pseudoplastic behaviour of the synovial fluid when considered with respect to $\alpha U << 1$.

The coefficient of friction depends only on the conformity ratio $\frac{\ell}{R}$ and it decreases as the conformity R increases. This suggests that the novelty of having good conformity in synovial joints is helpful in keeping the coefficient of friction fairly low.

It is also pointed out here that the load capacity decreases as the cartilage surface becomes more elastic. Further, the load capacity decreases as conformity increases but this decrease is less due to pseudoplastic behaviour of the fluid when seen with respect to $R > 1$.

CHAPTER - VII

EFFECTS OF CARTILAGE POROSITY AND VISCOSITY VARIATION OF SYNOVIAL FLUID

7.1 INTRODUCTION

In chapter V, we have studied the effects of cartilage porosity and pseudoplastic behaviour of the synovial fluid on the mechanism of joints. In this chapter, we study the characteristics of synovial joints by considering the synovial fluid as a Newtonian fluid whose viscosity varies with the concentration of hyaluronic acid molecules. Here, again, we take the porosity of the cartilage matrix into account whose permeabilities are different along and across the cartilage surface. Under loading the cartilage thickness is compressed and the liquid, filling the cartilage matrix, is squeezed out into the synovial fluid film. Further, under standing position, which we consider here, the squeezing of synovial fluid film also takes place. During this process, the consolidation and trapping of hyaluronic acid molecules occur in the fluid film, thus causing an increase in hyaluronate concentration in the synovial fluid film, Dowson et. al. [1970]. This in turn increase the effective viscosity of the synovial fluid, which can be written as follows [see chapterII, equation (2.49)],

$$\mu = \mu_o \{ 1 + \lambda C_o + \frac{\lambda M}{2D} (h^2 - y^2) \} \qquad (7.1)$$

As in chapter V, here also, we study the following two cases :

1. Rectangular parallel plates model.
2. Circular parallel plates model.

7.2 RECTANGULAR PLATES MODEL (KNEE JOINT)

As pointed out earlier, the load bearing region of the knee joint may be approximated by two porous rectangular parallel plates with the fluid film in between them, as shown in fig. 5.1. The equations governing the pressure in the porous matrix and in the fluid film region can be rewritten as follows [see chapterII, equations (2.40) and (2.43)].

$$\frac{d}{dx}\left\{-\frac{Hk_x}{\mu_o}\frac{dP}{dx}\right\} = V' - \frac{k_y(P-p)}{\mu_o H_s} \tag{7.2}$$

$$\frac{d}{dx}\left\{-F\frac{dP}{dx}\right\} = V + \frac{k_y}{\mu_o H_s}(P-p) \tag{7.3}$$

where,

$$F = \int_o^h \frac{y^2}{\mu}\,dy \tag{7.4}$$

and μ is given by equation (7.1).

The boundary conditions for P and p are taken as follows

$$\frac{dP}{dx} = 0 \quad \text{at } x = 0$$

$$P = P_o \text{ at } x = \ell \tag{7.5}$$

$$\frac{dp}{dx} = 0 \quad \text{at } x = 0$$

$$p = 0 \quad \text{at } x = \ell \tag{7.6}$$

Adding equations (7.2) and (7.3), we get

$$\frac{d}{dx}\left[\frac{H k_x}{\mu_o}\frac{dP}{dx} + F\frac{dp}{dx}\right] = -(V + V') \tag{7.7}$$

which on integration and using the boundary conditions (7.5) and (7.6), gives

$$P = P_o + \frac{\mu_o}{H k_x}\left[\frac{V+V'}{2}(\ell^2 - x^2) - Fp\right] \tag{7.8}$$

Substituting the expression of P in equation (7.2), the equation governing the pressure in the fluid film region is obtained as :

$$\frac{d^2p}{dx^2} - \beta^2 p = -\frac{1}{F}\left[V + \frac{k_y}{\mu_o H_s}\left\{P_o + \frac{\mu_o}{2H k_x}(V + V')(\ell^2 - x^2)\right\}\right] \tag{7.9}$$

where,

$$\beta^2 = \frac{k_y}{H_s}\left(\frac{1}{H \cdot k_x} + \frac{1}{\mu_o F}\right) \tag{7.10}$$

Solving equation (7.9) with the boundary conditions (7.6) for p, the pressure in the fluid film region is determined as follows :

$$p = \frac{\mu_o}{\mu_o F + H k_x}\left[\frac{V+V'}{2}(\ell^2 - x^2) + \frac{1}{\beta^2}\left(1 - \frac{\cosh \beta x}{\cosh \beta \ell}\right)\cdot\right.$$

$$\left.\left\{\frac{H k_x}{\mu_o}\left(\frac{V}{F} + \beta^2 P_o\right) - V'\right\}\right] \tag{7.11}$$

The pressure in the porous region can now be obtained from equations (7.8) and (7.11), as follows

$$P = P_o + \frac{\mu_o}{\mu_o F + H k_x}\left[\frac{V+V'}{2}(\ell^2 - x^2) - \frac{1}{\beta^2}\left(1 - \frac{\cosh \beta x}{\cosh \beta \ell}\right)\right.$$

$$\left. \cdot \{V + \beta^2 F P_o - \frac{\mu_o F}{H k_x} V'\}\right] \qquad (7.12)$$

Using equation (7.11) the load bearing capacity of the knee joint can be written as,

$$W = \frac{2\mu_o b \ell^3}{3(\mu_o F + H k_x)}\left[(V+V') + 3f\left\{\frac{H k_x}{\mu_o F} V + \frac{H k_x}{\mu_o} \beta^2 P_o - V'\right\}\right] \qquad (7.13)$$

or,

$$W = 2 \mu_o b \ell^3 \left[f_1 V + f_2 V' + f_3 \frac{P_o \ell}{\mu_o}\right] \qquad (7.14)$$

where,

$$f = \frac{1}{\beta^2 \ell^2}\left(1 - \frac{\tanh \beta \ell}{\beta \ell}\right) \qquad (7.15)$$

$$f_1 = \frac{\mu_o F + 3H k_x f}{3 \mu_o F(\mu_o F + H k_x)}$$

$$f_2 = \frac{1 - 3f}{3(\mu_o F + H k_x)} \qquad (7.16)$$

$$f_3 = \frac{k_y}{\mu_o F H_s \ell} f .$$

In the non-dimensional form, W can be written in the following form,

$$\bar{W} = \frac{W h^3}{2 \mu_o b V \ell^3}$$

$$= \frac{\bar{F} + 3f \bar{k}_x}{3\bar{F}(\bar{F}+\bar{k}_x)} + \frac{1-3f}{3(\bar{F} + \bar{k}_x)} \bar{V}' + \frac{f \bar{k}_y}{\bar{F}} \bar{P}_o \qquad (7.17)$$

where,

$$\bar{F} = \frac{\mu_o F}{h^3} , \quad \bar{k}_x = \frac{H k_x}{h^3} , \quad \bar{k}_y = \frac{k_y \ell^2}{H_s h^3} ,$$

$$\bar{V}' = \frac{V'}{V} , \quad \bar{P}_o = \frac{P_o h^3}{V \mu_o \ell^2} \qquad (7.18)$$

and $\beta^2 \ell^2 = \bar{k}_y \left(\frac{1}{\bar{F}} + \frac{1}{\bar{k}_x}\right)$

From equation (7.14), the time of squeezing can be obtained as follows :

$$t = 2\mu_o b \ell^3 \int_{h_f}^{h_i} \frac{f_1 dh}{W - 2b\mu_o \ell^3 (f_2 V' + f_3 \frac{P_o \ell}{\mu_o})} \qquad (7.19)$$

or

$$\bar{t} = \int_1^{\bar{h}_i} \frac{\bar{F} + 3\bar{k}_x f}{3\bar{F}(\bar{F} + \bar{k}_x) - \bar{F}(1-3f)\bar{V}' - 3f\bar{k}_y(\bar{F} + \bar{k}_x)\bar{P}_o} d\bar{h} \qquad (7.20)$$

where

$$\bar{t} = \frac{2b \mu_o \ell^3}{W h_f^2} t, \quad \bar{V}' = \frac{2 \mu_o b \ell^3 V'}{W h_f^3} ,$$

$$\bar{P}_o = \frac{2b \ell P_o}{W} , \quad \bar{h} = h/h_f, \quad \bar{h}_i = h_i/h_f.$$

and other dimensionless parameters are same as in equation (7.18) where h is replaced by h_f.

To see the effects of different parameters, the expression given by equations (7.13) and (7.19) can be approximated as follows for large $\beta\ell$ such that $\tanh \beta\ell \approx 1$ and $\frac{\bar{k}_x}{\bar{F}} \ll 1$, $\frac{\bar{k}_x}{\bar{F}} \cdot \bar{P}_o \approx 0$.

$$\frac{W}{2b\mu_o \ell^3} \approx \frac{1}{3} \frac{V}{\mu_o F + Hk_x} + \frac{1}{3} \frac{V'}{\mu_o F + Hk_x} \left(1 - \frac{3HH_s k_x}{k_y \ell^2}\right) \tag{7.21}$$

$$\frac{t}{2b\mu_o \ell^3} \approx \int_{h_f}^{h_i} \frac{dh}{3W(\mu_o F + Hk_x) - 2b\mu_o \ell^3 V \left(1 - \frac{3HH_s k_x}{k_y \ell^2}\right)} \tag{7.22}$$

In the above equations F is a function of h, λC_o, M and can be written as follows by using equations (7.1) and (7.2)

$$F = \frac{h^3}{\mu_o \bar{M}} \left[\frac{1}{2\bar{M}_c} \ln \frac{1 + \bar{M}_c}{1 - \bar{M}_c} - 1 \right] \tag{7.23}$$

where $\bar{M} = \frac{\lambda h^2 M}{2D}$, $\bar{M}_c = \frac{\bar{M}}{\bar{M} + 1 + \lambda C_o}$

This expression for F can be approximated for $\lambda C_o \ll 1$ as follows :

$$F \approx \frac{h^3}{3\mu_o} \left[1 - \frac{2\bar{M}}{5} - \lambda C_o\right]$$

Here it may be noted that F decreases as $\bar{M}$ or λC_o increases.

Keeping this behaviour of F in view, it can be noted from equations (7.21) and (7.22) that W and t increase as $\lambda\bar{U}_o$ and $\bar{M}$ increase. Further W and t also increase as k_y increases but they decrease with the increase in k_x. These behaviours can also be noted from the graphical representations of equations (7.17) and (7.20) as shown in figures 7.1 to 7.4, for different values of the parameters.

7.3 CIRCULAR PLATES MODEL (HIP JOINT)

As mentioned earlier, the hip joint geometry has been approximated by two circular parallel discs (see fig. 5.2). The discs are porous and permeable in both r- and y-directions. In this case, the equations, corresponding to the equations (7.2) and (7.3), governing the pressure in porous and fluid film regions, can be written as follows :

$$\frac{1}{r}\frac{d}{dr}\left\{\frac{Hk_x}{\mu_o}\left(r\frac{dP}{dr}\right)\right\} = -\left\{V' - \frac{k_y}{H_s\mu_o}(P-p)\right\} \qquad (7.24)$$

$$\frac{1}{r}\frac{d}{dr}\left\{Hr\frac{dp}{dr}\right\} = -\left\{V + \frac{k_y}{H_s\mu_o}(P-p)\right\} \qquad (7.25)$$

when μ_o is a constant, equations (7.24) and (7.25) are same as used by Ling [1974] .

The boundary conditions for P and p are taken as follows :

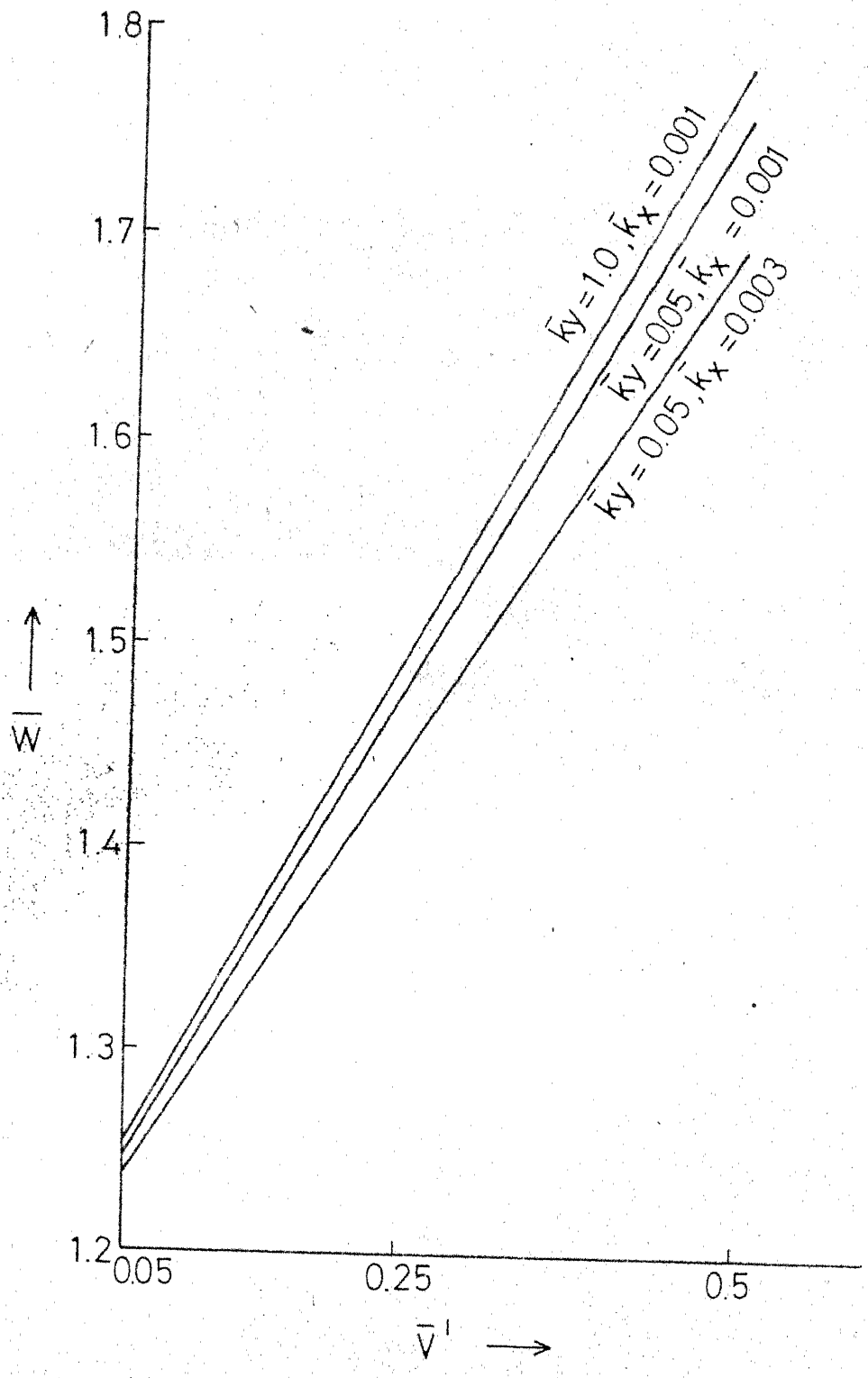

g. 7.1 Variation of $\bar{W}$ with $\bar{V}'$ for different values of $\bar{k}_x, \bar{k}y$ and $\bar{P}_o = 0.2$, $\lambda C_o = 0.1$, $\bar{M} = 0.25$

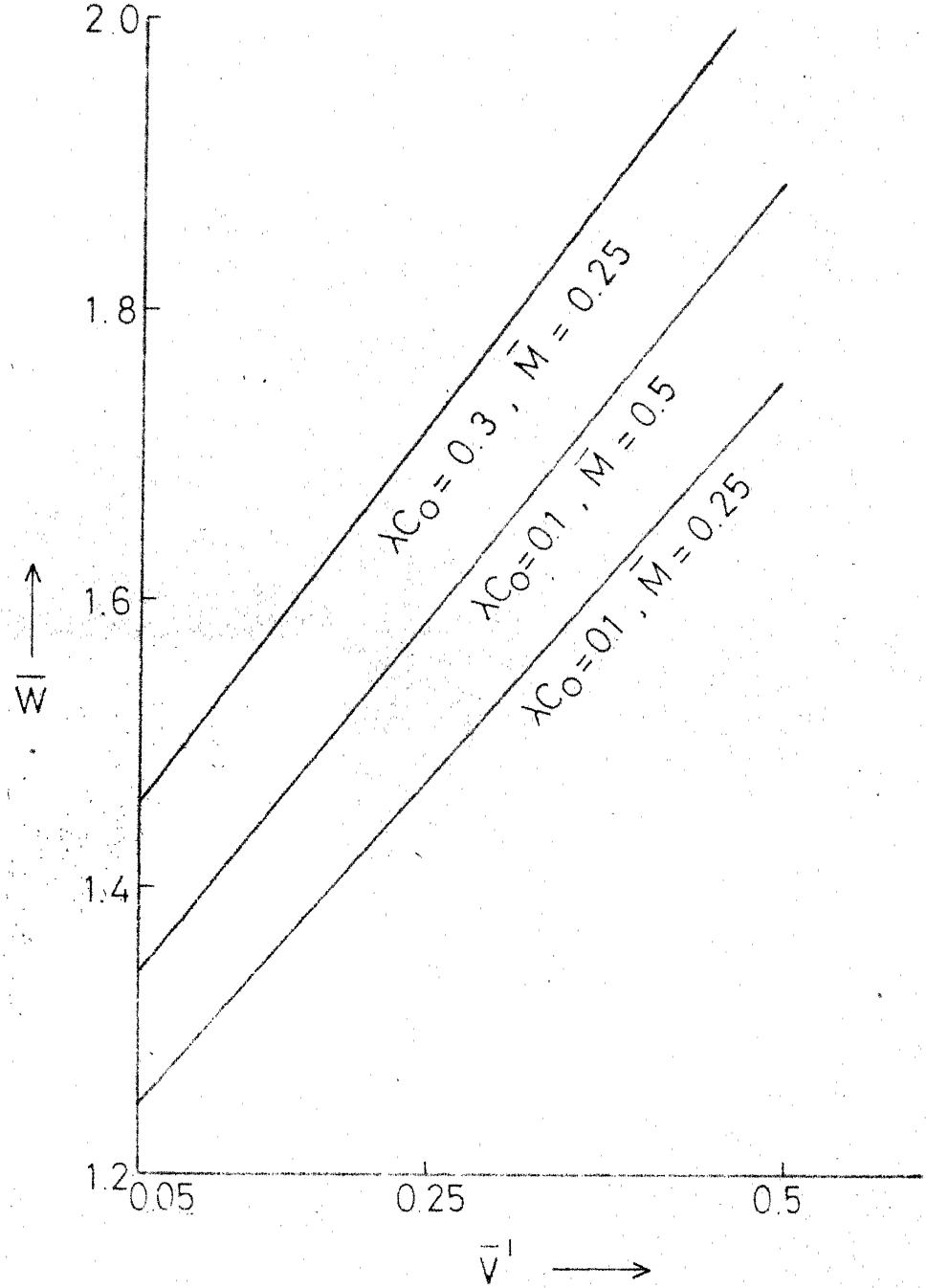

Fig. 7.2 Variation of $\bar{W}$ with $\bar{V}'$ for different values of λC_o and $\bar{M}$, and for $\bar{P}_o = 0.2$, $\bar{k}_x = 0.001$, $\bar{k}y = 0.05$

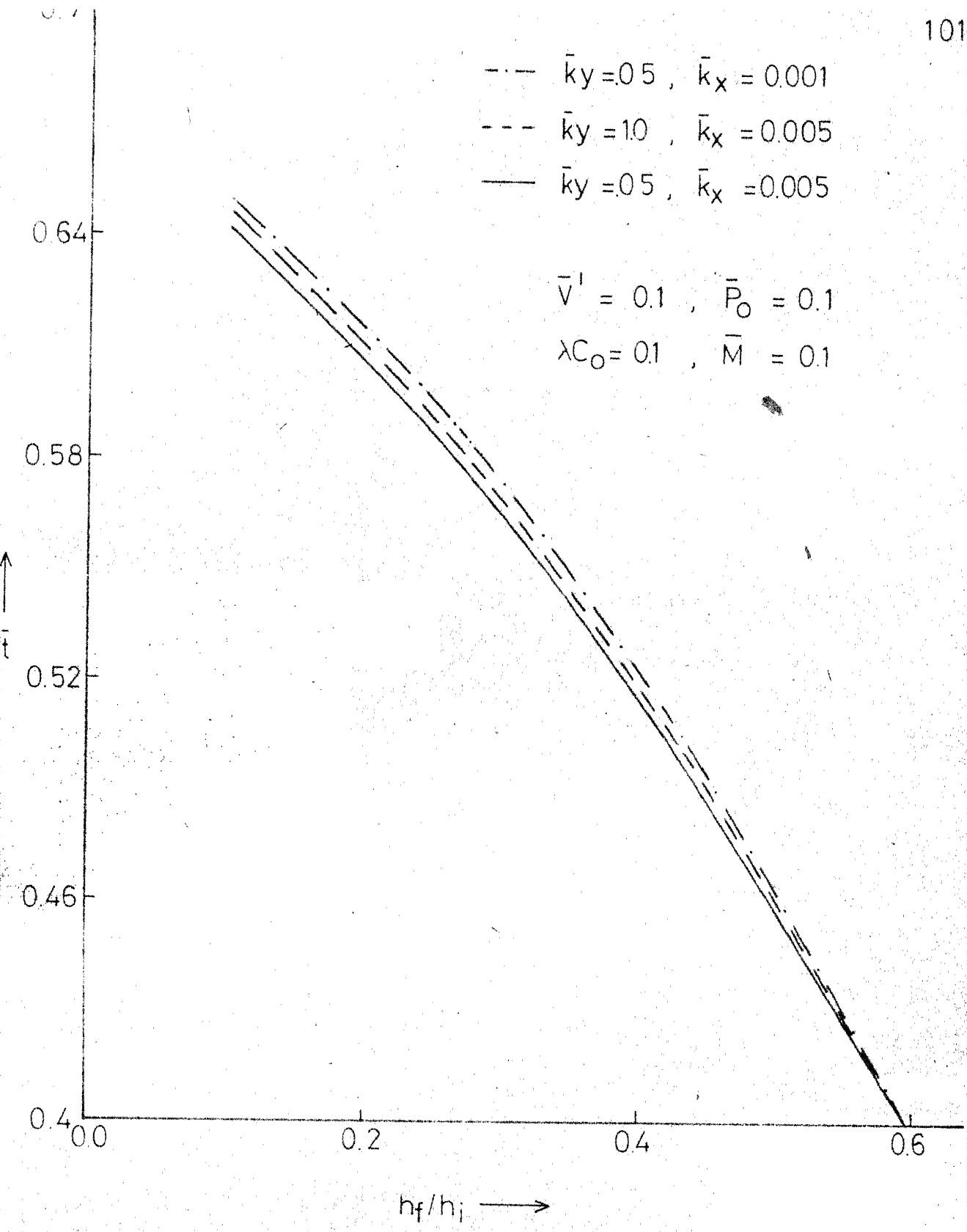

g. 7.3 Variation of $\bar{t}$ with h_f/h_i for different values of $\bar{k}_x$ and $\bar{k}$

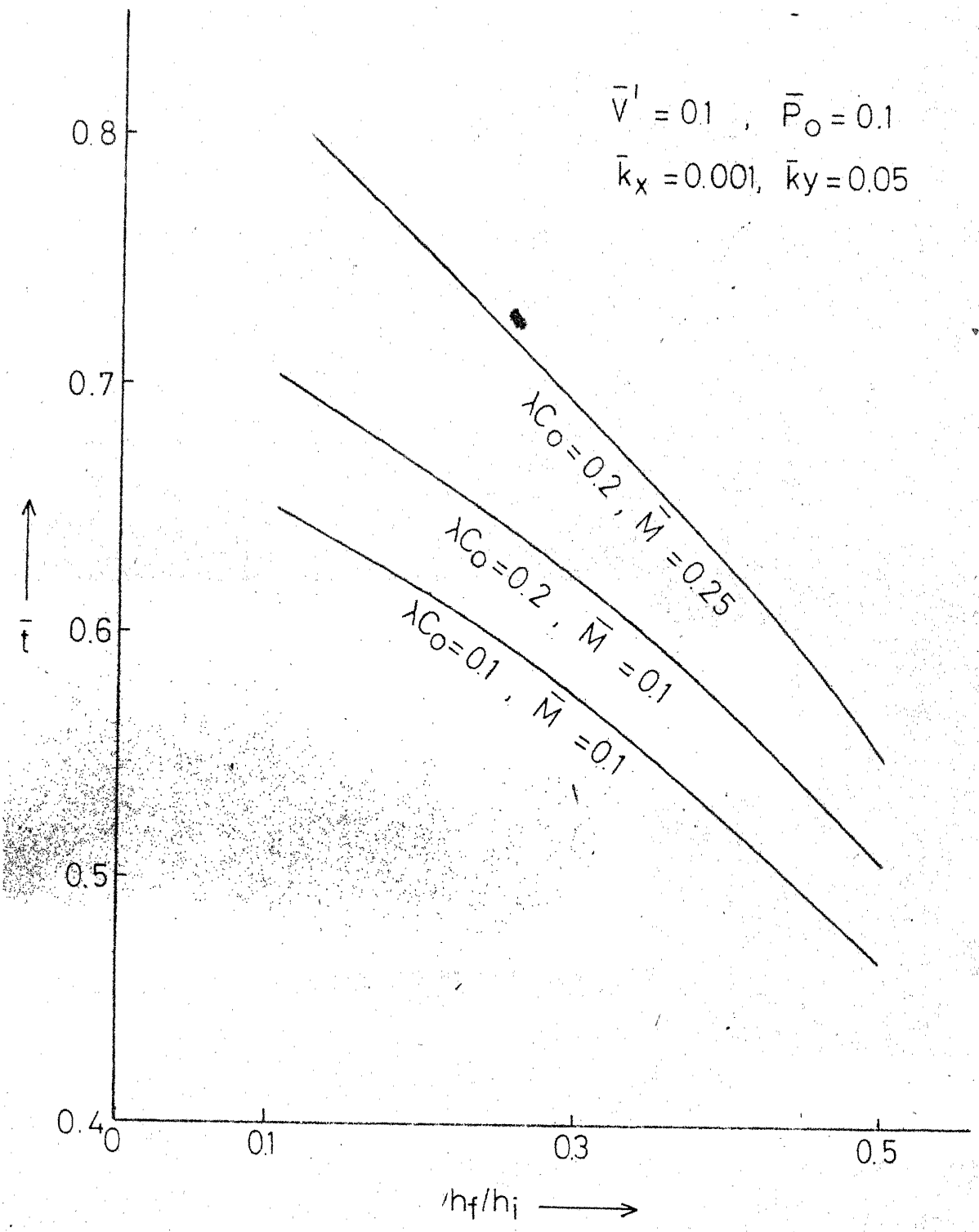

ig. 7.4 Variation of $\bar{t}$ with h_f/h_i for different values of λC_o and $\bar{M}$

$$\frac{dP}{dr} = 0 \quad \text{at} \quad r = 0$$

$$P = P_o \quad \text{at} \quad r = r_o \tag{7.26}$$

$$\frac{dp}{dr} = 0 \quad \text{at} \quad r = 0$$

$$p = 0 \quad \text{at} \quad r = r_o \tag{7.27}$$

Adding the equations (7.24) and (7.25), and integrating the resultant equation with the boundary conditions for P and p, we get,

$$P = P_o + \frac{\mu_o}{H k_r} \left[\frac{(V+V')(r_o^2-r^2)}{4} - F p \right] \tag{7.28}$$

The equations (7.25) and (7.28), on simplification give the following equation to determine the pressure p in the fluid film,

$$\frac{1}{r} \frac{d}{dr} \{ r \frac{dp}{dr} \} - \beta^2 p = - \frac{1}{F} \left[V + \frac{k_y}{\mu_o H_s} \{ P_o + \frac{\mu_o (V+V')(r_o^2-r^2)}{4 H k_r} \right] \tag{7.29}$$

where, in this case,

$$\beta^2 = \frac{k_y}{H_s} \left[\frac{1}{H k_r} + \frac{1}{\mu_o F} \right] \tag{7.30}$$

The equation (7.29) is modified Bessel's equation and its solution with the boundary conditions (7.27) is given as follows :

$$p = \frac{\mu_o}{\mu_o F + H k_r} \left[\frac{V+V'}{4} (r_o^2-r^2) + \frac{1}{\beta^2} \{ 1 - \frac{I_o(\beta r)}{I_o(\beta r_o)} \} \cdot \right.$$

$$\left. \{ \frac{H k_r}{\mu_o} (\frac{V}{F} + \beta^2 P_o) - V' \} \right] \tag{7.31}$$

The pressure in the porous matrix then can be written as [by using equation (7.28)]

$$P = P_o + \frac{\mu_o}{\mu_o F + H k_r}\left[\frac{V+V'}{4}(r_o^2 - r^2) - \frac{1}{\beta^2}\left(1 - \frac{I_o(\beta r)}{I_o(\beta r_o)}\right)\right.$$

$$\left.\{V + F\beta^2 P_o - \frac{\mu_o F}{H k_r}\}\right] \qquad (7.32)$$

The load capability, W, of the joint, in this case is given by

$$W = \frac{\pi\mu_o r_o^4}{8(\mu_o F + H k_r)}\left[V+V'+8g\left\{\frac{H k_r}{\mu_o}\left(\frac{V}{F} + \beta^2 P_o\right) - V'\right\}\right] \qquad (7.33)$$

or,

$$W = \pi\mu_o r_o^4\left[g_1 V + g_2 V' + g_3 \frac{P_o r_o}{\mu_o}\right] \qquad (7.34)$$

where,

$$g = \frac{1}{\beta^2 r_o^2}\left\{1 - \frac{2 I_1(\beta r_o)}{(\beta r_o) I_o(\beta r_o)}\right\} \qquad (7.35)$$

$$g_1 = \frac{\mu_o F + 8 g H k_r}{8 \mu_o F(\mu_o F + H k_r)}$$

$$g_2 = \frac{1-8g}{8(\mu_o F + H k_r)} \qquad (7.36)$$

$$g_3 = \frac{g k_y}{\mu_o F H_s r_o}$$

The non-dimensional form of W can be written as,

$$W = \frac{\pi\mu_o V r_o^4}{h^3}\bar{W} \qquad (7.37)$$

where,

$$\bar{W} = \frac{\bar{F}+8g\,\bar{k}_r}{8\,\bar{F}(\bar{F}+\bar{k}_r)} + \frac{1-8g}{8(\bar{F}+\bar{k}_r)}\bar{V}' + \frac{g\,\bar{k}_y}{\bar{F}}\bar{P}_o$$

$$\bar{F} = \frac{\mu_o F}{h^3}\ ,\ \bar{k}_y = \frac{k_y r_o^2}{h^3 H_s}\ ,\ \bar{k}_r = \frac{H k_r}{h^3}\ , \qquad (7.38)$$

$$\bar{V}' = \frac{V'}{V}\ ,\ \bar{P}_o = \frac{P_o h^3}{r_o^2\ \mu_o\ V}\ .$$

The time of squeezing can then be obtained as follows :

$$t = \pi\mu_o r_o^4 \int_{h_f}^{h_i} \frac{g_1\,dh}{W - \pi\mu_o r_o^4 (g_2 V' + g_3 \frac{P_o r_o}{\mu_o})} \qquad (7.39)$$

or

$$\bar{t} = \int_1^{\bar{h}_i} \frac{(\bar{F} + 8\bar{k}_r g)\,d\bar{h}}{8\bar{F}(\bar{F}+\bar{k}_r) - \bar{F}(1-8g)\bar{V}' - 8g\,\bar{k}_y(\bar{F}+\bar{k}_r)\,\bar{P}_o} \qquad (7.40)$$

where $\bar{t} = \dfrac{t\ W\ h_f^2}{\pi\mu_o\ r_o^4}$, $\bar{V}' = \dfrac{\pi\mu_o r_o^4\ V'}{W\ h_f^3}$,

$$\bar{P}_o = \frac{\pi r_o^2\ P_o}{W}\ ,\ \bar{h}_f = h/h_f,\ \bar{h}_i = h_i/h_f,$$

and the other demonsionless quantities are same as before when h is replaced by h_f.

As before, for large βr_o and $\dfrac{\bar{k}_r}{\bar{F}} \ll 1$, $\dfrac{\bar{k}_r}{\bar{F}}\bar{P}_o \approx 0$, the expression for W and t, given by equations (7.33) and (7.38), can be approximated

as follows :

$$W \approx \frac{\pi \mu_o r_o^4}{8(\mu_o F + H k_r)} \{V + (1 - \frac{8 k_r H H_s}{k_y r_o^2} V' \} \qquad (7.41)$$

$$\frac{t}{\pi \mu_o r_o^4} \approx \int_{h_f}^{h_i} \frac{dh}{8W(\mu_o F + H k_r) - \pi \mu_o r_o^4 V'(1 - \frac{8 H H_s k_r}{k_y r_o^2})} \qquad (7.42)$$

Again, it can be noted from equations (7.38) and (7.40) that W and t increase as λC_o, M, and k_y increase but they decrease as k_r increases. The expressions (7.41) and (7.42) are plotted in figures 7.5 to 7.8 respectively for various values of λC_o, k_y and k_r. From these figures, the above described results are obvious.

7.4 CONCLUSIONS

In this chapter, we have studied the behaviour of knee and hip joints by taking into account the porosity of the cartilage and the viscosity variation of the synovial fluid due to change in the concentration of hyaluronic acid molecules. It is shown that the load capacity and time of approach increases as the concentration of the hyaluronic acid molecules increases due to consolidation and trapping. Further, these parameters also increase as the permeability of the cartilage matrix in the normal direction increases but they decrease with the increase in the permeability of the cartilage in the parallel direction. As pointed out in chapter V, this situation does exist in the case of the cartilage of synovial joints.

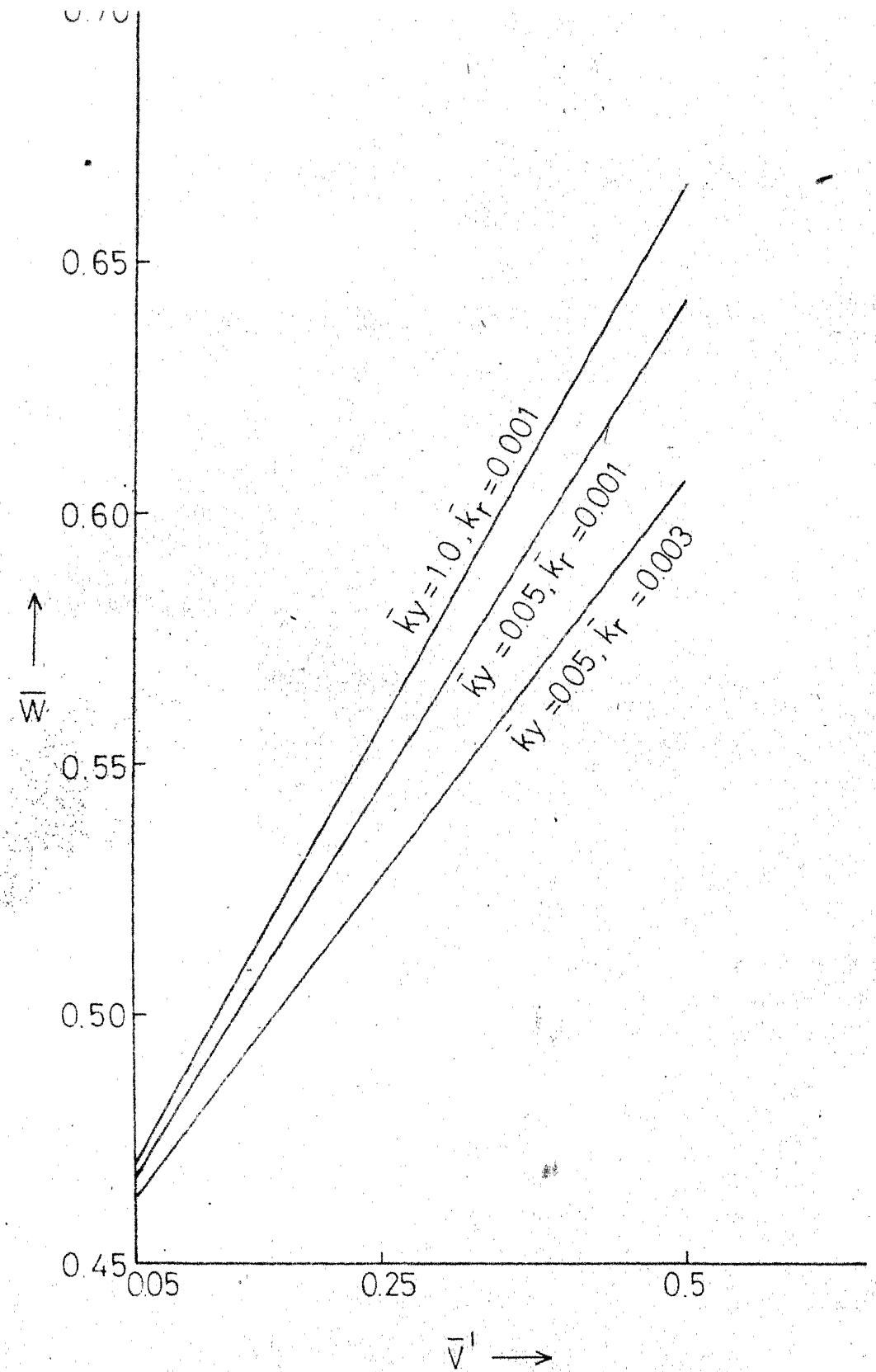

Fig. 7.5 Variation of $\bar{W}$ with $\bar{V}'$ for different values of $\bar{k}_r, \bar{k}_y$ and $\bar{P}_o = 0.2$, $\lambda C_o = 0.1$, $\bar{M} = 0.25$.

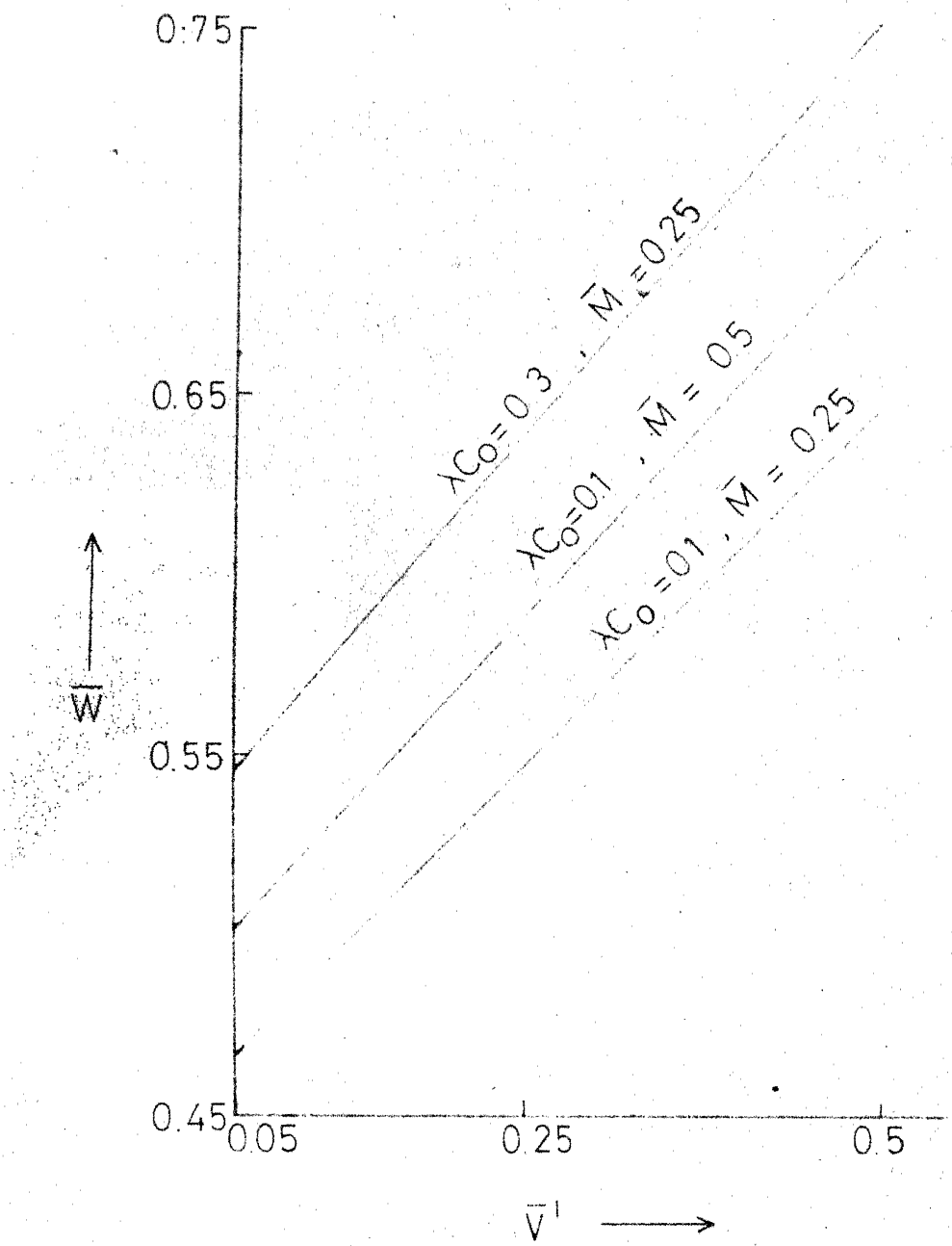

g.7.6. Variation of $\bar{W}$ with $\bar{V}'$ for different values of λC_o and $\bar{M}$, and for $\bar{P}_o = 0.2$, $\bar{k}_r = 0.001$, $\bar{k}y = 0.05$.

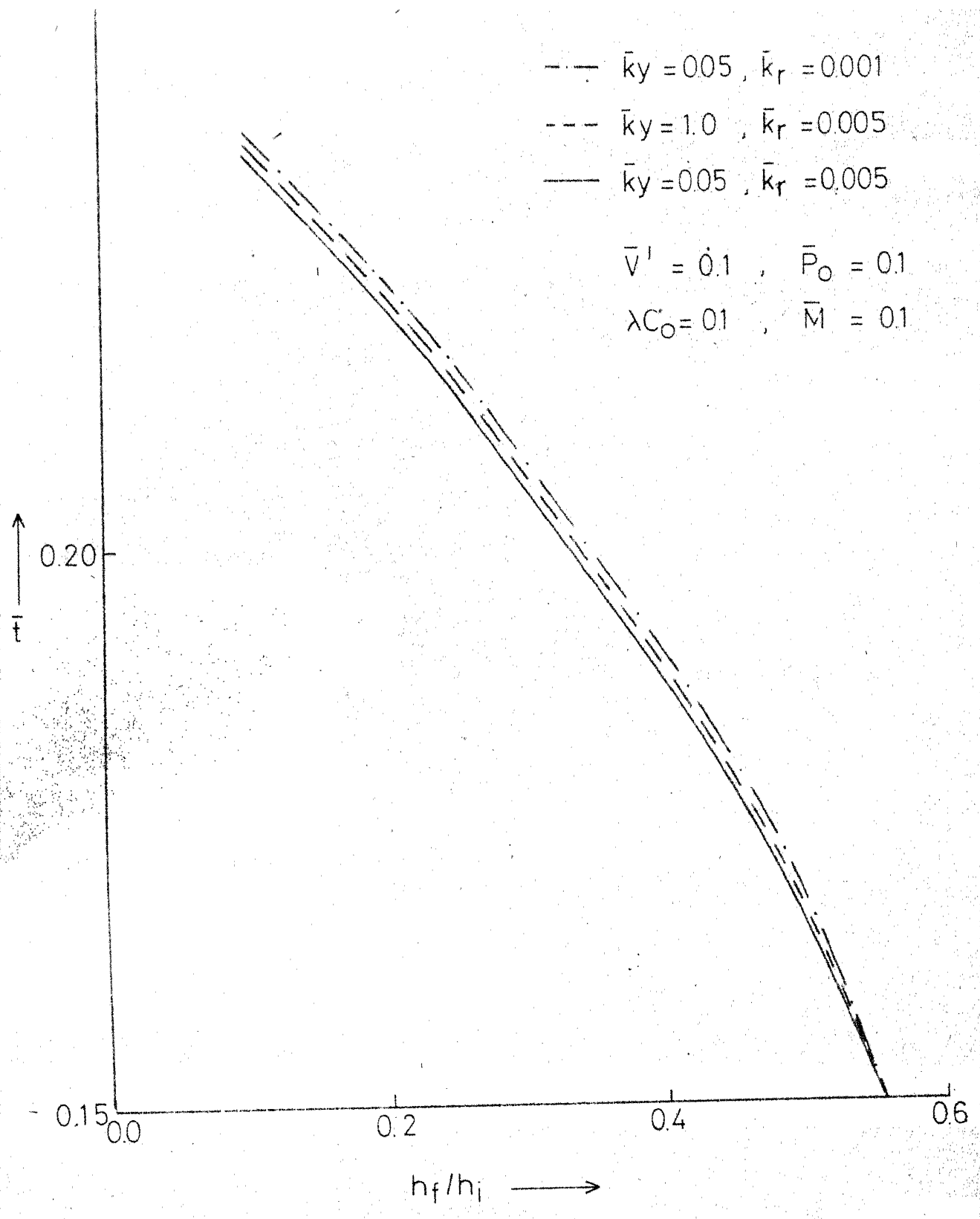

Fig 7.7 Variation of $\bar{t}$ with h_f/h_i for different values of $\bar{k}_r$ and $\bar{k}y$.

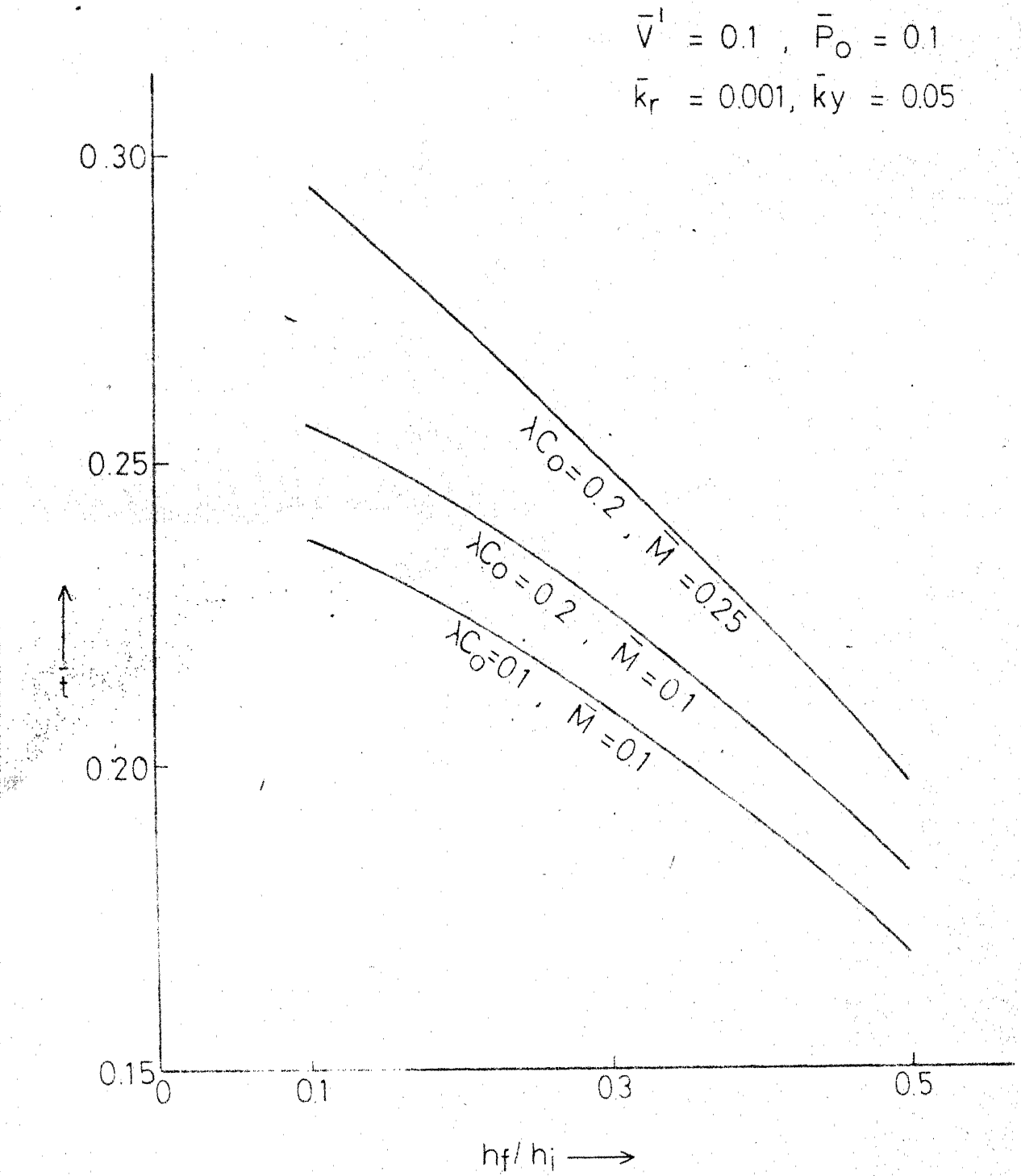

g. 7.8 Variation of $\bar{t}$ with h_f/h_i for different values of λC_o and $\bar{M}$

CHAPTER - VIII

ANALYSIS OF DISEASED JOINTS

8.1 INTRODUCTION

In previous chapters we have studied the characteristics of normal joints. In this chapter, we investigate the behaviour of the diseased joint i.e. the joint whose components such as synovial fluid and articular cartilage are diseased. As pointed out by Burch et. . al. [1960], the synovial fluid for diseased joint of rheumatoid arthritic patient looses its non-Newtonian character and the cartilage becomes cracked, frayed and less resilient. The pores of the cartilage matrix may become larger allowing a mass transfer of hyaluronate molecules at the cartilage surface and thus decreasing the hyaluronate concentration in the synovial fluid-film. Further, the disease causing bacteria , present in the diseased joint, may react biochemically with the hyaluronate molecules and destroy their concentration, structure etc. in the synovial fluid. These changes in hyaluronate may be responsible for the Newtonian character of the synovial fluid and for the decrease of its viscosity in the case of diseased joint.

In the analysis that follows it is assumed that the effective viscosity of the synovial fluid varies linearly with the concentration of hyaluronic acid molecules, Rutgers [1962] , as follows :

$$\mu = \mu_o [1 + \lambda C] \tag{8.1}$$

where μ_o is the viscosity of the fluid without hyaluronate molecules, λ is a constant and C is the concentration of the hyaluronic acid molecules which depends upon the process such as diffusion, biochemical reaction etc. (see chapter II). Further to present the results in a simple form, the effects of cartilage elasticity and porosity have not been considered.

Here the behaviour of the diseased joint in the standing position (squeeze film) has been studied by assuming the loaded region of the joint in following forms.

(i) rectangular parallel plates model.

(ii) circular parallel plates model.

(iii) cylindrical surface model.

8.2 RECTANGULAR PARALLEL PLATES MODEL

The joint geometry, when approximated to two parallel rectangular plates, is shown in figure 8.1a . The basic equation governing the pressure in the film can be written as follows [see chapter II, equations (2.43), (2.44) and (2.49-a)].

$$\frac{d}{dx}\left[F \frac{dp}{dx}\right] = -V \tag{8.2}$$

$$F = \int_o^h \frac{y^2}{\mu}\, dy \tag{8.3}$$

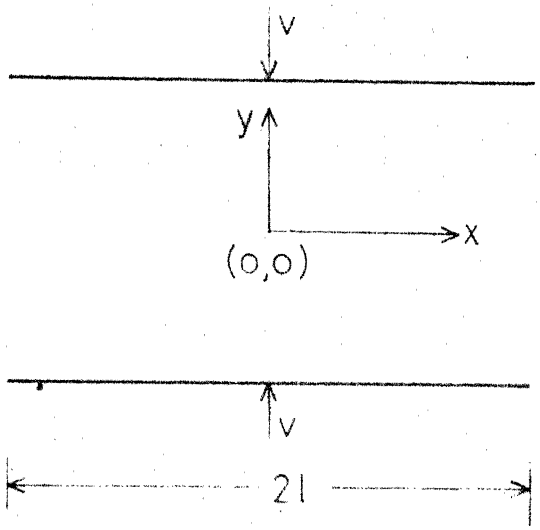

(a) Rectangular plates model

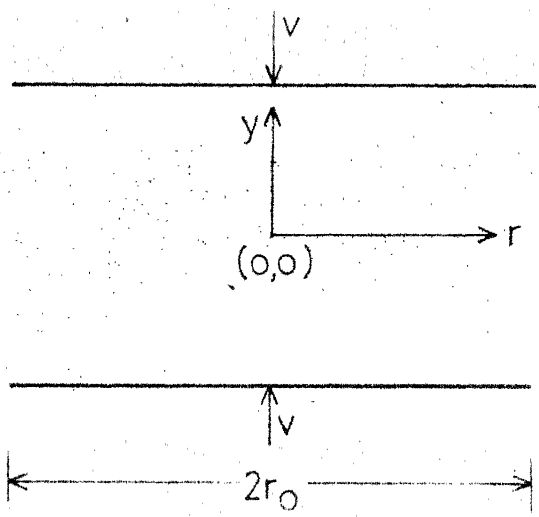

(b) Circular plates model

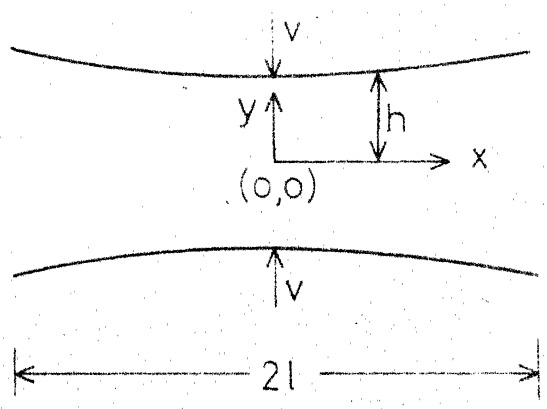

(c) Curved surfaces model

Fig. 8.1 Squeeze film geometries.

$$\mu = \mu_o \left(1 + \lambda C_d \frac{\cosh \gamma y}{\cosh \gamma h}\right) \tag{8.4}$$

where $\gamma^2 = \frac{\alpha}{D}$, α is the rate of decrease of hyaluronate concentration due to biochemical reactions etc., D is the diffusion coefficient and C_d is the concentration of hyaluronate at the surface $y = h$ of the diseased joint.

Integrating equation (8.2) with the following conditions for p,

$$\begin{aligned} p &= 0 \quad \text{at } x = \ell \\ \frac{dp}{dx} &= 0 \quad \text{at } x = 0 \end{aligned} \tag{8.5}$$

the pressure distribution is obtained as,

$$p = \frac{V}{F} \frac{\ell^2 - x^2}{2} \tag{8.6}$$

which gives the expression for the load capacity of the joint as,

$$W = \frac{2b\ V\ \ell^3}{3F} \tag{8.7}$$

The time of squeezing t for the upper surface to approach the position h_f from h_i is obtained, by putting $V = -\frac{dh}{dt}$ in equation (8.7) and integrating, as follows :

$$t = \frac{2b\ \ell^3}{3W} \int_{h_f}^{h_i} \frac{dh}{F} \tag{8.8}$$

To see the various effects approximately, the function F can be approximated as follows : ($\lambda C_d << 1$)

$$F = \frac{h^3}{3\mu_o}\left[1 - \frac{3\lambda C_d}{\gamma h}\left\{\left(1 + \frac{2}{\gamma^2 h^2}\right)\tanh(\gamma h) - \frac{2}{\gamma h}\right\}\right] \tag{8.9}$$

In such a case, the above expressions for W and t can be approximated as follows :

$$W = \frac{2\mu_o b V \ell^3}{h^3}\,\bar{W} \tag{8.10}$$

$$t = \frac{\mu_o b \ell^3}{W h_f^2}\,\bar{t} \tag{8.11}$$

where

$$\bar{W} = 1 + \frac{3\lambda C_d}{\gamma h}\left\{\left(1 + \frac{2}{\gamma^2 h^2}\right)\tanh(\gamma h) - \frac{2}{\gamma h}\right\} \tag{8.12}$$

$$\bar{t} = 2\int_1^{\bar{h}_i} \frac{\bar{W}}{\bar{h}^3}\, d\bar{h} \tag{8.13}$$

$$\bar{h}_i = \frac{h_i}{h_f}\,,\quad \bar{h} = \frac{h}{h_f}$$

The expressions for $\bar{W}$ and $\bar{t}$ have been plotted in figs. 8.2 and 8.3 respectively for various values of λC_d and γh. From fig. 8.2, it can be noted that $\bar{W}$(or W) decreases as λC_d decreases or as γh increases. Considering that the case $\gamma h = 0$, corresponds to a normal joint for a given λC_d, it can be seen that the load of the normal joint ($\gamma h = 0$) decreases about 14% corresponding to the case of diseased joint ($\gamma h = 10$) for $\lambda C_d = 0.2$.

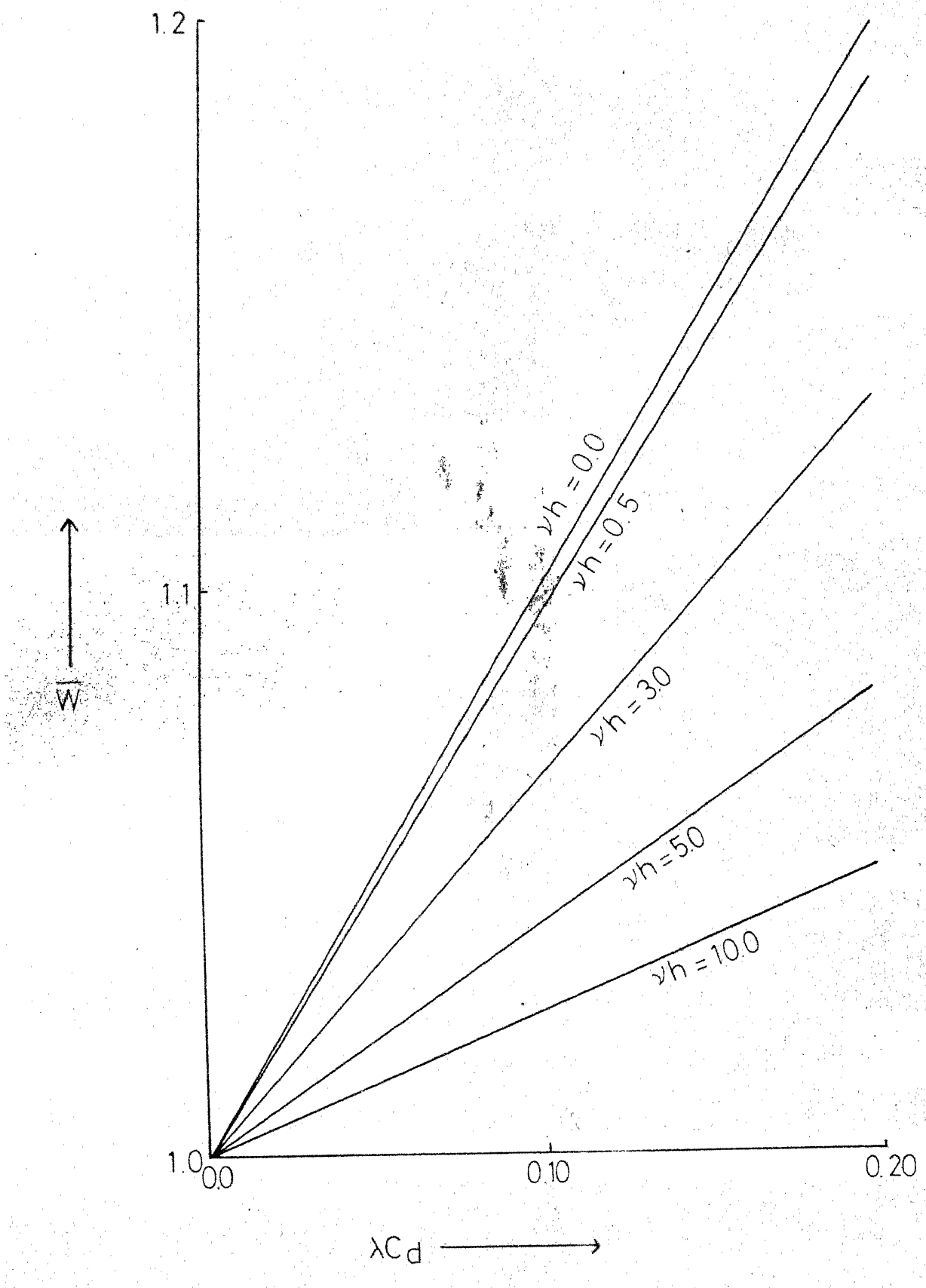

Fig. 8.2 Variation of $\overline{W}$ with λC_d for different values of ν

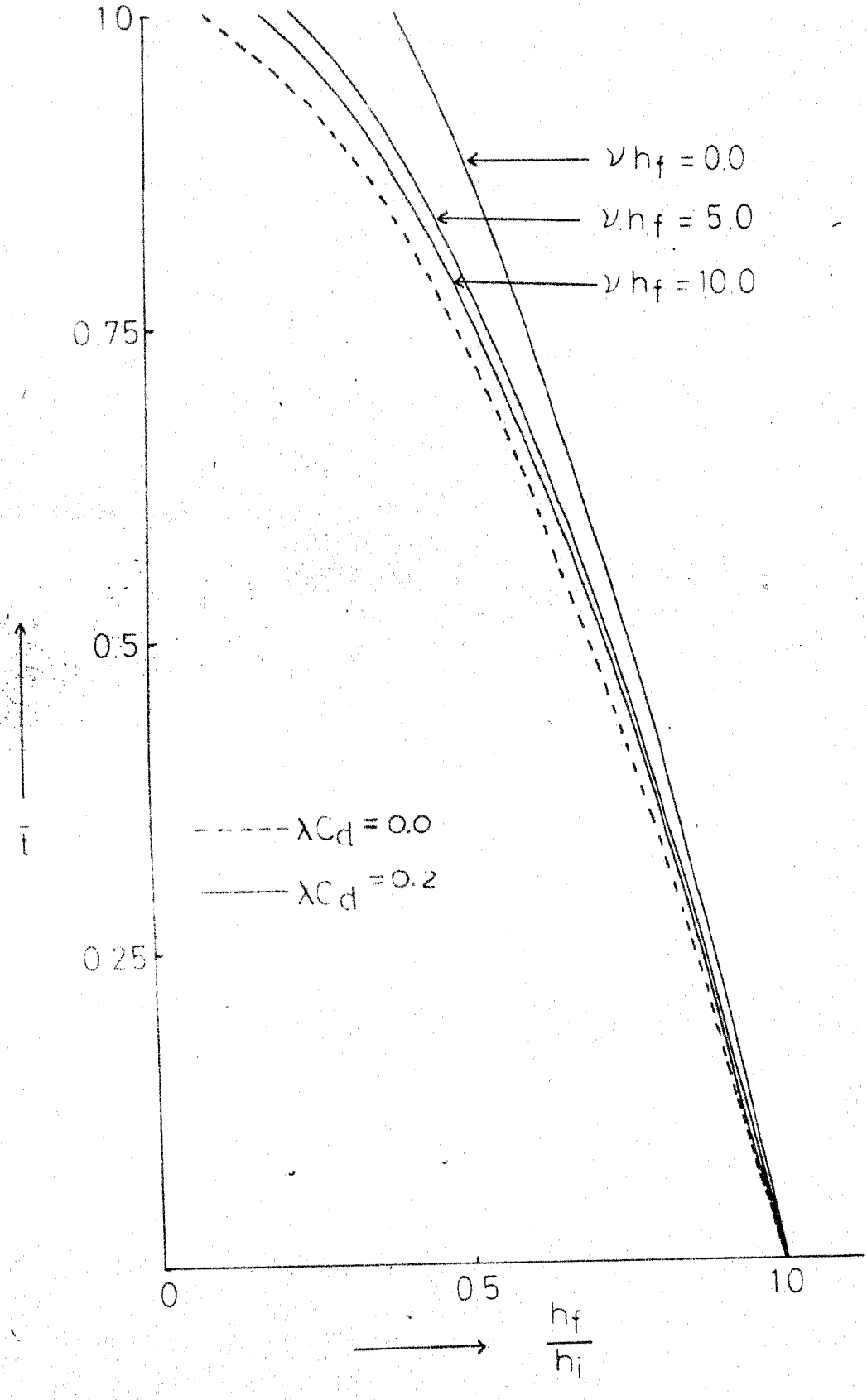

Fig 8.3 Variation of $\bar{t}$ with h_f/h_i

Further from fig. 8.3 it is seen that $\bar{t}$ (or t) also decreases as λC_d decreases or γh increases. It has also been found that the time of squeezing to reduce the film-thickness by 9×10^{-4} cm for the normal joint ($\gamma h_f = 0$) is reduced by 17% in comparison to the diseased joint ($\gamma h_f = 10$) for $\gamma C_d = .2$.

8.3 CIRCULAR PARALLEL PLATES MODEL

In this case, the joint geometry has been approximated by two circular parallel plates, as shown in fig. 8.1-b. The basic equation governing the pressure in the film is given by

$$\frac{1}{r}\frac{d}{dr}\left(rh^3\frac{dp}{dr}\right) = -V \tag{8.13}$$

The conditions on p are,

$$\begin{aligned} p &= 0 \quad \text{at } r = r_o \\ \frac{dp}{dr} &= 0 \quad \text{at } r = 0 \end{aligned} \tag{8.14}$$

Integrating equation (8.13) and using the conditions (8.14), the expressions for pressure and load capacity can be obtained as follows :

$$p = \frac{V}{4F}\left(r_o^2 - r^2\right) \tag{8.15}$$

$$W = \frac{\pi}{8}\frac{V}{F}r_o^4 \tag{8.16}$$

The time of squeezing t is then obtained as

$$t = \frac{\pi r_o^4}{8W} \int_{h_f}^{h_i} \frac{dh}{F} \tag{8.17}$$

As before for low concentrations $\lambda C_d << 1$, the expressions for W and t can be approximated in the following forms :

$$W = \frac{3\pi \mu_o V r_o^4}{8h^3} \bar{W} \tag{8.18}$$

$$t = \frac{3\pi \mu_o r_o^4}{16W h_f^2} \bar{t} \tag{8.19}$$

where $\bar{W}$ and $\bar{t}$ are same as defined in equations (8.12) and (8.13) respectively.

Since the expressions for $\bar{W}$ and $\bar{t}$ are same as in the previous case, the same behaviour follows here also.

8.4 CYLINDRICAL SURFACE MODEL

Here, we approximate, the joint geometry with two cylindrical surfaces as shown in fig. 8.1-c. The film thickness function h in this case is given by

$$h = h_m \left[1 + \frac{x^2}{2Rh_m} \right] \tag{8.20}$$

where $2h_m$ is the minimum film thickness and R is the equivalent radius of the cylindrical surfaces. The basic equation governing the pressure corresponding to this case is given as follows :

$$\frac{d}{dx}\left[F \frac{dp}{dx} \right] = - V \tag{8.21}$$

where, F is the same as defined in equation (8.3), and is a function of x.

Integrating equation (8.21) and using conditions (8.5) for p, the pressure is determined as follows :

$$p = \int_{x}^{\ell} \frac{Vx}{F}\, dx \tag{8.22}$$

The load capacity of the joint W is given as,

$$W = 2b\ V \int_{o}^{\ell} \frac{x^2}{F}\, dx \tag{8.23}$$

The time of squeezing t , then can be written as,

$$t = \frac{2b}{W} \int_{h_f}^{h_i} \left[\int_{o}^{\ell} \frac{x^2}{F}\, dx \right] dh \ . \tag{8.24}$$

To see the various effects qualitatively the expressions for W and t are approximated for $\lambda C_d << 1$, $\frac{\ell^2}{Rh_m} << 1$ and $\tanh \gamma h \approx 1$, as follows :

$$W = \frac{2b\ \mu_o\ V\ell^3}{h_m^3}\ \bar{W} \tag{8.25}$$

$$t = \frac{\mu_o b \ell^3}{W h_f^2}\ \bar{t} \tag{8.26}$$

where,

$$\bar{W} = \left(1 - \frac{9\ell^2}{10Rh_m}\right) + \frac{3\lambda C_d}{\gamma h_m}\left[\left(1 - \frac{6\ell^2}{5Rh_m}\right) - \frac{2}{\gamma h_m}\left(1 - \frac{3\ell^2}{2Rh_m}\right) + \frac{2}{\gamma^2 h_m^2}\left(1 - \frac{9\ell^2}{5Rh_m}\right)\right] \tag{8.27}$$

and,

$$\bar{t} = \{1-(\frac{h_f}{h_i})^2\} - \frac{3}{5}\frac{\ell^2}{Rh_f}\{1-(\frac{h_f}{h_i})^3\}$$

$$+ \frac{2\lambda C_d}{\gamma h_f}[\{1-(\frac{h_f}{h_i})^3\} - \frac{3}{2\gamma h_f}(\frac{3}{5}\frac{\ell^2}{Rh_f} + \frac{1}{\gamma h_f})\{1-(\frac{h_f}{h_i})^4\}$$

$$+ \frac{3}{5\gamma^2 h_f^2}(\frac{3\ell^2}{Rh_f} + \frac{2}{\gamma h_f})\{1-(\frac{h_f}{h_i})^5\} - \frac{9}{5\gamma^3 h_f^3}\frac{\ell^2}{Rh_f}\{(1-(\frac{h_f}{h_i})^6\}] \qquad (8.28)$$

In fig. 8.4 the function $\bar{W}$ has been plotted for different values of γh_m and λC_d with $(\frac{\ell^2}{Rh_m} = .2)$. It is noted from the fig. 8.3 that the $\bar{W}$ and hence, the load capacity W, decrease as λC_d decreases, or as γh_m increases. For $\frac{\ell^2}{Rh_m} = .2$ and $\lambda C_d = .2$, the decrease in load capacity for normal joint ($\gamma h_f = 0$), in comparison to diseased joint ($\gamma h_f = 10$) is about 11.7%.

In fig. 8.5, the graph has been plotted for $\bar{t}$ against h_f/h_i for different values of λC_d and γh_f. It is noted that, time of squeezing t, $(\bar{t})$, also decreases as λC_d decreases or as γh_f increases.

8.5 CONCLUSIONS

In this chapter, the characteristics of diseased joints have been studied in various cases by considering the Newtonian behaviour of the synovial fluid which is caused due to decrease in concentration of hyaluronic acid molecules and change in their structure. It has been shown that both the load capacity and time of approach decrease as the joints become more and more diseased.

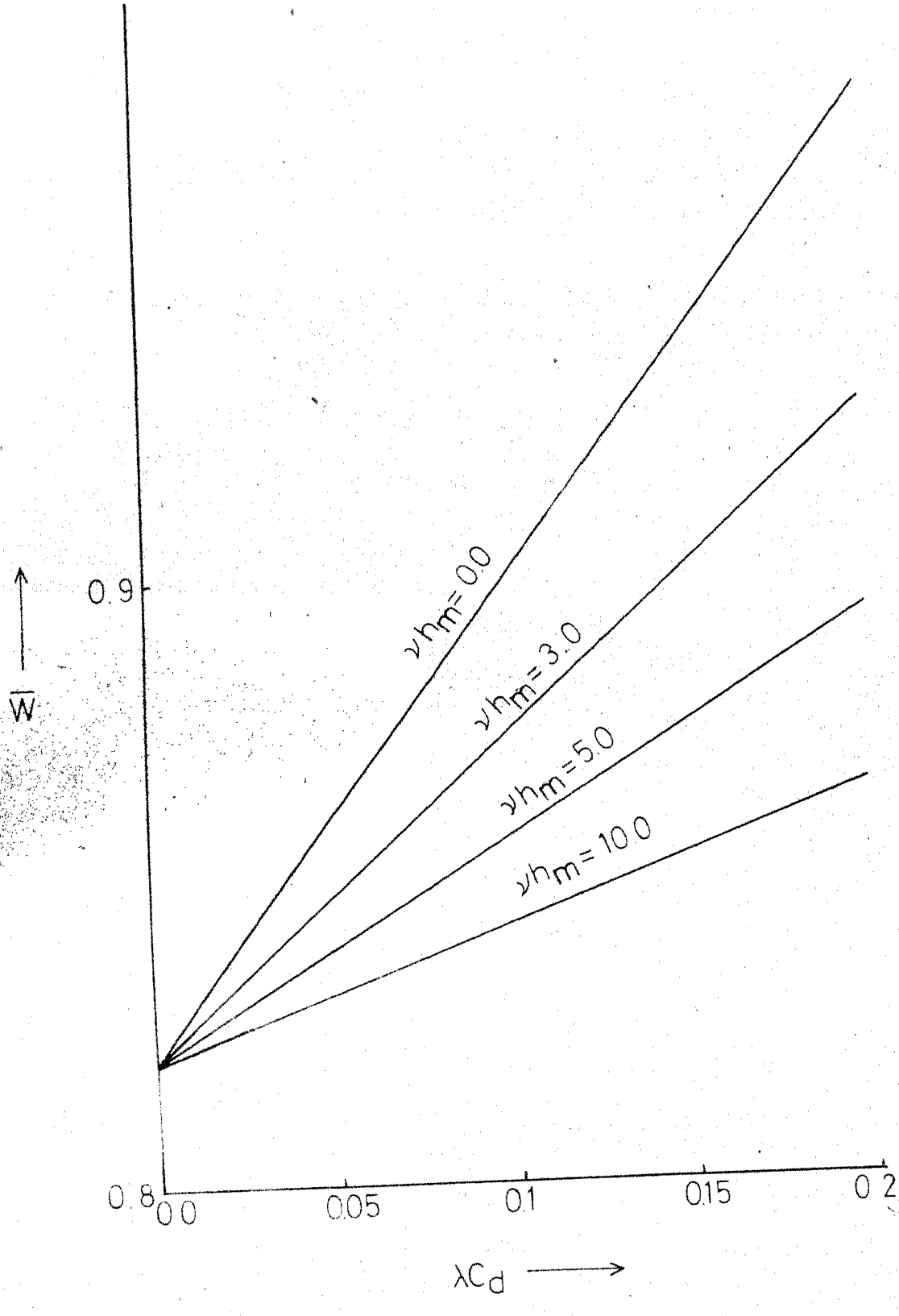

Fig. 8.4 Variation of $\overline{W}$ with λC_d, for $l^2 / Rh_m = 0.2$

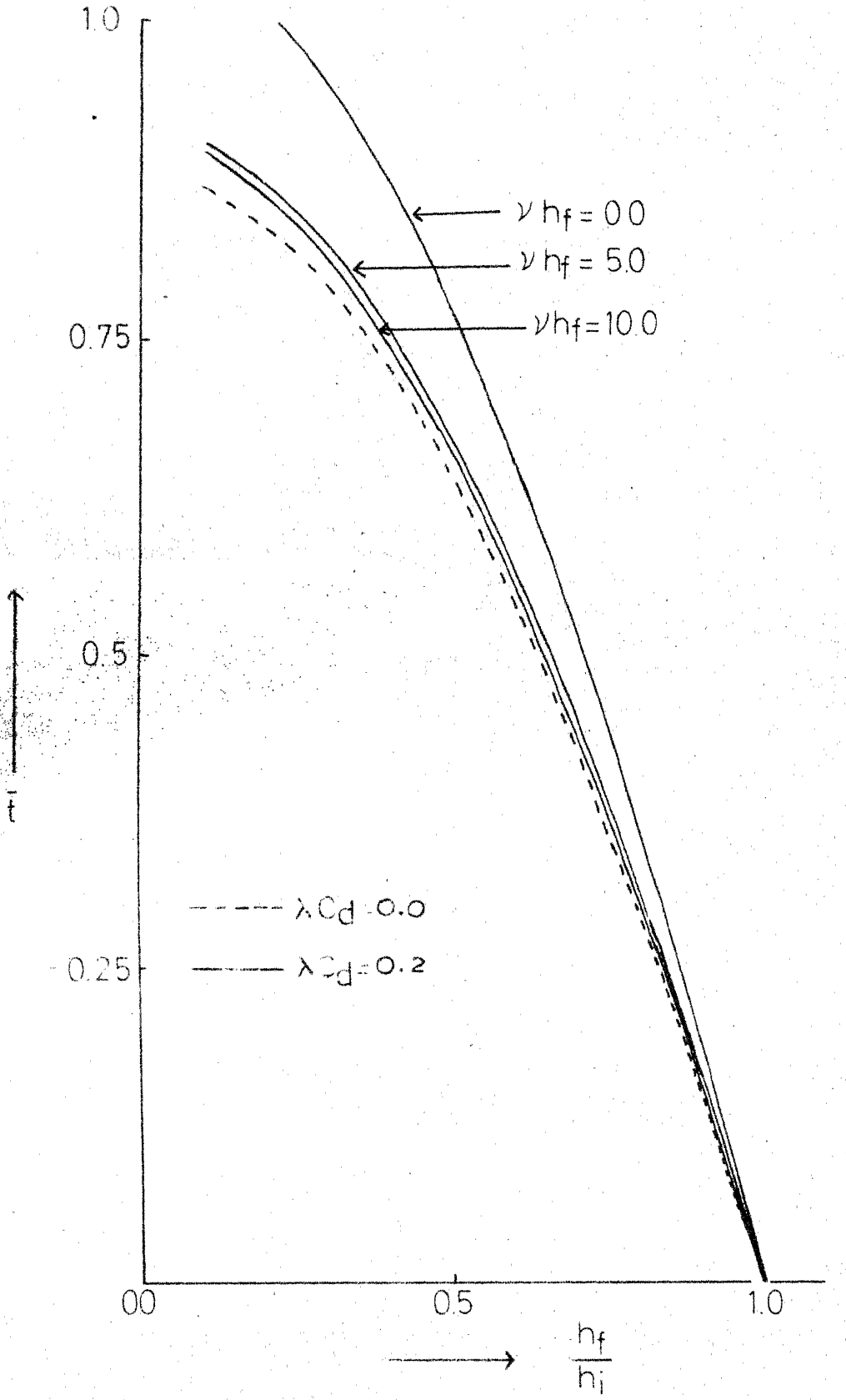

Fig. 8.5. Variation of $\bar{t}$ with h_f/h_i for $I^2/Rh_f = 0.2$

REFERENCES

Archard, J.F. and Kirk, M.T. (1963)
Influence of elastic modulus properties on the lubrication of point contacts.
Proc. Lubr. Wear Convention, Instn. Mech.Engrs., London, Paper No. 15, Vol.181.

Barwell, F.T. (1956)
Lubrication of Bearings.
Butterworths Scientific Publications, London.

Bird, R.B., Stewart, W.E. and Lightfoot, E.N. (1960)
Transport Phenomena.
John Wiley and Sons, Inc.

Bloch, B. and Dintenfass, L. (1963)
Rheological study of human synovial fluid.
Australian-NewZealand J. of Surgery, Vol. 33, p. 108.

Burch, G.E., Love, W.D. and Jeffrey (1960)
The waning joints.
Progress of Medical Science, January - Volume.

Castelli, V., Rightmire, G.K. and Fuller, D.D. (1966)
On the analysis and experimental investigation of a hydrostatic axisymmetric compliant-surface thrust bearing.
Lubrication Conference, Minneapolis, Paper No. 66-Lub.17.

Charney, J. (1959)
The lubrication of animal joints.
Proc.Symp. Biomechanics, Instn. Mech. Engrs., London, Paper no. 12.

Christensen, H. (1969)
Elastohydrodynamic theory of spherical bodies in normal approach.
Lubrication Symposium, San Fransisco, Paper No. 69-Lub S-3.

Clarke, I.C. (1971-a)
Articular Cartilage : a review and scanning microscope study.
J. Bone Jnt. Surg., Vol. 53B(4), p. 732.

Clarke, I.C. (1971-b)
Human articular surface contours and related surface depression frequency study.
J.Microscopy, Vol. 93, No. 1, p. 66.

Davies, D.V., Barnett, C.H., Cochrane, W. and Palfrey A.J. (1962)
Electron microscopy of articular cartilage in the young adult rabit.
Ann. Rheum. Dis., Vol. 21, p. 11.

Davies, D. V. (1966)
Synovial fluid as a lubricant .
Fed. Proc., Vol. 25, No. 3, p. 1069.

Davies, D. V. (1967)
Properties of synovial fluid.
Proc. Instn. Mech. Engrs., Vol. 181, (Pt 3J).

Dintenfass, L. (1963)
Lubrication in synovial joints : A theoretical analysis.
J. Bone Jnt. Surg., Vol. 45A(6), p. 1241.

Dintenfass, L. (1966)
Rheology of complex fluids and some observations on joint lubrication.
Fed. Proc., Vol. 25, p. 1054.

Dowson, D. and Higginson, G.R. (1959)
A numerical solution to the elastohydrodynamic problem.
J. Mech. Eng. Sci., Vol. 1, No. 1.

Dowson, D. and Higginson, G.R. (1960)
The effect of material properties on the lubrication of elastic rollers.
J. Mech. Eng. Sci., Vol. 2, No. 3.

Dowson, D. (1962)
A generalized Reynolds' equation for fluid film lubrication.
Int. J. Mech. Sci.,Vol. 4, p. 159.

Dowson, D. and Taylor, C.M. (1966)
Elastohydrodynamic lubrication of circular plate thrust bearing.
Lebrication Symposium, New Orleans, La, Paper No. 66 + Lub S-15.

Dowson, D. and Higginson, G.R. (1966)
Elastohydrodynamic lubrication; the fundamentals of roller and gear lubrication.
Pergamon Press, Oxford.

Dowson, D. (1967)
Modes of lubrication in human joints.
Proc. Instn. Mech. Engrs. London, Vol. 181, Pt. 3J, p. 45.

Dowson, D., Unsworth A. and Wright, V. (1970)
Analysis of 'Boosted Lubrication' in human joints.
J. Mech. Eng. Sci., Vol. 12, No. 5, p. 364.

Dowson, D. and Wright, V. (1973)
Bio-Tribology.
The Rheology of lubricants, ed. by T.C. Davanport, Applied Science, England, p. 81.

Edwards, J.(1967)
Physical characteristics of articular cartilage.
Proc. Instn. Mech. Engrs. London, Vol. 181, Pt. 3J, p. 16.

Engin, A.E. and Korde, M.S. (1974)
Biomechanics of normal and abnormal knee joint.
J. Biomechanics, Vol. 7, p. 325.

Fein, R. S. (1967)
Are synovial joints squeeze -film lubricated?
Proc. Instn. Mech. Engrs., London, Vol. 181, Pt 3J, p. 125.

Gardner, D. L. and McGillivray, D. C. (1971)
Living articular cartilage is not smooth.
Ann. Rheum. Dis., Vol. 30 (3), p. 11.

Gatcombe, E. K. (1945)
Lubrication characteristics of involute spur gears.
Trans. A.S.M.E., Vol. 67, p. 178.

Herrebrugh, K. (1970)
Elastohydrodynamic squeeze films between two cylinders in normal approach.
J. Lub. Tech. (Trans. A.S.M.E.) Vol. 92F (2), p. 292.

Higginson, G.R. and Norman, R. (1974)
The lubrication of porous elastic solids with reference to the functioning of human joint .
J. Mech. Eng. Sci., Vol. 16, No. 4, p. 250.

Hooke, C.J., Lines, D.J. and O'Donoghue, J.P. (1966)
Elastohydrodynamic lubrication of O-ring seals.
Proc. Instn. Engrs., Vol. 181, No. 9.

Hsing, F.C. (1971)
The effect of fluid inertia on a porous thrust plate - an analytic solution.
J. Lub. Tech. (Trans. A.S.M.E.), Vol. 93F(1) p. 202.

Isa, M. (1974)
Contributions to recent frontiers in tribology.
Ph.D. Thesis, I.I.T. Kanpur.

Kamal, M.M. (1968)
A high pressure seal.
J. Lub. Tech. (Trans. A.S.M.E.), Vol. 90F(2) p. 412.

Kapur, J. N. (1963)
A note on the boundary layer equations for power law fluids.
J. Phys. Soc., Japan, Vol. 18,p. 144.

Kempson, G. E., Freeman, M.A.R. and Swanson, S.A.V. (1968)
Tensile properties of articular cartilage.
Nature, Vol. 220,p. 1127.

Ling, F.F. (1974)
A new model of articular cartilage in human joints.
J. Lub. Tech. (Trans. A.S.M.E.) Vol. 96, No. 3, p.449.

Linn, F.C. and Sokoloff, L. (1965)
Movement and composition of interstitial fluid of cartilage.
Arth. Rheum., Vol. 8, p. 481.

MacConaill, M.A. (1932)
The function of intra-articular fibrocartilages.
J. Anat., Vol. 66, p. 210.

MacConaill, M.A. (1966)
The synovial fluid.
Labrotary Practice, Vol. 15, No. 1 (LABP-15-4; Special article), p. 60.

MacConaill, M.A. (1967)
Basic anatomy of weight-bearing joints.
Proc. Instn. Mech. Engrs., London, Vol. 181 (Pt 3J), Paper No. 5.

Matthews, B. F. (1952)
Collagen chondroitin - sulfate ratio of human articular cartilage related to function.
Brit. Med. J., Vol. 2, p. 1295.

McCutchen, C.W. (1959)
Mechanism of animal joints.
Nature, Vol. 184, p. 1284.

McCutchen, C.W. (1962-a)
Animal joint and weeping lubrication.
New Scientist, Vol. 15, p. 412.

McCutchen, C.W. (1962-b)
The frictional properties of animal joints.
Wear, Vol. 5, p. 1.

McCutchen, C.W. (1966)
Boundary lubrication by synovial fluid : demonstration and possible osmotic explanation.
Fed. Proc., Vol. 25(3), p. 1061.

McCutchen, C.W. (1967)
Physiological lubrication.
Proc. Instn. Mech. Engrs., London, Vol. 181 (Pt 3J), Paper No. 1.

McKee, G.K. (1967)
Developments in total hip joint replacement.
Proc. Instn. Mech. Engrs., London, Vol. 181 (Pt 3J), Paper No. 4.

Meachim, G. and Roy, S. (1969)
Surface ultrastructure of mature adult human articular cartilage.
J. Bone Jnt. Surg., Vol. 51B(3), p. 529.

Mital, M.A. and Millington, P.F. (1971)
Surface characteristics of articular cartilage.
Micron., Vol. 2, p. 236.

Mori, H., Yabe, H. and Ono, T. (1965)
Theory of externally pressurised circular thrust porous gas bearings.
J. Basic Engg. (Trans. A.S.M.E.), Vol. 87D(3) Paper No.64-Lub. 19, p. 613.

Morrison, J. B. (1970)
The mechanism of the knee joint in relation to normal walking.
J. Biomechanics, Vol. 3, p. 51.

Mow, M.C. and Ling, F.F. (1969)
On weeping lubrication.
ZAMP, Vol. 20, p. 158.

Mow, V.C. (1969)
The role of lubrication in biomechanical joints.
J.Lub. Tech. (Trns. A.S.M.E.), Vol. 91F (2).

Mow, V.C., Lai, W.M. and Redler, I. (1974)
Some characteristics of articular cartilage - I : A scanning electron microscopy study and a theoretical model for the dynamic interaction of synovial fluid and articular cartilage.
J. Biomechanics, Vol. 7, p. 449.

Negami, S. (1964)
Dynamic mechanical properties of synovial fluid.
M.S. Thesis, Lehigh University, Penn, U.S.A.

Ogston, A.G. and Staneir, J.E. (1953)
The physiological function of hyaluronate acid in synovial fluid; viscous elastic and lubricant properties.
J. Physiology, Vol. 119,p. 253.

Paul, J.P. (1967)
Forces transmitted by joints in the human body.
Proc. Instn. Mech.Engrs., London, Vol. 181 (Pt 3J), Paper No. 8.

Pinkus, O. and Sternlicht, B. (1961)
Theory of hydrodynamic lubrication.
McGraw Hill Book Company, Inc.

Radin, E.L., Paul, I.L. and Pollock, D. (1970)
Animal joint behaviour under excessive loading.
Nature, Vol. 226, p. 554.

Radin, E.L. and Paul, I.L. (1972)
A consolidated concept of joint lubrication.
J. Bone Jnt. Surg., Vol. 54-A(3), p. 607.

Rashevsky, N. (1973)
The principle of adequate design.
Foundations of mathematical biology, edited by Robert Rosen , Academic Press.

Rutgers, I.R. (1962)
Relative viscosity of suspension of rigid spheres in Newtonian liquids.
Rheological Acta, Vol. 2(1), p. 74.

Sasaki, T., Mori, H. and Okino, N. (1962)
Fluid film theory of roller bearing, Part I.
J. Basic Engg., (Trans. A.S.M.E.), Vol. 84D(1), p.166.

Scales, J.T. (1967)
Arthroplasty of the hip using foreign materials : a history.
Proc. Instn. Mech. Engrs., London, Vol. 181 (Pt 3J), Paper No. 13.

Shukla, J.B. (1963)
Conical step bearing using a power law lubricant.
Wear, Vol. 6, p. 371.

Shukla, J.B. (1964-a)
Load capacity and time relation for squeeze films in conical bearings.
Wear, Vol. 7, p. 378.

Shukla, J.B. (1964-b)
Theory for the squeeze film for power law fluid lubricant.
A.S.M.E. Publication, Paper No. 64-Lub S-4.

Shukla, J.B. (1972)
Effect of additives in lubrication.
Proc. World Conference in Industrial Tribology, Delhi; Paper No. B-5.

Shukla, J. B. and Prasad, R. (1966)
Effects of roughness in hydromagnetically lubricated bearings.
Lubrication Symposium (A.S.M.E.), New Orleans, La ; Paper No. 66 - Lub S-9.

Sokoloff, L. (1966)
Elasticity of aging cartilage.
Fed.Proc., Fedn. Am.Soc. Exp. Biol., Vol. 25(3), p. 1089.

Steindler, A. (1955)
Kinesiology.
Charles C. Thomas Publishers, Spring field, Ill.

Tanner, R.I. (1966)
An alternative mechanism for the lubrication of synovial joints.
Phys. Med. Bio., Vol. 11(1), p.119.

Walker, P.S., Dowson, D., Longfield, M.D. and Wright, V. (1968)
Boosted lubrication in synovial joints by fluid entrapment and enrichment.
Ann. Rheum. Dis., Vol. 27 (6), p. 512.

Walker, P.S., Sikorski, J., Dowson, D., Longfield, M.D., Wright, V. and Buckley, T. (1969)
Behaviour of synovial fluid on surfaces of articular cartilage : a scanning electron microscope study.
Ann. Rheum. Dis., Vol. 28 (1).

Weiss, C., Rosenberg, L. and Helfet, A.J. (1968)
An ultrastructure study of normal young adult human articular cartilage.
J. Bone Jnt. Surg., Vol. 50 A(4), p. 663.

Wilson, J.N. (1967)
Problems of acetabular fixation in total hip replacement.
Proc. Instn. Mech. Engrs., London, Vol. 181 (Pt 3J), Paper No. 9.

Wright, V., Dowson, D. and Kerr, J. (1974)
The structure of joints.
(Private communication).

Wu, H. (1970)
Squeeze film behaviour for porous annular disks.
J. Lub. Tech., (Trans. A.S.M.E.) Vol. 92 F(4), p. 593.

46228

d on the